Strathprints Institutional Repository

Fedorov, Maxim and Kornyshev, Alexei A. (2014) Ionic liquids at electrified interfaces. Chemical Reviews, 114 (5). pp. 2978-3036. , http://dx.doi.org/10.1021/cr400374x

This version is available at http://strathprints.strath.ac.uk/47256/

Ionic liquids at electrified interfaces

Maxim Fedorov[*,†] and Alexei Kornyshev[*,‡]

Department of Physics (Scottish University Physics Alliance), University of Strathclyde, John Anderson Bldg, 107 Rottenrow, Glasgow G4 0NG, United Kingdom , and Department of Chemistry, Faculty of Natural Sciences, Imperial College London, C1Bldg, South Kensington Campus, London, SW7 2AZ, United Kingdom

E-mail: maxim.fedorov@strath.ac.uk; a.kornyshev@imperial.ac.uk

Contents

---

*To whom correspondence should be addressed
†University of Strathclyde
‡Imperial College London

8 Examples of other applications of RTILs at EIs   109

9 Conclusions   115

10 Nomenclature   119

11 Acknowledgment   122

1 Introduction

Until recently, 'room-temperature' (<100-150 C) liquid-state electrochemistry was mostly electrochemistry of *diluted* electrolytes[1–4] where dissolved salt ions were surrounded by a considerable amount of solvent molecules. Highly *concentrated* liquid electrolytes were mostly considered only in the narrow (albeit important) niche of *high-temperature* electrochemistry of molten inorganic salts[5–7] and in the even narrower niche of 'first-generation' **r**oom **t**emperature **i**onic **l**iquids, RTILs (such as chloro-aluminates and alkylammonium nitrates).[8–12] The situation has changed dramatically in 2000s after the discovery of new moisture- and temperature-stable RTILs.[13,14] These days, the 'later generation' RTILs attracted wide attention within the electrochemical community.[15–29] Indeed, RTILs, as a class of compounds, possess a unique combination of properties (high charge density, electrochemical stability, low/negligible volatility, tunable polarity etc) that make them very attractive substances from fundamental and application point of view.[30–36] Most importantly, they can mix with each other in 'cocktails' of one's choice to acquire the desired properties (e.g. wider temperature range of the liquid phase[37]) and can serve as almost 'universal' solvents.[35,38,39]

However, RTIL systems are far from a conventional 'text-book picture' describing an electrolyte (e.g NaCl aqueous solution) as small (atomistic) 'roundish' ions with *uniform* charge density on their surface dissolved in a large amount of solvent, interacting with each other via *long-range* Coulomb forces. On the contrary, there is no solvent in a neat RTIL electrolyte, unless it is deliberately added or they sorb water from the environment; neither the *molecular* RTILs ions are 'small' (on an atomistic scale) nor they are 'roundish'. To make things even more complicated, their molecular charge density is highly non-uniform.[40–44] But it is this complexity that makes them liquid at room and in some cases even much lower temperatures.[45] That means that the effects of *short-range* ion-ion interactions, molecular shape of ions and ion molecular charge distribution are very important for their properties both in the bulk and at interfaces. We also note that the large electrochemical window of many commercially available RTILs[11,15,46] allows one to achieve high electrode charge densities that are inaccessible for conventional (aqueous) electrolytes; and, therefore, several interesting effects that were considered mostly as a 'theoretical exotics' in the past can be

found now experimentally in RTIL-based systems.[47] This all makes the RTILs at electrified interfaces (EIs) to be an important field of research (and this view is justified by the ever growing number of publications on the subject).

There is a large number of known RTIL cations and anions readily available.[30,35,49,50] Moreover, as mentioned, many RTILs can be easily mixed with each other and with various organic and ionorganic polar solvents, giving practically infinite number of solvent-free or solvent-enriched electrolytes with tunable properties.[15,19,30,35,51] That makes the task of choosing the most optimum RTIL for any given application to be highly non-trivial. Therefore, the main goal of the article is to overview the main qualitative *trends* in the RTIL behavior at EIs in order to reveal the most important **factors** that determine their properties and behaviour there.

The fact that RTILs are far from conventional diluted electrolytes sets a number of challenges, both for theorists as well as experimentalists. To a large extent this is due to inapplicability of standard models (e.g. Gouy-Chapman theory) for theoretical studies of these systems and interpretation of experimental results on RTILs.[52] Not unrelated to this, RTILs attract the attention of not only chemists and applied scientists but also of theoretical physicists, based on purely fundamental grounds. Indeed, RTILs represent unique examples of highly concentrated, dense room temperature ionic plasma that exhibits strong 'Coulomb correlations',[53–55] the field lying at the frontier line of modern statistical mechanics.[56–58]

Each RTIL is an overall neutral assembly of charged particles. As the majority of their applications deal with their behaviour near interfaces[30–36] and, particularly, near electrified interfaces, understanding of the charge and electric potential distribution in RTILs at interfaces is crucial for understanding their performance as electrolytes.[61] This article is devoted to the discussion of the properties of RTILs at different electrified interfaces, in particular the RTILs response to charging the interface and how it manifests itself in a number of selected applications.

Response of electrolyte to a charged electrode surface is described within the so-called theory of electrical double layer (EDL). We will overview the current status of the theory of EDL in RTILs, showing that the structure of EDL there is dramatically different from that of a diluted electrolyte, although having certain common features with that of high temperature

molten salts, HTMSs (to avoid confusion, we will use this abbreviation or simply 'molten salts' below when we discuss *high temperature* ionic liquids).

It is well known that the EDL plays a crucial role in 'electrodics'.[2,59] The potential drop across in the EDL and its response to charging determines the electrical capacitance of the electrode/electrolyte interface, i.e. thereby the energy stored in the EDL capacitors. The potential distribution in the EDL controls electrochemical kinetics, because the voltage difference between the electrode and the point where the reactant (donor or acceptor of the electron) sits is the driving force of electrochemical reactions.[2,3,60,61] Since the electrochemical current depends exponentially on this driving force, even small changes in the value of the potential drop may change the current by orders of magnitude. Obviously, understanding the potential distribution in RTILs and its dependence on the applied potential that are both expected to be different from what they are in ordinary electrolytes, is a primary task for electrochemistry of RTILs.

Understanding the double layer properties is equally important for other applications. In electrowetting applications that use RTILs as the material of the organic droplet surrounded by aqueous electrolyte and lying at the electrode surface, the way how the droplet will change its shape with varying voltage of the electrode is determined by the potential distribution in the droplet.[62–65] In the recently discovered phenomenon of 'quantized' friction between spontaneously charged solid surfaces,[66] the lubrication capacity of the nano-layers of RTIL is determined by the distribution of ions between them.[66–70] In molecular gating applications of RTILs the current across a molecule which bridges two electrodes in a nanogap the EDL determines the ability to control independently the potentials of the two electrodes (relative to the reference electrode).[65] This list could be continued.

We will therefore devote a large part of this article to understanding the main properties of the EDL in RTILs. We start with the EDL at flat electrodes and then proceed to electrodes with enhanced, volume filling, surface area.

In many applications not only EDL equilibrium properties are important, but also the dynamics of its charging-discharging.[19,22,71–74] The dynamics determines the time response of the EDL capacitor, but this is not the whole story: impeded dynamics is accompanied by ohmic losses, and, thereby, worsened power delivery.[75] This equally refers to electroactuators

for artificial muscles (such a flashy name is often assigned to all electroactuators, although the whole muscle is a more complicated hierarchical construction),[76] as well as for sensor applications.[77,78] Ion transport dynamics also determines how fast the electrowetting lens will be changing its shape.[51] Not going into details of this yet poorly explored territory, we only briefly discuss main mechanisms of charge transport of ions in RTILs and some aspects of the EDL transient behaviour, as there are yet more questions than answers here, and the work in this area is in progress.

The review is organised as follows. We will start with the main principles of the EDL theory in RTILs, then proceed to (molecular-scale) computer simulations of RTILs at EIs , and then discuss recent experiments that investigate the validity of theoretical/modeling predictions. Clarifying this picture as far as we can, we will then overview some manifestations of the EDL in RTILs in the properties of the selected applications, such as EDL supercapacitors, electroactuators, electrode kinetics, extraction of metals, and quantized friction.

Trying to be as comprehensive as possible, we will nevertheless have to restrict ourselves to most recent developments, on former achievements referring the readers to earlier surveys (see e.g.[14–22,27]).The last note before we begin; this article is not a handbook: it overviews main principles and qualitative features rather than specific data. Some of those will be drawn in the context of ideas discussed in this review.

To set the scene, we start with a definition of RTILs and a brief overview of some of their pertinent physico-chemical and electrochemical properties, to which we will sporadically refer later in the review.

2 RTILs and some of their properties

2.1 What to we imply by RTILs? The *main* features and applications.

The commonly accepted definition of Room Temperature Ionic Liquids these days can be formulated as follows: RTILs are materials that are composed solely from anions and cations

and melt at or below 100-150°C.[17,30,35,50,79] In the following we will use this (broad) definition, if not stated otherwise. In this section we only briefly overview some pertinent properties of RTILs because there is a number of excellent reviews on this subject already in the context of synthesis and catalysis,[35,50,79] industrial applications[30,33] etc.[36,80,81] A short but comprehensive overview of the history of the subject can be found in the Wilkes' 2002 review.[82]

The first accounts of RTILs is commonly attributed to Walden, who reported in 1914 synthesis and characterisation of a new organic salt, ethylammonium nitrate, that was liquid at room temperature (m.p. 12°C).[83] However, analysis of the literature shows that the discovery date of the first RTIL as well as the names of discoverers might be disputed.[30,82] E.g. Gabriel and Weiner reported in 1888 a new organic salt, ethanol-ammonium nitrate with m.p. 52-55°C;[84] (for more historical details we address the readers to Refs[30,82]). Later on in 1930s and 1940s several other RTILs were discovered[85] that were mixtures of alkylpyridinium-based organic salts (halides) with aluminium (III) chloride.[8] Since then there were several attempts to explore this intriguing class of substances,[86,87] particularly by electrochemists[88] that soon recognized an enormous potential of RTILs as 'electrolytes without solvent' (or only with minor solvent additives) for applications in batteries,[89] supercapacitors and electrodeposition.[8]

In 1980s Wilkes and Hussey with co-workers discovered that alkylimidazolium halogenoaluminates[90] have much larger liquid range than alkylpyridinium halogenoaluminates and these RTILs are more stable in terms of reduction of the alkylimidazolium cation.[90–98] In parallel with the research on halogenoaluminate-based RTILs, several groups explored other low-temperature molten salts known by that time such as tetra-n-alkylammonium-based RTILs and alkylammonium nitrates and thiocyanates.[16,99]

However, until mid 1990s, research on RTILs was somewhat outside the mainstream of electrochemistry due to various problems with synthesis and purification of the 'first-generation' RTILs that resulted in high costs of these compounds. Moreover, most of the first-generation RTILs (e.g. alkylimidazolium/alkylpyridinium halogenoaluminates) are very sensitive to moisture and have difficulties with regulation of their acidity/basicity.[90,100] Therefore, until recently the main focus in electrochemistry of concentrated ionic fluids

(particularly in 50s-70s of the past century) was in high temperature ionic liquids - the molten inorganic salts (m.p. 300-1000°C) and their applications in metal production processes.[5,101,102]

A 'rediscovery' of RTILs two decades ago was mainly due to (i) discovery of RTILs with stable organic anions (such as PF_6-, BF_4-, and, $[(CF_3SO_2)_2N]$-) in 1990s[13,103] and (ii) breakthroughs in organics synthesis of RTIL components that reduced their costs (such as e.g. the Biphasic Acid Scavenging Utilizing Ionic Liquids (BASIL) process introduced by the BASF company in 2002[104]). This was followed by an exponential explosion of interest to RTILs with thousands of papers published annually on various aspects of their chemistry and physics. For enthusiasts of metrics in science one can draw just one illustrative figure: according to the ISI Web of Knowledge, in 2012 the overall number of papers published on the subject 'ionic liquids' during only this year was around 10^4. The enormous 'popularity' of RTILs is related to their unique properties and the vast number of applications that are already employing RTILs or can potentially employ them in the future.[30,33,36,105]

Following Stark[106] the 'chemical space' of functional variations of RTILs can be represented as a three-dimensional domain with anions, cations and their (chemical) functional groups as (generalised) coordinates (see Figure 1).

The features of RTILs that make them special are, briefly, as follows:

- Unlike molten salts composed of small, 'roundish' inorganic ions, the ions of RTIL are ordinarily large organic ions (at least one of them – usually the cation), containing substantial amount of hydropobic constituents[35,79] (see Figure 1). They often have anisotropic and asymmetric shapes. These two features, that principally differ them from molten inorganic salts, reduce the freezing temperature of the liquid: the Coulomb interactions are weaker in the range of their action, whereas their complicated shape does not let the RTIL ions easily acquire stable ordered crystal structures.[45]

- RTILs are electrolytes without solvents staying liquid in a broad temperature interval around the room temperature.[11,107]

- Still, strongly kept together by electrostatic interactions of cations and anions, many RTILs have low or ultra-low volatility.[48,49,108–111]
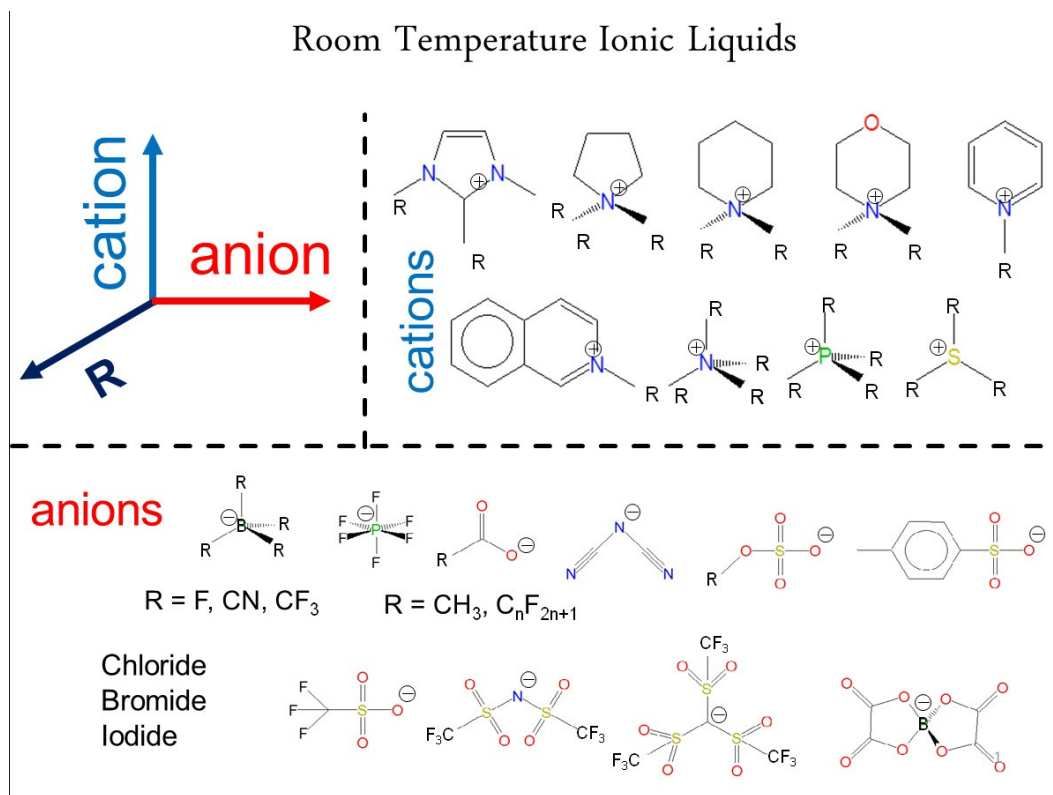
Figure 1: General representation of the the 'chemical space' of functional variations of RTILs. **R** states for the functional group. Most popular choice for **R** is the alkyl substituent $CH_3(CH_2)_n$ ($n = 1, 3, 5, \dots$); there are also many other choices available.[35,79] The layout of the figure was inspired by Fig. 1 in Ref.[106]

- Those RTILs that a composed from less reactive ions are more inert electrochemically than many standard electrolytes; i.e. as solvents at electrodes they can sustain higher voltages before their electrochemical (and thermal[213]) decomposition.[11,46,107,113–118]

- Different RTILs can be mixed with each other and one can make 'cocktails' of them.[38,39] Moreover, RTILs can be slightly diluted by adding to them organic dipolar solvents.[119,120] The resulting mixture can be called a designer solvent, as it can be adjusted to provide targeted functions for reactions of substances dissolved in them.[35,50] Since thousands of RTILs has been or can be synthesized, the discovery of RTILs made a revolution in chemistry: one in principle can have practically unlimited number of solvents and electrolytes, whereas in the past they all could be counted.[3,121]

Calling RTILs green electrolytes is more of a wishful thinking[122–124] as quite many of them are not green at all,[125,126] some are toxic[127,128] and hazardous,[129,130] and most of them

are difficult to wash away.[131] But the other listed properties make them very promising in various applications (we focus on those applications where interfacial and electrical double layer properties of RTILs are important).

What are these? They can be used as:

- designer solvents for homogeneous and surface catalysis and synthesis.[35,50,132]

- extraction liquids for purification of metals,[133] proteins and colloids[30] and biomass conversion;[134,135]

- media for electrochemical reactions, electrocatalysis, and electrodeposition;[11,15,16,19,136–140]

- electrolytes for power sources and generators, such as supercapacitors,[37,72,73,141–144] batteries,[113,118,145,146] solar cells,[147–151] and, prospectively, fuel cells (once RTILs with high proton conductance will be found);[152]

- liquids for electrowetting based variable lenses and microfluidics applications;[153–155]

- lubricants, from macromechanisms to micro and nanodevices;[66,68,70,156,157]

- the organic liquid component for self-assembled nanoplasmonic devices;[158]

- electronic gating media for single molecule devices[159,160] and electrolyte-gated transistors for organic and printed electronics[160–164] and superconductors;[165]

- chemical and electrochemical sensing;[21,166,167]

The list could be continued but these are those applications that are clearly seen now.

2.2   A closer look at *some* of RTILs'properties

In this section we will provide a brief (and non-extensive) overview of several main properties of RTILs focusing on those that are important for understanding their behaviour at EIs. Emphasis is set on a few examples of commercially available RTILs that are frequently used in experimental and simulations studies of electrical double layer and various applications. For extensive reviews of RTIL properties we refer the readers to the following databases, books and essays.

- A large collection of *thermodynamical, thermochemical* and *transport* properties data of RTILs and their mixtures is given in the IL Thermo database.[168] There is also recent critical review by Aparicio et al[169] on thermo-physical properties of new RTILs that analyses different experimental methods for measuring thermophysical properties and possible sources of errors.

- Book of Zhang et al "Ionic liquids: physicochemical properties".[170] To the best of our knowledge this is the most extensive handbook on physico-chemical properties of ionic liquids currently available (the book was preceded by an earlier publication by the same group of authors[171]). The book contains a large database of physical properties of ionic liquids[172] including density, viscosity, phase transition temperatures, thermal decomposition temperature, polarity and the electrochemical window.

- The 2005 compiled book "Electrochemical aspects of Ionic Liquids" edited by Ohno[17] provides a large amount of data on electrochemical behaviour of RTILs. The book also provides good introduction to the subject and contains many innovative ideas that were later developed by the authors of the contributed chapters and other groups.

- The 2008 complied volume "Electrodeposition from ionic liquids" edited by Endres, MacFarlane, and A. Abbott[173] provides a good introduction to electrochemistry of RTILs and contains a large amount of information on relevant electrochemical and physical-chemical properties that might be difficult to find elsewhere.

- The 2008 review by Hapiot and Langost on electrochemical reactivity in RTILs[140] that discusses different physical and electrochemical properties of RTIL-based system in a view of their applications as reactive media for electrochemical reactions at interfaces. See also the Chapter 4 in the review by Yoshida et al[139] on modern strategies in electroorganic synthesis that also discusses applications of RTILs as reactive media for electrocatalytic reactions.

To overview the typical *ranges* of main properties of RTILs that are relevant to the subject of the article we provide here an updated and extended version of the Table 1 from the 2010 review of RTIL applications in chemical engineering by Werner, Haumann and

Wasserscheid.[33] Several important properties of RTILs are also discussed in more details below.

Table 1: Typical ranges of RTILs properties.*

Property	Lower limit example	Typical values for most of RTILs	Upper limit example
Melting Point/glass transition	[EMIM]Cl/AlCl$_3$ = (1:2) = $-96\,^\circ$C (glass transition)	$0\,^\circ$C - $60\,^\circ$C	$100-150\,^\circ$C depending on the defenition of RTILs
Density	[HMPyr][N(CN)$_2$] = 0.92 gL^{-1}	1.1 - 1.6 gL^{-1} $^{(i)}$	[EMIM]Br-AlBr$_3$:1/2 = 2.2 gL^{-1}
Viscosity	[EMIM]Cl-AlCl$_3$:1/2 = 14mPa s$^{(i)}$	40-800 mPa s$^{(i)}$	[BMIM]Cl (supercooled) = 40.89 Pa s$^{(i)}$
Thermal stability	[EMIM][OAc] = $\sim 200\,^\circ$C$^{(ii)}$	$230\,^\circ$C-$300\,^\circ$C$^{(ii)}$	[EMIM][TFSA] = $400\,^\circ$C$^{(ii)}$
Surface tension	[C$_{12}$MIM][PF$_6$] = 23.6 mNm^{-1}	30-50 mNm^{-1}	[MMIM[MeSO$_4$] = 59.8 mNm^{-1}
Heat capacity	[BMIM][MeSO$_4$] = 247 Jmol^{-1}K^{-1}	300 to 400 Jmol^{-1}K^{-1}	[OMIM][TFSA] = 654 Jmol^{-1}K^{-1}
Water miscibility	[TFSA]$^-$, [P(C$_2$F$_5$)$_3$F$_3$]$^-$	many ILs do not mix with water but also can be extracted from water	[RSO$_3$]$^-$, [RSO$_4$]$^-$, [R$_2$PO$_4$]$^-$
Hydrolytic stability	[BF$_4$]$^-$, [PF$_6$]$^-$	heterocyclic cations can hydrolyze under extreme conditions	[TFSA]$^-$, [OTf]$^-$, [CH$_3$SO$_3$]$^-$
Base stability	[Al$_2$Cl$_7$]$^-$, [HSO$_4$]$^-$	all 1,3-dialkylimidazolium RTILs are subject to deprotonation	[PR$_4$]$^+$, [OAc]$^-$
Corrosion	[TFSA]$^-$, [OTf]$^-$	most RTILs are corrosive versus Cu; additives available	Cl$^-$, HF formed from [MF$_x$]$^-$ hydrolysis
Toxicity	[cholinium][OAc]	often increasing toxicity for aquatic systems with increasing lipophilicity	[EMIM][CN]
Static dielectric constant	[HMIM][PF$_6$]=8.9[174]	10-15[174,175]	(2-hydroxyethyl)ammonium lactate=85.6 ± 3[175]

*Large part of the table is reproduced from Ref.[33] (Table 1 there); data taken from the Ref.[33] and references therein if not specified otherwise. The abbreviations in the table are as follows [EMIM]: 1-ethyl-3-methylimidazolium, [HMPyr]: 1-hexyl-1-methyl-pyrrolidinium, [BMIM]: 1-butyl-3-methylimidazolium, [C$_n$MIM]: 1-alkyl-3-methylimidazolium, [TFSA]: [(CF$_3$SO$_2$)$_2$N]-, [BMMIM]: 1-butyl-2,3 dimethylimidazolium.
$^{(i)}$ At room temperature.
$^{(ii)}$ TGA experiments at 10 K min^{-1}.

2.2.1 Thermophysical parameters

Most RTILs at normal atmospheric pressure stay in the liquid state up to temperatures as high as 200-300 °C where water and the most common organic solvents already evaporate.[169] Due to the strong ion-ion interactions, volatility of RTILs is typically very low.[49] Therefore, in principle, RTILs themselves could also withstand high operation temperatures in energy storage devices.[179] However, if these are double layer supercapacitors, elevated temperatures[180] can activate undesired electrochemical reactions,[213] involving RTIL ions both at cathodes and anodes, which will narrow down the window of electrochemical stability of RTIL (see also discussion below).

We note that at temperatures higher than 200-300 °C most RTILs start to decompose; moreover, the RTIL thermal decomposition process can generate flammable and toxic gases.[36,80]

Following to Aparicio, Atilhan and Karadas,[169] the melting point of ionic liquids depends on a balance between cation and anion symmetry, flexibility of chains in the ions, and charge accessibility. Increasing the length of alkyl chains in the cations and/or increasing the anion size generally leads to decrease in the RTIL melting points.[168,169,181]

We note that there are already available quite advanced procedures for predictions of melting points and thermodynamic stability of RTILs,[182] (as well as other thermophysical parameters, see Ref.[183]); however their usage is still not widely applied in the field. As was pointed by Coutinho, Carvalho and Oliveira in their recent review on predictive models for thermophysical and transport properties of pure RTILs,[184] the major problems in development of a reliable model for predicting thermophysical properties of RTILs are that "many ILs do not have a melting point, that the boiling temperatures of the ILs are as elusive as their critical temperatures, and consequently that the uncertainties associated with those estimates are necessarily very large."[184] That correlates with opinions discussed in a recent critical review by Aparicio, Atilhan and Karadas on experimental methods for measurements of thermophysical properties of RTILs.[169]

2.2.2 Transport properties

As was mentioned in the Introduction, transport properties of RTILs directly affect performance of RTIL-based electrochemical applications.[185] In fact, high viscosity and low diffusion of ions of most of electrochemically stable RTILs are the main bottlenecks in the development of electrochemical applications of RTILs in energy storage and electrodeposition areas. Indeed, at room temperatures viscosity of RTILs varies between 20-40,000 cP[30] (compare with viscosity of standard solvents that varies in the range of 0.2-100 cP). Even low-viscous RTILs have viscosity around 20-30 cP at room temperatures[186] that is an order of magnitude higher that viscosity of water at these temperatures ($\sim$1 cP)[30] and molten inorganic salts at high temperatures (1-3 cP).[55]

Transport properties of RTILs are also of considerable fundamental interest to liquid and soft matter scientists due to a large number of intriguing phenomena there.[187,188] For example, experimental results on ion mobility in RTILs show that small anions have a reduced mobility compared to (much larger) cations;[187,189,190] this interesting counterintuitive phenomenon can be explained by their stronger solvation by the counterions. Many RTILs show also non- Arrhenius behavior of kinetic coefficients.[191]

Following Kowsari et al[192] the main factors that determine the magnitude of self-diffusion in imidazolium-based RTILs are the ion size, the geometric shape of the RTIL anion and the charge delocalization in the anion. Tsuzuki in his recent mini-review[193] summarized the main factors controlling the diffusion of ions in ionic liquids and their mixtures: the size and shape of ions; the magnitude of interaction between cation and anion; conformational flexibility; molecular mass of ions; solvent additives, and the effects of formation local nanostructures. See also the work by Okoturo and Van der Noot[191] that discusses several molecular-scale factors influencing the viscosity of RTILs. An overview of transport properties of common RTILs can be found in the Galinski et al review on RTIL-based electrolytes.[11]

In general, viscosity of RTILs decreases with the increase of the size of ions and temperature.[184,194] Also, Krossing and co-workers observed that for a given class of RTILs the viscosity and conductivity of RTILs have strong dependence on the RTIL molecular volume.[195,196] Vila, Varela and Cabeza performed systematic experimental study of the conductivity of nine

different imidazolium-based RTILs with BF$_4$-anion and its dependence on temperature.[197] They found that the values of the electrical conductivity decrease value as the alkyl chain of the studied cations increases. The authors of this work also studied effects of anions on the conductivity of EMIM-based RTILs, systematically varying the anion size.[197] They found that there is an optimum size of anion (that correspond to BF$_4$-) where the conductivity reaches its maximum value (15.71 mS cm^{-1} at room temperature for [EMIM][BF$_4$]).

First-generation chloroalumiate-based RTILs usually show low viscosity and high ionic conductivity compared to the hydrophobic RTILs based on large hydrophobic anions (e.g. TFSA);[191,201] therefore, chloraluminates and halogen-based other RTILs have favorable electrochemical properties for processes like electrodeposition that stimulates researchers to continue to investigate these substances (e.g. in a view of developing electroplating applications)[12,202,203] despite several issues with stability and large hydrophilicity of chloroaluminate-based RTILs (many of them dangerously react with water especially at higher Lewis acidity).[30] It should be noted, however, that it is more difficult to prepare a high-purity hydrophilic RTIL than a hydrophobic RTIL.[173,201]

In the context of comparing viscosities of different classes of RTILs we also would like to refer to the research paper of Okoturo and Van der Noot[191] that presents thorough investigation of the absolute viscosity behaviour of ten air/moisture-sensitive acidic chloroaluminate-based RTILs and thirteen air/moisture-tolerant RTILs. They reported that "the Arrhenius plot was not linear for the majority of the RTILs and some of these RTILs were better fitted with the Vogel-Tammann-Fulcher (VTF) equation. Those RTILs which obeyed the Arrhenius law typically contained asymmetric cations and the majority did not contain functional groups. Those RTILs which obeyed the VTF law contained small and symmetrical cations with low molar mass. Those RTILs which obeyed neither the Arrhenius nor the VTF law consisted of cations which were less symmetric, contained functional groups (e.g., OH and C=O) and had higher molar mass. The glass transition temperatures T$_0$ (calculated from the VTF fittings) generally decreased with increasing size and molar mass of the cation and anion. The chloroaluminate RTILs containing oxygenated cations were more volatile than the corresponding de-oxygenated RTILs making them unsuitable for applications as solvents and/or electrolytes above ambient temperature."

16

We also note that slow dynamics of most RTIL systems poses a challenge to modelling transport and dynamic properties of RTILs.[188] In general, molecular simulations of RTIL systems require specific adjustments of standard molecular models and force fields; otherwise, the calculated values of diffusion coefficients, viscosity and ionic conductivity can be far from even qualitative correlations with experimental data.[198–200]

Due to the high viscosity and low ion mobility, neat RTILs have low conductivity (in spite of high concentration of charge carriers) that is in the range of 0.1-18 mS cm^{-1},[107] which is much lower than the conductivity range for conventional aqueous electrolytes applied in electrochemistry that is around 400-800 mS cm^{-1}.[11] Conductivity at the level of 10 mS cm^{-1} is typical for ionic liquids based on the [EMIM]+ cation (14 mS cm^{-1} for [EMIM][BF$_4$]). RTILs based on such cations as pyrrolidinium or piperidinium show lower conductivities that are at the level of 1-2 mS cm^{-1}. We note that dissolution on Li+ ion in neat RTILs increases their viscosity and lowers conductivity.[107]

In many electrochemical applications RTILs are mixed with organic solvents (mostly acetonitrile and propylene carbonate) to decrease viscosity and increase conductivity.[204,205] Such, [EMIM][BF$_4$] mixture with acetonitrile at the concentration of 2 mol/dm solution in acetonitrile shows a conductivity of 47 mS cm^{-1} (compare with the conductivity of the neat [EMIM][BF$_4$] that is 14 mS cm^{-1}).[11]

2.2.3 Dielectric properties

Ionic liquids are conductive, so strictly speaking their static dielectric constant is infinite, because they will fully screen an electric field which will penetrate into the liquid within the range of its short range structure.[207,208] But there are many other degrees of freedom than those of the translational motion (rotational, vibrational etc); these degrees of freedom contribute to polarizability of the liquids at different frequencies.[190] Thus the term 'static dielectric constant' must be used with care, assuming that it encompasses the contribution of all the polarization active modes, such as polarizability of atoms, vibrations of ionic pairs and decaying phonon modes, librations and rotations of ion pairs and larger ionic clusters. Since the translational motions of ions in RTILs are strongly coupled to many of these modes, it makes the measurement of the 'static dielectric constant' of RTILs

challenging.[174,209] The most popular method for determining the static dielectric constant values is different dielectric relaxation spectroscopy techniques.[79,174–176] We note, however, that several other parameters and techniques are used in the general context of determining RTIL polarity such as Kosower's Z values determined by the charge-transfer absorption band of 1-ethyl-4-(methoxycarbonyl)pyridinium iodide,[177] and the Kamlet-Taft solvent parameters[178] (hydrogen-bond acidity (α), hydrogen-bond basicity (β), and (particularly) dipolarity/polarizability π^*); see extended discussions on this subject in Refs.[174,209,210]

According to Refs.[79,174,175] static dielectric constants of different RTILs vary in the range of 7 to 85 with many of widely used RTILs having the dielectric constant around 10-15. The work of Kobrak[174] shows interesting trends in relationships between the dielectric response of RTILs and the molecular structure of RTIL ions. Kobrak pinpoints that "if a high dipolarity/polarizability is desired for a certain task, the liquid should either (1) incorporate very small ions, or (2) incorporate ionic structures that frustrate the formation of nanoscale domains." From another side we would like to cite in this context the recent work of Choi et al[176] on imidazolium acrylates and methacrylates and their ionomers. Using dielectric spectroscopy, they shown that polymerization of ionic liquids can significantly enhance their static dielectric constant (they report values as high as ~ 140 at room temperature). They explain this effect by synergistic dipole alignment of long polymer segments in response to the external field.[176]

2.2.4 Electrochemical Stability

For electrochemical applications of RTILs, their stability at charged interfaces is of special interest. Electrochemical window (EW) is usually defined as the operating potential range or the difference between the maximum oxidation and reduction potentials for a given solvent-electrode system. In many modern applications of RTILs (batteries, supercapacitors, electrocatalysys, electrodeposition etc), there is a strong need for ionic liquids that electrochemically stable at as wide as possible potential range (we will discuss this in more details below). Most of commonly used RTILs have much higher electrochemical windows (up to 5-6 V but typically about 2-3 V) than aqueous electrolytes (see[107,211]). A large collection of data on electrochemical windows of many RTILs at different electrodes can be found in

Refs.[26,46,170,173,212]

Lane recently overviewed main mechanisms of electroreduction of RTIL cations.[212] Following this review, the best estimates of maximum cathodic stabilities for main types of RTIL cations can be arranged as pyridinium<sulfonium<1,2-dialkylimidazolium<1,2,3-trialkylimidazolium<morpholinium<phosphonium <quaternary ammonium (see Fig.16 in Ref.[212]) with the cathodic limit of -2.7V for phosphonium and quaternary ammonium cations. A comprehensive study of Hayyan et al[46] summarises the electrochemical stability of cations of as follows: $[P_{4,666}]+ > [N_{112,102}]+ > [HMpyr]+ > [EMIM]+ > [MOEMMor]+ = [MOPMPip]+ > [S222]+ > [BMPy]+$. The oxidative limits for anions reported in this paper were found to follow the sequence of $[TFSI]- > [TPTP]- > [TfO]- > [DCA]- > [TFA]-$.[46]

Moreover, a recent work by Fletcher et al[213] reported two RTILs with electrochemical windows at the platinum electrode to be as high as 8-9 V, hexyltriethylammonium bis(trifluoromethylsulfonyl)imide ([HTE][TFSI]) and butyltrimethylammonium bis(trifluoromethylsulfonyl)imide ([BTM][TFSI]). The authors of the work[213] also discuss some observed trends in relationships between the ion geometry and their electrochemical stability and melting point. Such, they find that increasing the chain length of the alkyl groups leads to improved chemical inertness of the RTIL ions. They also note that decreasing the symmetry of the quaternary ammonium cations lowers the melting points of the corresponding ionic liquids (see also discussions on relationships between the molecular structure of RTIL ions with their melting points and other transport and thermophysical properties in[35,50,214]). These results need verification by other groups and tests that such enormous enhancement of electrochemical stability is not an artifact related to formation of passivation layers on platinum electrodes. However, if approved, it could open new avenues towards development of RTILs of exceptional electrochemical stability.

Naturally, the electrochemical window of a particular RTIL strongly depends on the type of electrodes used.[173] A good summary of types of electrodes that have been used in conjunction with RTILs is given by Endres et al.[173] Following this source as well as analysis of the literature data,[26,107,170,211] one may conclude that for fundamental studies of RTILs at EIs most popular electrodes are made from Au, Hg and Pt due their stability. Au and Pt electrodes are also used in analytical and sensor applications of RTILs.[215] However, a

recent work of Lust and co-workers attracted attention to potential use of Bi electrodes for fundamental studies on RTILs as well as applications.[216] Indeed, Bi electrodes have certain advantages: their costs are much less than for Au and Pt electrodes, they are much less toxic than then Hg electrodes, they are stable and operationally efficient.[217] From another side, it was shown that copper electrodes sufficiently decrease elecrochemical stability of RTILs with fluorinated ions.[218]

There has recently been great interest in RTIL properties at the interface with carbon-based electrodes (amorphous carbon, graphite, carbide-derived-carbon, carbon cloth, nanocarbon composites etc)[27,179,219–222] due to large amount of current and potential applications of these materials (see more detailed discussion on this subject later on in the manuscript).

For ions in aqueous solutions, surface charge densities between -40 to +80 μC/cm^2 have been reported.[223] The determination of experimentally accessible electrode charge densities in RTILs is rather difficult. Upon considering the area under an experimentally measured capacitance/potential-curve starting from the potential of zero charge, the surface charge density can be roughly estimated[224] that shows that for the spherical ion PF$_6$- at a Au(111) electrode, the surface charge density can be as high as +30 +40 μC/cm^2.[225] In their recent work Costa, Pereira and Silva[226] reported that the surface charge densities for different imidazolium-mased RTILs and their mixtures at a Hg electrode can be as high as -/+ 25 μ C/cm^2 for a potential window of ~ 2.5 V. Therefore, we anticipate that for RTILs with higher electrochemical windows the cathodic/anodic limits for the electrode charge density could be at least around -40/+50 μC/cm^2. The cathodic upper values are comparable with the surface charge density on muscovite mica that has a fixed layer charge of around -32 to -34 μ C/cm^2.[73,227,228]

Even a small amount of water impurities (as well as some other additives) have a profound effect on electrochemical stability of RTILs at EIs. Such, it was shown in Ref.[229] than even a small amount of water intake from atmosphere significantly decreases electrochemical window for several types of RTILs. Because even hydrophobic RTILs absorb some minor amounts of water from the atmosphere[229] this issue becomes important both for fundamental studies of RTILs at EIs[230,231] as well as for developing applications.[130,232]

3   EDL before RTILs

The first concepts of EDL were developed a century ago in the context of ordinary inorganic electrolytic solutions.

The earliest model for EDL was suggested by Helmholtz in 1853.[233] In this model the EDL is described mathematically as a simple, plane dielectric capacitor, assuming that the counter charge of ions forms the second plate of the capacitor, oppositely charged with respect to the first plate - the electrode. This picture corresponds to a single layer of ions driven to the surface by the electric field of the electrode and totally screening it. Helmholtz model did not imply any space charge of ions behind that layer. Presumably because of the Helmholtz model, the mere term *double layer* (sometimes quite confusing, because the EDL is normally not one layer thick) has forever established itself in the scientific literature. In the Hemholtz model, the electrostatic potential drops linearly between the electrode and electrolyte, and the whole drop is confined between those two plates. The capacitance of such EDL is just the same as of a macroscopic capacitor and it is given as

$$C = C_H = \frac{\epsilon^*}{4\pi d},\tag{1}$$

where d is the distance between the plates and ϵ^* is the effective dielectric constant of the medium between them (note that throughout the paper all electrostatics related equations, will be consistently written in Gaussian system of units[234]). With $d = 0.5$nm and $\epsilon^* = 5$ for a water layer with 'frozen' orientational polarizability with only librations allowed, one gets $C = 8.5 = \mu\text{F/cm}^2$ which is of the order of the typically measured capacitance of inorganic electrolytes.

However, in real systems the EDL is (generally) not one layer thick because of entropy: thermal disorder does not allow all counterions to gather on a monolayer-thick plane. Instead, a space charge of ions forms at the polarized interface, which was clarified half a century later. French physicist Gouy has pioneered a theory of such space charge in 1909-1910[235,236] and British physical chemist Chapman in 1913 developed it in a form that we now call the Poisson-Boltzman theory of diffuse EDL, or the **G**ouy-**Ch**apman theory (GCh theory). The distribution of counterions in the GCh theory is smeared within the so-called Gouy length,

λ_G, the value of which is found self consistently and it depends on the potential drop across the EDL, U. For 1-1-electrolyte, using modern notations, this expression reads as follows

$$\lambda_G = \frac{\lambda_D}{\cosh(u/2)} \quad , \quad u = \frac{eU}{k_B T} \quad , \quad \lambda_D = \sqrt{\frac{1}{8\pi L_B c_0}} \quad , \quad L_B = \frac{e^2}{\epsilon k_B T}. \tag{2}$$

Here $u = eU / k_B T$, i.e. it is the potential drop across the double layer measured in the units of the so called 'thermal voltage', $k_B T/e$ where k_B is the Boltzmann constant, T is the absolute temperature and e is the elementary charge; at room temperature $k_B T$ $e=0.0256$ V/e, usually memorised as $25 mV$. λ_D is the Debye length expressed here through the Bjerrum length, L_B (the length at which the energy of the Coulomb interaction of two elementary charges in a dielectric medium with a macroscopic dielectric constant ϵ is equal to the thermal energy $k_B T$), and the bulk electrolyte concentration. Note that it is nowadays that we express the Gouy length, λ_G, through the Debye length, λ_D; whereas λ_D itself was introduced by Debye and Hückel a decade later[237] with, however, a reference to the Gouy paper.

As a function of the electrode surface charge density σ, the Gouy length reads as

$$\lambda_G = \frac{\lambda_D}{\sqrt{1 + 4\pi^2 L_B{}^2 \lambda_D{}^2 (\sigma/e)^2}}. \tag{3}$$

The Gouy length turns into the Debye length at small voltages, $u \to 0$, $\lambda_G \to \lambda_D$; at large voltages, $u \gg 1$, $\lambda_G \approx 2e^{-u/2}$, i.e. λ_G becomes exponentially small with increasing electrode polarization; as a function of the electrode charge at large charges it, however, diminishes only hyperbolically as $\lambda_G \approx \frac{1}{2\pi L_B |\sigma/e|}$. Hence the differential capacitance of the diffuse EDL,

$$C = C_{GC} \equiv \frac{\epsilon}{4\pi \lambda_G}, \tag{4}$$

has a U-shape (Figure 2), growing *unlimitedly* with the electrode polarization regardless of its sign, in contradiction to experiments in which the capacitance always levels off at large voltages.

It was clear that the GCh theory should break down at large voltages, as long as the estimated Gouy length approaches the diameter of the ion or even earlier. Indeed, the Gouy
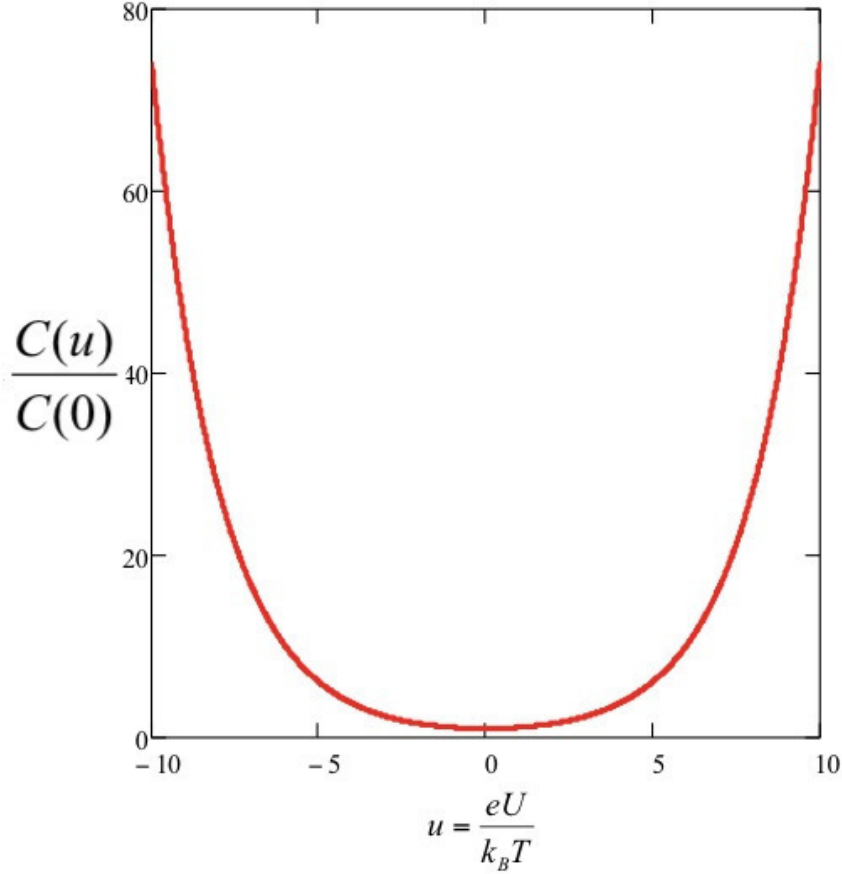
Figure 2: The U-shape of the capacitance predicted by the Gouy-Chapman theory (eq 4).

length diminishes unlimitedly, because there is no finite size of ions or any discreteness scale in the Gouy-Chapman theory.

An attempt to introduce such discreteness effect was made by Stern,[238] motivated in the first place by that controversy. To avoid the unlimitedly large capacitances of the EDL, contradicting experimental observations, he introduced a 'cut-off', having added a compact layer capacitance, the analogue of the Helmholtz capacitance, in series to the Gouy-Chapman capacitance, such that

$$\frac{1}{C} = \frac{1}{C_H} + \frac{1}{C_{GC}(u(u_{tot}))}. \tag{5}$$

In the Gouy-Chapman-Stern model, the potential drops down linearly within the compact layer, and then decays quasi-exponentially in the diffuse layer. Generally the overall potential drop u_{tot} splits into two parts, u_{tot} - u across the Stern layer and u across the Gouy-Chapman diffuse layer. The value of $u(u_{tot})$ must be found subject to the values of C_H and C_{GC},

according to the equation:

$$U = \frac{V}{1 + \frac{K_{GC}(u)}{K_H}},$$ (6)

where the symbol K stands for the integral capacitance, defined as the ratio of the minus-charge accumulated in the compact layer (equal to the charge of the electrode) to the voltage drop across the layer minus its value at zero charge, i.e. **p**otential of **z**ero **c**harge (p.z.c). The integral capacitance is related to the differential one as:

$$K = \frac{1}{u - u_0} \int_{u_0}^{u} C(u')du' = \frac{\sigma}{\int_0^{\sigma} \frac{1}{C}d\sigma}$$ (7)

where u_0 is the pzc.

However, for moderate electrode polarizations (and not too high ion concentrations) the original GCh theory (eq 2 and 4) has proved to work very well. Therefore, it became a background of many estimates not only in electrochemistry but also in colloid science and biophysics.[239–244] Practically every textbook starts the introduction of the principles of EDL from the GCh theory. The latter suggests that the minimum of capacitance in solution without specifically adsorbing electrolyte coincides with p.z.c, at least in dilute electrolytes where the diffuse layer capacitance dominates the total one in a wide range of electrode potentials. This has offered an easy method for estimating the value of p.z.c for different electrode/electrolyte interfaces. More involved methods have also been developed,[245,246] but the early one still remains to be one of the easiest and most reliable.

For large electrode polarization and not too dilute electrolytes, it is the compact layer that determines the capacitance. That contribution has been evaluated from experiments by drawing the so called Parson-Zobel plots,[247] namely showing the experimental values of the inverse capacitance $C^{-1}_{experimental}$ vs. the calculated inverse Gouy-Chapman capacitance C^{-1}_{GC}, at varied electrolyte concentrations. If eq 5 is valid and the value of C_H does not depend on electrolyte concentration (the so called 'Graham ansatz', for review see[2]), one must get a straight line with the intercept in the limit of high concentrations, usually extrapolated, giving the value of C^{-1}_H. Such lines can be plotted for different electrode polarizations and, notably, C_H assessed in this way usually revealed strong dependence on

the charge of the electrode voltage.[2,248]

Hence, many models were proposed to describe the nonlinear polarization of the compact layer, for review see monographic articles.[248,249] These models spanned from descriptions of the monolayers of solvent molecules at the interface, adsorption-desorption of organic molecules if present in the solution, to the profiles of the electronic excess charge density at electrodes and even surface reconstruction.[2,250]

Most importantly the Graham ansatz is valid only in the absence of specific adsorption of ions. An extension of the theory that takes into account effects of the specific ion adsorbtion has been made first by Graham and Parsons,[5,251,252] and a review of further developments can be found in the Vorotyntsev's monographic chapter.[253]

Much effort was devoted later on to develop a unified theory of EDL without distinguishing compact and diffuse part, either on a phenomenological level[248,254,255] or on the molecular level considering ions and solvent molecules on the same footing.[4,256–258] The upshot of those studies is that in the systems without specific ionic adsorption, there is a contribution to capacitance that is independent of electrolyte concentration. Therefore, the apparent compact layer contribution appears automatically upon incorporation of the structure of the solvent into the theory. We refer the reader to the corresponding reviews mentioned above; the progress along those lines for the cases when the ions adsorb specifically was also reviewed in detail.[248]

In the last few years we witness a renaissance in developing more sophisticated statistical mechanical or extended mean-field models for the EDL within the so called restrictive primitive model of electrolytes (charged hard spheres in a background with a constant dielectric permittivity), which we will selectively cover in sections to follow later in the review in the context of potential applications to RTILs.

For the subject of this article, we will need first to focus on one direction in this research area. Conceptually, one of the main weaknesses of the GCh theory is the neglect of the finite size of ions (that allows them to accumulate at large voltages at any concentration at the electrode). Such, 1999 simulation work of Boda, Henderson and Chan[259] showed that the GCh theory fails to reproduce the qualitative behavior of the electrical double layer capacitance of high-temperature molten salts where the effects of the finite ion size

25

are important. However this drawback usually does not manifest itself in the theory of ordinary (diluted) electrolytic solutions. With increase of the voltage, long before the ions will start 'feeling' their excluded volume, electrochemical reactions involving these ions or solvent at the corresponding electrodes will take place. For this reason the pioneering works that were devoted to the inclusion of the excluded volume effects in the EDL theory[260–264] did not receive enough credit and attention in electrochemical community (as well as some follow up literature that also missed to notice those works;[265–267] more detailed exploration of the history of this subject and more references of this kind one can find in Ref.[268]). All these works were rediscovered only recently in the context of such highly concentrated ionic systems as RTILs or in microfluidics, where the effects of the finite size of ions start playing important role at voltages below the onset of electrochemical reactions. In fact, several results from these works were independently reproduced again. We will dwell on the most important of them and generally on a detailed description of the excluded volume effects in the context of the problems where they become crucial: EDL in RTILs.

Obviously, integral characteristics of the double layer are not the whole story. Whereas the capacitance is an important characteristics of energy storage devices, as a diagnostic feature it integrates out many details which one must be interested to reveal. The key characteristics are the molecular-scale distribution of ions and the whole molecular picture of the EDL. The greatest interest is nowadays in a direct assessment of that structure through X-ray[269–271] and neutron scattering,[272,273] angle-resolved and energy-resolved X-ray photoelectron spectroscopy (XPS),[274,275] metastable induced electron spectroscopy (MIES) scanning probe techniques,[276] neutral-impact-collision ion scattering spectroscopy (NICISS, that recently became popular method for investigating interfacial properties of RTILs),[231,277–279] or any other in situ methods, including STM and AFM measurements.[280]

As we have stressed already, the study of the highly concentrated ionic systems was very much 'catalyzed' by the interest in molten salts. In particular, pioneering theoretical works of Tosi and collaborators[281–284] for molten salts have discovered a spectacular phenomenon, that they termed "overscreening". It was found there that at small electrode polarizations, the first layer of ions delivers a counter charge greater in absolute value than the one on the electrode. The next layer was on average oppositely signed, but with the absolute value

of the charge larger than the absolute value of the difference between the charge of the electrode and the charge of the first layer. And off these decaying charge oscillations go over several layers before reaching electroneutrality in the 'bulk'. Torrie and Valleau were among the first who used simulation techniques (Monte-Carlo) for systematical studies of EDL formation at charged interfaces in concentrated electrolytes. In their 1980 work they have shown that at high concentration of ions in an electrolyte, the charge density in the EDL starts to oscillate.[285] Their pioneering works on modelling EDL in concentrated electrolytes have shown apparent limitations of the GCh theory.[286,287]

However, the physical nature of overscreening, to our knowledge has never been clearly rationalized in the literature. We will get back to this issue, when discussing the situation with RTILs, where it becomes central for small and medium electrode polarizations.

Note that the papers by Tosi et al on molten salts did not study the effect of the voltage on the ionic distribution near the interface, having limited the analysis to the linear response.[284] The nonlinear response was much more difficult to handle, and here simulation has started to play a pivotal role, as we discuss later in this review. For molten salts such study has been performed in Ref.,[288] albeit not for a wide set of charges of the electrode. It has, however, detected some suppression of overscreening at large electrode polarization. We will dwell on a similar phenomenon in the context of RTILs later in this review.

The detailed Monte Carlo simulation studies of overscreening by Tosi et al were inspired by a short note by Dogonadze and Chizmadzhev.[289] Based on the experimental evidence (well established at that time) for the decaying oscillating structure of the bulk binary correlation function in simple liquids, Dogonadze and Chizmadzhev correctly deduced that the charge density correlation function in an ionic liquid should also have a form of decaying oscillations. They related the EDL capacitance with the features of the bulk correlation function of that charge distribution; such relationship is possible in the linear response regime, and neglecting the breakdown of the translational invariance of the system in the direction perpendicular to the electrode. They came to a conclusion that the capacitance is simply inversely proportional to the distance to the first peak. Their suggestion has paved the way to much later statements that the EDL in ionic liquids is effectively one layer thick. This was bold and novel at that time, but in fact appeared to be not always accurate.

Indeed, it can be shown exactly that that the differential capacitance of EDL is inversely proportional to the centre of mass of the excess charge distribution in the double layer

$$\lambda(\sigma) = \lim_{\delta\sigma \to 0} \left[\frac{\int_0^{z*} dz \delta\rho_{ion}(\sigma,z)z}{\int_0^{z*} dz \delta\rho_{ion}(\sigma,z)} \equiv \frac{\int_0^{z*} dz \delta\rho_{ion}(\sigma,z)z}{-\delta\sigma} \right] = \int_0^{z*} dz \left\{ -\frac{d\rho_{ion}(\sigma,z)}{d\sigma} \right\} z \qquad (8)$$

where $\delta\rho_{ion}(\sigma,z) = \rho_{ion}(z)|_{\sigma+\delta\sigma} - \rho_{ion}(z)|_\sigma$ is the difference between the charge densities in the liquids at the charge of the electrode equal to $\sigma + \delta\sigma$ and σ and z is some distance in the electroneutral bulk which may be put equal to infinity for large separation between the electrodes. Namely,

$$C = \frac{\epsilon_*}{4\pi\lambda(\sigma)} \qquad (9)$$

where ϵ^* is the *is the effective dielectric function of the dipole active degrees of freedom in the electrolyte* - due to vibrations and rotations of ionic pairs and clusters, electronic polarisability of ions of the solute and solvent molecules, etc. In the case of solvent-free RTIL it is the polarizability of all the degrees of freedom that are faster than translational motions of the same ions of RTIL, and it redresses Coulomb interactions in RTIL. Systematic measurements show that for many RTILs ϵ^* is of the order of 10, c.f. Refs.[174,189,290] But in the case of molten salts this is just due the electronic polarizability of ions, and $\epsilon^* \sim 2$.

Oscillations in the potential distribution are related with the oscillations in $\rho_{ion}(\sigma,z)$ as a function of z, because the distribution of electrostatic potential in the double layer is given by

$$\Phi_{IL}(z) = -\frac{4\pi}{\epsilon_*} \int_0^z (z - z')\rho_{ion}(z')dz'. \qquad (10)$$

All in all, had the first peak in $\delta\rho_{ion}(\sigma,z)$ been totally dominating, the Dogonadze-Chizmadjhev conjecture would have been justified. However, even in HTMSs more than one peak is seen on the density profiles (not talking about RTILs). The way how all these peaks get restructured with applied voltage is decisive for the capacitance dependence upon voltage.

Measurements of the EDL capacitance at high temperatures typical for molten salts using electrochemical impedance techniques,[5,291,292] are generally very difficult and are prone

to all sorts of experimental artifacts (for critical review see Ref.[292]). In particular, the controversy in the data for the temperature dependence of the EDL capacitance in molten salts (different trends reported by different authors) that challenged theorists for decades, remains unresolved (see also discussion on this subject in the following sections below).

There is one issue to be mentioned before we conclude this section. In the mid-late 1980s there was a great interest in understanding the role of the electrons of the electrode in the result for EDL capacitance, specifically the effect of the spillover of the surface electron cloud into the solvent, and of the response of the surface electronic profile to charging (for reviews read.[2,293,294] Indeed, the distance to the centre of mass of the excess charge distribution should be calculated not from the hypothetical 'edge of the electrode', say the edge of it ionic skeleton, but from a position of the excess charge in the electrode. This position is determined by the distribution of electrons near the interface and the latter is affected by the net charge of the electrode. The effect on the compact layer capacitance and its dependence on the electrode potential could be substantial, the surface electronic profile of the electrode being sensitive to the electrode polarization.[2] How important this effect is for ionic liquids is not clear, as so far all the attention has been addressed to the double layer on the liquid side. It is, however, very important for any electrolyte, whether the electrode is an ideal metal, semiconductor or semimetal.

From the very first steps of the electrochemistry of semiconductors it was made clear that the potential distribution on the electrode side of the interface can be very important. Semiconductor electrode essentially contributes a capacitance in series, due to the penetration of electric field in it, because of the finite screening length and, consequently, the space charge forming in it. If the concentration of charge carriers is low there, this space charge will be ever extended and that space charge region will totally dominate the overall capacitance of the interface. Gerischer[295,296] has noted some 30 years ago that the measured capacitance of the semi-metal graphite electrode/electrolyte solution will unlikely display any information on the EDL in the electrolyte, being totally determined by the EDL in the electrode! Indeed, the two capacitances add in series and thus the smaller one will determine the capacitance. As calculated by Gerischer et al, it appears that the dominant contribution is due to the graphite side, unless one goes to very low electrolyte concentrations. It will be worth to keep

this in mind, when trying to interpret experimental data on various carbon electrodes. We note that this conclusion has not been approved by recent findings of Shklovskii et al.[297] Theoretical estimates reported in that work suggested that the electric field should decay to zero within the first graphite layer. However, the recent *quantum* **d**ensity **f**unctional **t**heory (DFT) study by Luque and Schmickler that explicitly considered the layered structure of the graphite electrode showed that "on the basal plane of graphite, an external field penetrates over a distance of a few tenth of a nm into the surface".[298] Luque and Schmickler also showed that the induced charge density inside the first several layers of graphite strongly oscillates (displaying Friedel-like oscillations). This work used a combination of the quantum DFT results with the hard-sphere model for the electrolyte solution to calculate the overall capacitance of the graphite/electrolyte interface. The computational and theoretical results presented in this work were shown to be in an excellent agreement with experimental data.[298]

Therefore, one may conclude that, indeed, the interfacial capacity between graphite and an electrolyte solution with high ionic concentration is dominated by the electronic response of graphite. However, there are still many open questions in this area (e.g effects of surface roughness, impurities, chemical modification of the surface and surface adsorption). Further detailed investigations of the appropriate quantum chemistry level combined with an adequate description of the liquid side are needed for various carbon materials. This is perhaps one of the most important challenges for the theory, in view of a wide use of carbon materials in supercapacitors, batteries and other electrochemical applications.[27,71,74,142,144,179,299–310]

4 Principles of the theory of EDL in RTILs at flat electrodes

4.1 Mean field theory

Mean field theories are usual first steps in description of complex statistical-mechanical systems. They serve as common reference bases for more sophisticated theories and computer simulations. The simplest mean field theory of EDL for RTILs at a flat interface was sug-

gested in a 2007 feature article[52] in the context of the overall broad discussion of various new features that EDL in RTILs may exhibit in contrast to EDL in ordinary diluted electrolytes. The approach used simple principles of the lattice gas model, in which N_+ cations and N_- anions, with a fixed total number $\bar{N} = N_+ + N_-$, are distributed over N available lattice sites. The distribution is random except for when it is influenced by electric field. The electrostatic potential Φ of this field is self-consistently determined by the distribution of ions near the boundary with the electrode the polarization of which is taken into account through the boundary condition.

The free energy of such system may be approximated by

$$F = e\Phi(N_+ - N_-) + B_+ N_+{}^2 + B_- N_-{}^2 + CN_+N_- - k_BT \ln \frac{N!}{(N - N_+ - N_-)!N_+!N_-!}. \quad (11)$$

Here the electrostatic potential Φ and the distribution of ions are related via the Poisson equation, which for a system with the anisotropy axis (the one perpendicular to the surface of the flat electrode), z, reads as

$$\epsilon_0 \frac{d^2\Phi}{dz^2} = 4\pi e[c_- - c_+] \quad (12)$$

with concentrations $c_- = N_i/\Omega$, $c_+ = N_+/\Omega$ where Ω is the total volume of the system. The second, third, and fourth terms in eq 11 take into account for specific interactions between cations and anions, the nontrivial consequences of which were the subject of intensive investigations in this class of models in different contexts in the past.[311–313] In the first approximation, however, as in Ref.[52] one can drop these terms out, just putting $B_+ = B_- = C = 0$ as this is the only way to keep the algebra simple and get analytical results. Minimization of the free energy with respect to N_+ and N_- gives 'Fermi-like' distributions of cation and ion densities as a function of electrostatic potential:

$$c_+ = c_0 \frac{exp\left(-\frac{e\Phi}{k_BT}\right)}{1 - \gamma + \gamma \cosh\left(\frac{e\Phi}{k_BT}\right)} = c_0 \frac{exp\left(\frac{e\Phi}{k_BT}\right)}{1 - \gamma + \gamma \cosh\left(\frac{e\Phi}{k_BT}\right)} \quad (13)$$

controlled by a single parameter of the model, the ratio of average concentration in electroneutral region (where, $\Phi = 0$ and $c_+ = c_- = c_0$) to the maximum possible local concen-

tration,

$$\gamma = \bar{N}/N = 2c_0/c_{max}.$$ (14)

The physical meaning of this parameter is straightforward (see Figure 3). In solvent-free ionic liquids: $1-\gamma$ is the portion of free volume, i.e. the portion of voids in the system (analogous to what is called *porosity*, with γ being equivalent to what is called *compacity*[314]). Some RTILs spontaneously absorb some small amount of water from the air[20,30,38,130,229,231,315,330] or they can be deliberately mixed with some amount of organic solvents (usually for the purpose of increasing the mobility of ions);[35,50,120,316–320] $1-\gamma$ will then characterise the volume portion of those molecules. The case of $\gamma = 1$ corresponds to an ultra dense system with no voids (or no solvent). The value of γ should vary for different RTILs, but for many of them is expected to lie around or above $1/2$; however, in the case of an RTIL with solvent additives it can be substantially lower.

Combination of eq 12 and eq 13 gives the so called Poisson-Fermi equation,

$$\frac{d^2\Phi}{dz^2} = \frac{8\pi e c_0}{\epsilon_*} \frac{\sinh\left(\frac{e\Phi}{k_B T}\right)}{1 + 2\gamma \sinh^2\left(\frac{e\Phi}{2k_B T}\right)}.$$ (15)

This nonlinear second order differential equation can be easily integrated subject to the corresponding two boundary conditions, and this solution will give us the distribution of potential $\Phi(z)$. For a single double layer at one electrode located at $z=0$, one may use as the boundary conditions (i) the Gaussian law at the electrode/electrolyte interface, $-\epsilon_* \frac{d\Phi}{dz}\big|_{x=0} = 4\pi\sigma$, where σ is the surface charge density, and (ii) the absence of the electric filed in the electroneutrality region, $\frac{d\Phi}{dz}\big|_{x\to\infty} = 0$. Setting the potential in the bulk, $z \to \infty$, at zero, together with the full solution for $\Phi(x)$, one gets the potential drop across the EDL, $V = \Phi(0)$, thus establishing the relationship between V and σ. The capacitance per unit surface area of the electrode then is obtained $C = \frac{d\sigma}{dV}$ at any value of electrode potential.

As noted in the previous section, devoted to the introduction to EDL in ordinary electrolytes, the Poisson-Fermi equations have been earlier solved in different contexts in a number of recent and much older works[260–264,266,267] starting with the pioneering paper by Bickerman;[260] for a comprehensive review see Ref.[268] For details of the potential distribution
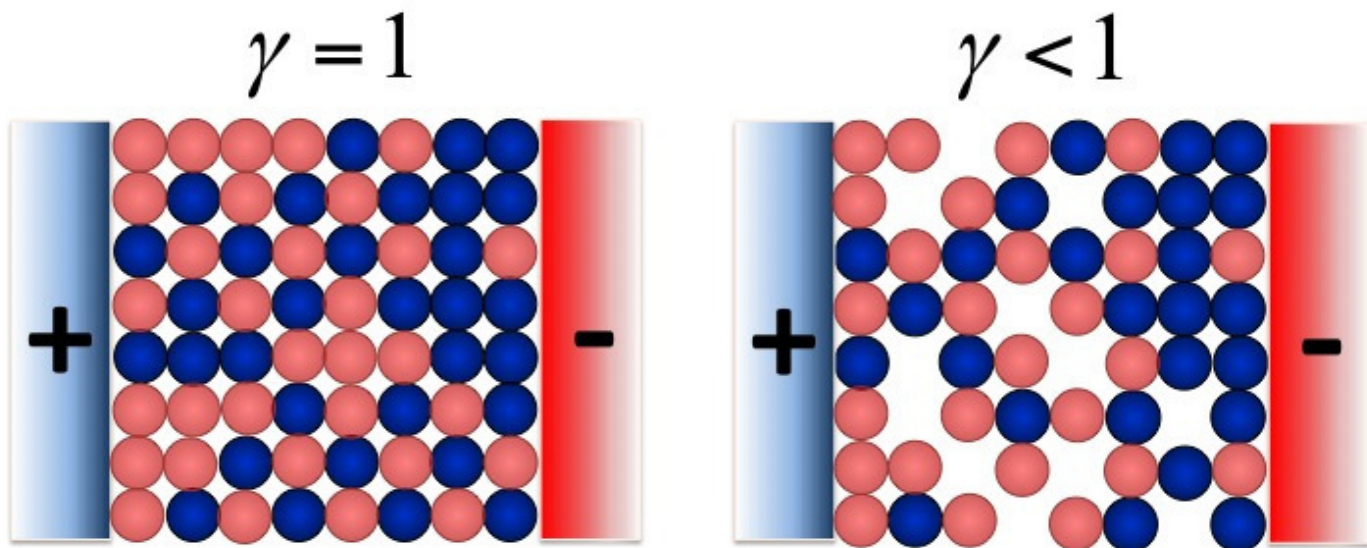
Figure 3: A cartoon showing an ionic liquid between two electrodes, representing the concept of the compacity parameter γ (red spheres standing for anions, blue spheres - cations, and empty space in the lattice representing voids) For these 2D cartoons, $\gamma = 1$ for the left picture and $\gamma = 13/18$ for the right picture.

$\Phi(x)$ at the flat interface we refer the reader to the Ref.[52] here outlining just the main points: the absolute value of the potential decreases from $\Phi(0)$ to zero (i) *monotonously* (mean-field solution!); and, (ii) slower than the Gouy-Chapman solution. How much slower? This is determined by the compacity factor, γ. When $\gamma = 0$ the shape of $\Phi(z)$ is the same as in the Gouy-Chapman theory; however, when γ approaches 1 the shape becomes much less prolate because of the volumetric constraints on the density of counterions that accumulate in the double layer in response to the polarization of the electrode. This effect is often called 'lattice

saturation' or 'crowding' and it has an important consequence on the voltage-dependence the EDL differential capacitance.[47,321]

The resulting expression for the latter through the overall potential drop across the double layer, written for compactness in dimensionless units, $u = eU/k_BT$, reads

$$C = C_D \cosh\left(\frac{u}{2}\right) \frac{1}{1 + 2\gamma\sinh^2\left(\frac{u}{2}\right)} \sqrt{\frac{2\gamma\sinh^2\left(\frac{u}{2}\right)}{\ln\left[1 + 2\gamma\sinh^2\left(\frac{u}{2}\right)\right]}}. \tag{16}$$

The particular case of $\gamma = 1$ can also be retrieved:

$$C = C_D \cosh\left(\frac{u}{2}\right) \frac{\sqrt{2}\,|\sinh(u/2)|}{\sqrt{\ln[\cosh u]}\cosh u}. \tag{17}$$

In the both expressions

$$C_D = \frac{\epsilon_*}{4\pi L_D} \;\;,\;\; \lambda_D = \sqrt{\frac{1}{8\pi L_B c_0}} \;\;,\;\; L_B = \frac{e^2}{\epsilon_* k_B T}. \tag{18}$$

which are the Debye capacitance, the Debye length, and the Bjerrum length, respectively. These three factors have the same form as in electrolytic solutions, but they use ϵ_*, the 'high frequency dielectric constant' of the RTIL that for pure, solvent- free RTILs is determined by all dipole-active collective excitations in RTIL (see subsection 2.2.3 above); an addition of organic solvent molecules can affect (usually increase) that value.

The first of the three factors in eq 16 is the Gouy-Chapman capacitance, but the two other factors convert the result into something very different. Such, the second factor in eq 17 makes the voltage-dependence of capacitance opposite to the Gouy-Chapman one: the curve takes a bell-shape instead of the U-shape. The behaviour of the more general case, 16, depends on the value of γ. For $\gamma > 1/3$ it has a bell shape, whereas for $\gamma < 1/3$ it has a double hump shape, called *camel shape* in Ref.[52] In Figure 4 we reproduce plots of that paper that show these qualitatively different modes of behaviour.

The physical nature of the two different modes of behaviour is clear. The crossover from the bell shape to the camel shape takes place when the density of electrolyte is diminished. The parameter γ is the key measure of the density of electrolyte, scaled to the maximum
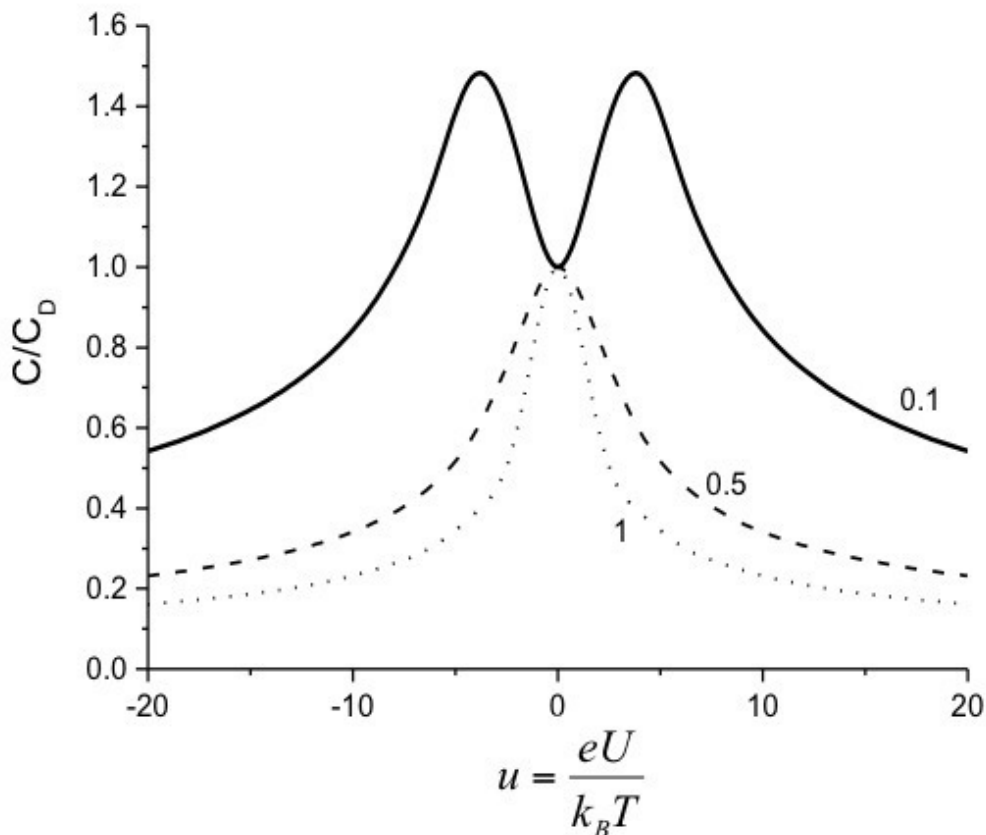
Figure 4: The capacitance given by the mean-field theory, eq 16, for indicated values of the compacity parameter, γ. The graph shows 'camel' and 'bell' shapes, for small and large values of γ, respectively. Reproduced from Ref.[52]

possible local density. For small γ there is some room to make the double layer more dense with the increase of voltage, filling up the voids (the free volume) in the liquid, or if instead of voids we have some space occupied by organic solvent, expelling solvent molecules out of the double layer.[323] This will provide the Gouy-Chapman like behaviour (see Figure 2 above). On the contrary if there are no voids/no solvent to realize the drive to compress the double layer with the increase of the voltage, the counterions will start to line up in front of the electrode and the double layer will be getting thicker and the capacitance will fall, demonstrating the bell shape.

In this mean-field theory the border line between the two modes of behaviour is at $\gamma = 1/3$. We fail to see any general law that could have dictated this; in reality the position of the demarcation line in terms of the average density of electrolyte (i.e. of parameter γ) should depend on details of the modelled system.[47,322]

Simultaneously with Ref.,[52] which was focused entirely on RTILs, the formula eq 16 in a different physical context was reported by Kilic, Bazant and Ajdari;[324] a year later, in connection with RTILs its particular case of $\gamma = 1$ was reported by Oldham.[325] References[52,325] became particularly popular in the community that deals with electrochemistry of RTILs; that analysis was also subjected to various extensions.[326,327]

The papers[52,325] missed, however, an early article by Freise,[264] who had derived similar formula as eq 17 but in the context of the double layer in concentrated electrolytes. Again, that early work was essentially ignored at the time of its publication (1952); we think that this happened mainly because the decreasing wings of the capacitance shape in electrochemical experiments had not been reported before RTILs. Indeed, the Freise's theory predicted them for voltages at which electrochemical reactions already turn on in common electrolytes. For this reason, electrochemists did not pay enough attention to it: in 1950s the time of the Freise's findings did not come. It was due Martin Bazant and his colleagues with their passion for the history of science[268,324] that the Freise's work has been retrieved from oblivion and began to be quoted, at least in the microfluidic community.

Note that the mean-field model can be modified to take into account the asymmetry of ion sizes. The easiest thing, as suggested in Ref.[52] and implemented in Ref.,[328] is to assume that c_{max} on the two wings of polarization will be different. If cations are larger than anions, then close to the positively polarized electrode (the anode) c_{max} will be higher than near negatively polarized electrode (the cathode). Consequently, γ will be smaller for positive polarization of the electrode than for negative polarization. This can be phenomenologically implemented into the previous equations by attributing to γ a voltage dependence. In the spirit of Refs.,[52,328] avoiding introduction of any new parameters, such dependence can be parametrized as

$$\gamma(u) = \gamma_- + (\gamma_+ - \gamma_-)/(1 + e^u). \tag{19}$$

This will immediately introduce an asymmetry in the capacitance curve around the p.z.c.: the positive wing lying higher than the negative wing, with the maximum/ maxima shifted from the p.z.c. to positive potentials.

The temperature dependence of capacitance, the subject of controversy in experimental data, in the mean-field theory enters through the value of $u = eU/k_BT$, and through the expression for the Debye length, eq 2, which it enters explicitly as well as through some mild dependence of $\epsilon_*(T)$. Graphs, plotted in Ref.[329] show that the increase of temperature broadens maxima in capacitance but leaves practically unaltered the large voltage wings (c.f. the next section).

4.2   Model independent result

Reference[52] has addressed attention to an interesting fact: the behaviour of the wings is likely to be universal, independent of the model. The mean-field theory formula gives it as an asymptotic law, $C = \frac{\epsilon}{4\pi L_{eff}(u)}$ where the effective thickness of the double layer is $L_{eff} \approx L_D\sqrt{2\gamma|u|}$, so that

$$C \approx C_D\sqrt{\frac{1}{2\gamma|u|}}. \tag{20}$$

As it has been shown in Ref,[52] this asymptotic law can indeed be derived in the so-called 'de Gennes' style, i.e. without any complicated algebra or any model. It is worth to reproduce those arguments here. In the saturation regime, when ions of one sign in the double layer are densely packed, $|\sigma| \approx L_{eff}ec_{max}$. Equally, using the Gauss theorem, $|\sigma| = \frac{\epsilon_*}{4\pi}\left|\frac{d\Phi}{dx}\right|_{x=0}\left| \approx \frac{\epsilon_*}{4\pi}\frac{(k_BT/e)|u|}{L_{eff}}\right.$. Equalizing these two expressions for $|\sigma|$, $\frac{\epsilon_*}{4\pi}\frac{(k_BT/e)|u|}{L_{eff}} \approx L_{eff}ec_{max}$, we get

$$L_{eff}^2 \approx \frac{\epsilon_*}{4\pi}\frac{(k_BT/e)|u|}{ec_{max}} = \frac{\epsilon_*k_BT}{8\pi c_0e^2}\frac{2c_0|u|}{c_{max}} = L_D^2\gamma|u|, \tag{21}$$

i.e. $L_{eff} \approx L_D\sqrt{\gamma|u|}$, which, to the accuracy of the factor $\sqrt{2}$, coincides with the limiting law of the mean field theory. In other words,

$$C \propto |u|^{-1/2}, \tag{22}$$

is the universal, *model independent* law imposed by the overall conservation of charge.

From here it follows that the capacitance at the wings must weekly depend on the temperature. Indeed,

$$C \approx \frac{\epsilon_*}{4\pi L_D} \cdot \frac{1}{\sqrt{2\gamma|u|}} = \frac{\epsilon}{4\pi\sqrt{\frac{\epsilon_* k_B T}{8\pi e^2 c_0}} \cdot \sqrt{2\gamma e \frac{|U|}{k_B T}}} = \sqrt{\frac{\epsilon_* e c_{max}}{4\pi|U|}}. \tag{23}$$

Hence the temperature dependence can enter here only through the value of $\sqrt{\epsilon_* c_{max}}$. The ϵ_* factor may have some mild temperature dependence, but c_{max}-factor is unlikely to have it at all, so that their product, square-rooted, will have very weak temperature dependence.

4.3 Notes on the structure and capacitance of the EDL in RTIL mixtures with neutral solvents

The above discussed conclusions about the EDL structure of RTIL will not be valid if we deal with a highly diluted solution of organic ions in organic solvents, but they should be to a high degree relevant for the case of a minor addition of the molecules of organic solvent to RTIL, the often used trick to decrease the RTIL's viscosity.[11,204,205]

How will adding small amount of neutral solvents to RTIL change the structure of the EDL and affect capacitance?[206] From the definition of the compacity parameter γ, eq 14, it follows that this would strongly affect this key parameter of the mean-field theory.[52] Indeed, the c_0 decreases with dilution, proportionally to the volume portion of the solvent component mixed with the ionic liquid, whereas c_{max} remains the same. This effect should tend the capacitance to change its shape from the bell like to the camel shape. But this is only a part of the story.

If the RTIL and the solvent wet differently the electrode surface, phase separation near the interface may take place, coupled with electric field induced wetting/dewetting transitions. Generally the ionic liquid phase should be closer to the electrode at large electrode potentials (independently of the sign) than a neutral solvent. At low voltages it all depends on the solvent, whether it wets the surface of the electrode better than the ionic liquid or not. The

phenomenon of stabilization of one phase in a film near the surface phase, with other phase moved away from the surface, and the peculiar behaviour of this phase separation when the system is close to the critical point is called critical wetting. It was a subject of intensive research in theoretical physics in 80s (for review see[331]).

Phase separation may take place as a first order or a second order transition. When one of the phases is stabilized near the surface, either spontaneously or with applied electric field, the thickness of the wetting layer near the critical point of the bulk solution can jump or even diverge (as in the case of the second order transition). Correspondingly sharp changes in response functions or divergences will take place when varying the temperature or electric field. In the EDL problem in liquid electrolytes, such response function is the differential capacitance, and it may reveal singularities.

We note that similar effects have been studied long time ago in context of the potential induced desorption of organic molecules, replaced by water (the effects were rationalised as competitive adsorption of water, organic molecules and ions in a two-dimensional-like compact layer of EDL); the effect laid into the basis of the famous Frumkin adsorption isotherm.[332] Similar problems also attracted attention in the context of the structure and properties of diffuse EDL in ordinary electrolytes.[333] In the context of the mixture of ionic liquids with neutral solvents, ordinarily motivated by the reduction of viscosity and facilitation of migration of ions, this problem has been revisited by Szparaga, Woodward and Forsman.[334] Using the classical density functional theory they showed that close to the critical point of the bulk solution, there indeed may be an extraordinary increase of capacitance. The authors speculate about the possible exploitation of the predicted effect for energy storage. It will be very interesting to test this prediction experimentally. Note, however, that the stored electrical energy in the capacitor is given by $\int_{U_{p.z.c}}^{U} C(U) \cdot U dU$, and just one peak at a critical value of the voltage may not change the integral dramatically. We will discuss various aspects of this problem below, in the section on optimized energy storage of supercapacitors.

4.4 Beyond the mean-field: direct simulations of ionic liquids at electrified interfaces

Even the most advanced theories have serious limitations due to a number of approximations behind them. The main points of concern are: (i) correct account of multi-body correlations; (ii) correct account of the effects related with the molecular geometry of ions; (iii) geometry of the electrode, which may be more easily handled by or sometimes only by computer simulations. In turn, simulations may not intend to consider the problems in their all complexity at once. The cleverest way is to increase sophistication of the model step by step, in order to reveal the role of different factors.

Therefore, since the middle of 70s researchers actively use Monte-Carlo and Molecular Dynamics simulation methods to study structural and thermodynamic properties of molten salts in the bulk[53,101,102] (these early achievements were summarized in Ref.;[335] see also Ref.[291]). Later on, first studies appeared on the properties of molten salts and concentrated electrolytes at electrified solid interfaces.[336,337]

In the early simulations of molten salts at electrified interfaces, much attention was paid to the temperature dependence of the electrical double layer capacitance. Several pioneering theoretical works (MSA, integral equations)[258,281] in 1980s suggested that at low reduced temperatures the capacitance firstly increases and then starts to decrease. The topic was later revisited by Boda and Henderson and their co-workers who investigated in detail several model systems of concentrated electrolytes[338] and molten salts as well as their mixtures.[339] The main messages from those early works were:

- The electrode/molten salt interface has a multilayer structure with several layers that penetrate to the bulk up to several nanometers from the interface;

- The effects of ion size are important;

- Mixtures (other salts, solvent etc) strongly affect properties of the electrical double layer;

Despite the many achievements during this first wave of interest to simulations of molten salts at electrified interfaces, the low-temperature regimes were not sufficiently explored.

Partially it was due to the fact that the investigated models operated with ion sizes in that range typical for mineral salts (like alkali halides). As a result, the systems (as well as the real alkali halides) become solid at low temperatures. Partially it was also due to the high viscosity of the ionic systems and other technical problems with simulations[259] (see also the discussion below).

That can explain, why the bell-shape of the electrical double layer capacitance was not seen in these simulations. As we discussed above this regime is characteristic for low-temperatures and at high temperatures the capacitance becomes flat or even U-shaped.

General methodological comments on simulations of highly concentrated electrolytes/ionic liquids The first works on concentrated electrolytes/molten salts already identified several general methodological problems:

- very accurate methods for electrostatics calculations are absolutely necessary to simulate such systems; these methods (such as Ewald summation[340,341]) are more computationally expensive than simple cut-off methods and they require large computational resources;

- the slab geometry pertinent for electrostatic calculations for most of the electrochemical systems demands the use of the so-called 2D Ewald summation method[340] that is very computationally expensive and poorly parallelizable;

- strong short-range correlations between the ions lead to large viscosity in these systems, and as a result, increase the sampling/simulation time as compared to neutral liquids;

- due to the highly pronounced interfacial oscillations, a relatively large distance between the electrodes is necessary to achieve bulk-like regime in the middle of the simulations box, which increases the size of the simulation cell.

We also note that incorporation of the polarisability of electrodes/image forces in molecular models of electrochemical interface is non-trivial and leads to significant increase of the computational time.[342–344]

Overall, these problems made simulations of ionic liquids a challenging task at that time, when even the fastest supercomputers had computational power not more than several Gflops (which corresponds to a typical modern laptop).

It has been shown that the 3D Ewald method and other 3D electrostatic methods (like e.g. Particle Mesh Ewald, PME[345]) that are less expensive than the 2D Ewald method can be still used for simulations of a 2D slab geometry with some corrections. Such, Torrie and Valeu suggested a so-called Charged-Sheet correction (CS).[286,337] Later on, in 1999 Yeh and Berkowitz suggested another correction method for using 3D Ewald methods in slab-like geometries, 3D-EWC.[346]

Effects of electrostatic boundary conditions and system size on results of simulations of interfacial properties in aqueous electrolyte systems were thoroughly investigated by Spohr. In Ref.[347] he showed that appropriate long-range corrections are mandatory for simulations of interfacial properties of electrolyte solutions. Indeed, the existing truncation schemes lead to unphysical electric fields in the solution, which prevent the formation of a 'bulk' region in the simulation cell. Later on Spohr, Henderson and co-workers investigated both CS and 3D-EWC corrections in Refs.[348,349] in a view of applications to concentrated electrolytes and molten salts. This works identified several problems associated with using CS for the approximation of long-range forces in the x and y directions in electrolyte systems with high particle density. In turn, Ref.[348] showed that in 3D-EWC there is no abrupt minimum image discontinuity in the x and y directions, and therefore the system size effect gets much smaller, as compared to the CS method. Thus, Ref.[348] concluded that 3D-EWC is preferred over CS for use in simulations with high particle density. Overall, Spohr recommended to use the 3D-EWC correction rather than the CS despite the fact that 3D-EWC is more computationally demanding.[347] Till now, the 3D-EWC is the most accepted technique in this field.

Today, one can roughly classify direct simulation models for modelling ionic liquids into two main categories: *Simple Models* (also referred as "*Coarse Grain*" models or "*Toy Models*") and *Molecular Models* (also referred as "*Atomistic Models*").

The Simple Models operate with a coarse-grain representation of the ion and solvent molecular structure. The Molecular models use more sophisticated atomistic description of molecular structures of the electrolyte components, sometimes in its full chemical complexity.

The exact borderline between these classes of models is somewhat arbitrary. Indeed, even simple spherical models of ions can be a good *quantitative* approximation for monoatomic molten salts systems (e.g. molten alkali halides). On the other hand, even fully atomistic models of *classical* Molecular Mechanics are 'force-field'-sensitive, and do not reproduce all features of the systems (e.g. charge transfer, electron distribution and polarizabilty, chemical reactivity etc; to model these phenomena more sophisticated *Quantum Mechanics* models are necessary).

4.4.1 Course-grained models: forest behind the trees

Overscreening *vs* crowding physics

The mean-field results published in Ref.[52] were beneficial for explanations of (somewhat puzzling) experimental capacitance curves in RTILs that do not display the Gouy-Chapman-like U-shape[398,463–468] (some of these experimental works will be discussed in details below). However, it was clearly underlined in the same paper[52] that the strong Coulomb correlations at the nano-scale[56] in such a dense 'ionic plasma' as RTILs should inevitably make the mean-field unreliable at least in some range of potentials.

The questions, (i) what is this range, (ii) what are the features of the simple mean-field theory that will retain after a more sophisticated analysis, and (iii) what will be the new features coming from those Coulomb correlations, remained to be answered.

The motivation for that quest had several reasons. First, it was known from the theory and computer simulation of HTMSs that electrostatic potential as well as the charge density near a mildly polarized electrode oscillates, exhibiting the above mentioned phenomenon of overscreening. Similar effects were expected to see for RTILs, the more so that first molecular-scale computer simulations of interfacial behaviour of RTILs have shown decaying oscillation potentials at interfaces.[350–353] Secondly, there were structural experiments for concentrated electrolytes in the bulk[227,354] and first-generation RTIL (ethylammonium nitrate).[354] They all showed oscillating structures in very concentrated electrolytic solutions. Third, overscreening, oscillating potentials and charge distributions were well established in dipolar liquids, such as water,[355–359] HTMSs;[259,288,288,360,361] similar kind of motifs[56] caused by proximity of positive and negative charges were to be expected for RTILs. Moreover, a

series of recent experiments by different surface-specific techniques have shown that, indeed, charge density distributions oscillate in RTILs at interfaces.[231,275,276,278,279] Last but not least, the capacitance predicted by the mean-field theory seemed to be too large at small electrode potentials as compared to the experimental values indicating that there is something missing in the mean-field theory, at least in that range of potentials.

As a result, the recent wave of interest to coarse-grained simulations of *low-temperature* ionic liquids at EIs[47,322,328,362–367] was to our opinion stimulated by several factors: (i) the increased number of applications of *different* RTILs demanded development of *toy models* that could capture *main trends* in the RTIL behavior at EIs; (ii) as summarized above, there was a list of fundamental questions about the behavior of RTILs at electrified interfaces that were poorly understood and required to go beyond simple theories (see also Ref.[52]); (iii) the computational power of supercomputers increased and access to high performance computing facilities became easily available for wide circles of researchers.

Moreover, coarse-grained models of RTILs provide input for advanced theories[368–374] as well as *classical* DFT models[364,375–378] that recently became increasingly popular for theoretical/computational studies of RTIL behaviour at flat EIs[377–382] as well as in porous electrodes.[372,383–385]

In Refs.[47,322,328,362] several coarse grained RTIL models of different complexity were used. The main features of these models and the main results of these works are discussed in details below. The works[328,362] studied dense liquid-like assembles of spherical charged particles. The main results of these works shown that:

- the electrical double layer capacitance in dense ionic liquid systems has an overall bell-shaped character as a function of electrode potential, with no signs of the Gouy-Chapman behavior;

- there is substantial over-screening effect at small electrode polarizations; here the double layer in RTILs has an oscillating structure, in which counter-ion-rich layers alternate with co-ion-rich layers;

- such structures are eliminated at large polarizations, replaced by the 'lattice saturation' effect.

44

More complicated models were later used to understand the effects of *non-spherical geometry* of RTIL ions and the nonpolar part of the RTIL molecules.[47,322] The main conclusions from these works were later confirmed by more sophisticated molecular models of RTILs.[208,386–390]

The analysis of those effects had started first with computer simulations of a deliberately simplified system[362] that we briefly overview below:

- Electrodes were considered as flat squares, each filled with charged spheres (spherical 'atoms') with the same inter-sphere distance; the partial charge of the spheres is equal in absolute value and opposite in sign on the cathode and anode, its absolute value being fixed for each simulation; by varying the partial charge of the spheres the surface charge density on the electrodes, σ, was varied in different simulations from 0 to $48\mu/\text{cm}^2$.

- The gap distance between the electrodes was set 30 nm to avoid overlap between the EDLs of the electrodes. Thus in a set of simulations the charge of the electrodes is controllably varied, and the potential variation across the double layers, which never overlap in such large system, as well as the overall potential drop across each of the double layers is calculated from the simulation data.

- The gap between the electrodes was filled with equal numbers of RTIL spherical particles, cations and anions, both considered as soft Van der Waals spheres (with only the repulsive part of the Lennard-Jones potential considered) of the same radius, 0.5nm and charge 1e for a cation and -1e for anion; partial densities of cations and anions, c_+ and c_- were the same (about 0.3 ion/nm^3) giving the total particle concentration around 0.6 ion/nm^3. Taking into account the actual size of the ions this concentration corresponds to the value of γ (see eq 14) around 0.43.

The polarisability of RTIL species was implemented in this model in a crude way by scaling the charges in the model by an effective factor $\frac{1}{\sqrt{2}}$. A similar approach was later used in other works on coarse-grained[224,328] and non-polarizable atomistic RTIL models[391,392] as an easy way to take into account the polarisabilty of RTIL molecules. Simulations themselves used periodical boundary conditions in the lateral dimension and perpendicular to

the electrodes with 15 nm of an empty space till the next pair of electrodes (necessary for correct use of the 3D-EWC correction[346]); standard molecular dynamics with Gromacs MD software[393–396] were used; because such idealistic symmetric system freezes much easier than the ionic liquids composed of real ions the temperature in the simulation was elevated and kept at $T = 450$.

Such approach ignored all the effects of the polarisability of real conducting electrodes (image forces), as well as attractive Van der Waals forces between the RTIL ions (such effects have been considered in later works), but the task of this study was to reveal the effects of Coulomb correlations in its pure form, and the results[362] were lessening.
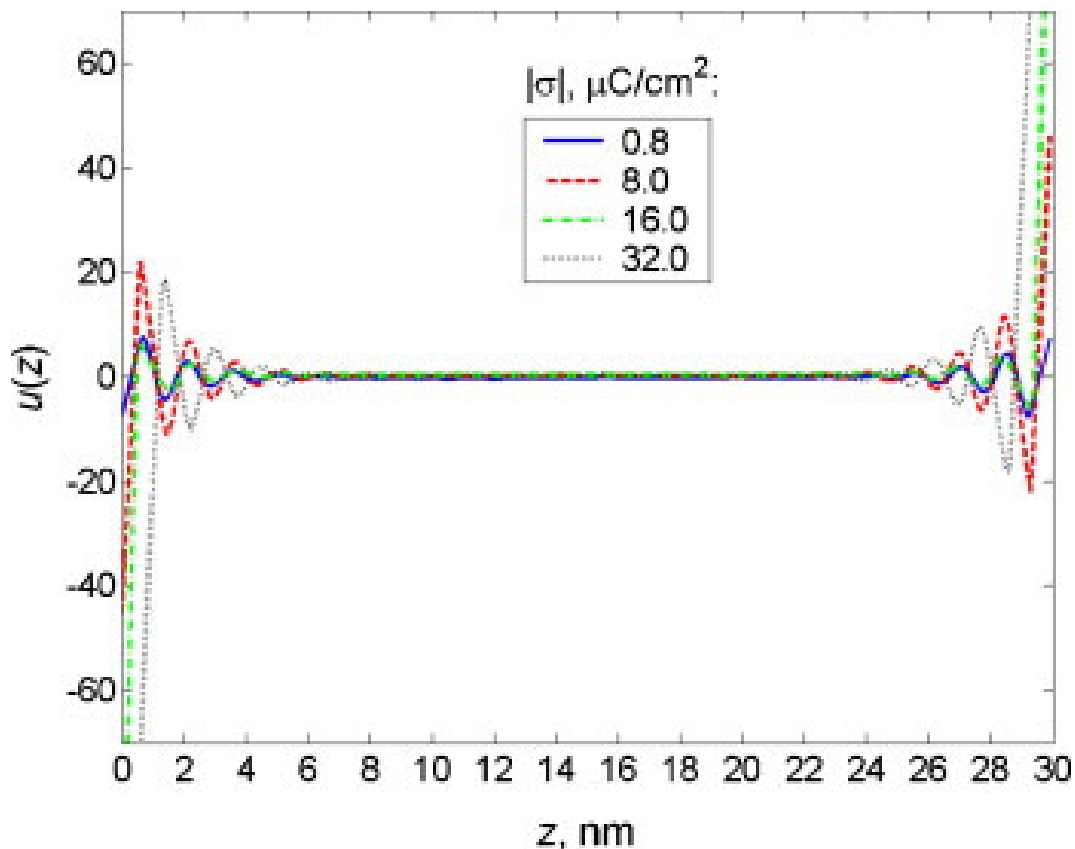
Figure 5: Simulated[362] profiles of dimensionless potential $u(z) = eU/k_BT$ (z is the direction perpendicular to the electrode planes), between the cathode (left) and anode (right). Note that for the temperature of the simulation, $k_BT/e = 38.8$ mV. For the symmetric systems used in this work (cations and anions distinguishable only via their charge) the profiles on the two electrodes are mirror images of each other. Reprinted with permission from Reference.[362] Copyright 2008, Elsevier.

The potential profiles, reproduced in Figure 5, show sharp decaying oscillations with

at least 5 visible peaks. We note that such oscillating patterns at the RTIL/EI interface, although for a smaller system with overlapping double layers have been published earlier by Pinilla et al for a molecular model of selected RTIL.[353] But what can one learn from such figures? To answer this question the following analysis has been performed. Exploiting the symmetry of the system, the liquid slab between the electrodes was split into a set of slit 'bins', each i-th bin having the same width, only slightly larger than the diameter of the ions (subject to the density of the liquid). In each bin the average charge of cations and anions per unit surface area was calculated, scaled to the absolute value of the charge of the corresponding electrode (due to the symmetry of the system the charts are mirror images of each other at the cathode and the anode). Such charts for the anode are reproduced in Figure 6.

This Figure demonstrates a dramatic overscreening effects at small and medium electrode polarization. In the upper left corner -charge density of the electrode, 0.8 $\mu C/cm^2$ - we see that the first bin has approximately 2.5 larger counter charge than the charge of the electrode. Increasing the charge of the electrode 10 times, upper right corner, the first bin delivers 1.4 times larger counter charge than the charge of the electrode. But then this 40% positive charge excess is overscreened in the next layer by 60% of negative charge. For even higher charge density, 16 $\mu C/cm^2$, lower left corner, there is almost no room in the first layer to overscreen the charge of the electrode of that surface charge density. There is, perhaps, only 5% overscreening, and this excess is dramatically overscreened, as it should be, in the next layer by a 20 times larger charge that that minute charge difference. Only when we further increase twice the charge of the electrode (the lower right corner) we see the onset of the lattice saturation: there is room to accommodate only 70% of the net counter charge in the first layer (cations only). The next layer, however, endorse slightly more that 30% of the missing balance showing yet some overscreening. Had we plotted the results for even higher charges, we would have presumably encountered with more pronounced lattice saturation, when more successive layers would have been dominated by ions of the same sign.

We went through this analysis in such detail, first of all because the overscreening patterns is actually what differs the real double layer structure in RTILs from the behaviour predicted by the mean field theory. Another reason is (as we will discuss later) that the os-
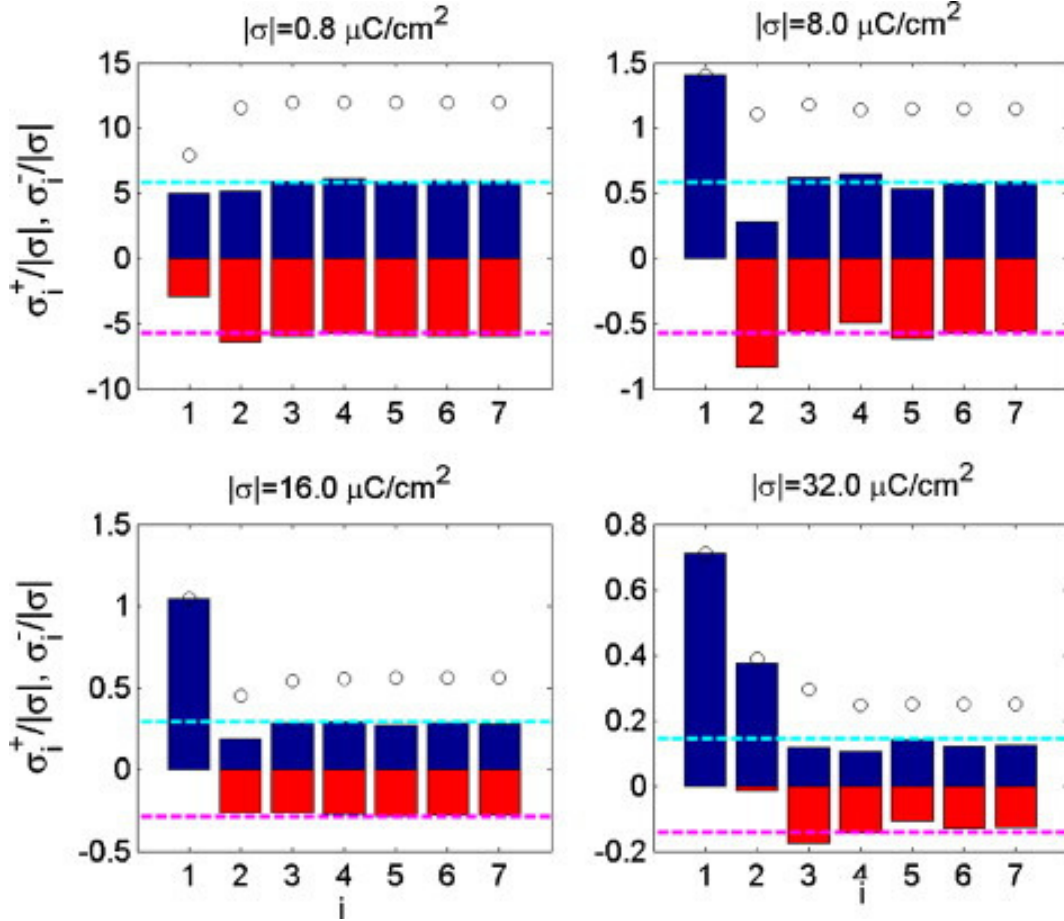
Figure 6: Partial charge densities per unit cross-section area in the first 7 mono-layers of near the cathode, scaled to the absolute values of surface charge density of the electrode, shown for the cathode ($1e/nm^2 = 16\mu C/cm^2$). The figure is reprinted with permission from Ref.[362] Copyright 2008, Elsevier.

cillating overscreening profiles may play crucial role in electrode kinetics when using RTILs as 'solvents' for the reacting ions.[397]

The main lesson from this analysis is that at small electrode polarizations the over-screening effect is maximal. With increase of the absolute value of the electrode charge, i.e. voltage drop across the double layer, overscreening is gradually replaced by crowding of ions of the same sign (lattice saturation) described by the model-independent limiting law (see the subsection 4.2 above) - simulations reproduce the tendency to reach the limiting law, Eq.22.

The EDL differential capacitance calculated from the simulation data[362] has a bell shape that correlates very well with the predictions by the mean-field theory[52] for the estimated

value of compacity $\gamma \sim 0.43$ for the system (that is higher than $1/3$); however, due to the integral effect of overscreening a substantial reduction of the capacitance value was observed compared to the one given by the mean-field theory.

In Ref.[328] the same analysis has been performed for ions modeled by spheres of the different size: cations twice as large as the anions. As the general arguments would suggest (c.f. the consequence of eq 19, discussed in subsection4.1), the curve should shift to positive potential, the positive wing lying higher than the negative wing. This is exactly what has been observed in Fig.1 of Ref.[328] Because of the 'proper' asymmetry of the curve that paper is somewhat more often quoted, than the, perhaps, more fundamental Ref.[362]

Further insight into the generic structure of the double layer in RTIL was given by a toy model of Ref.[322] which used the same class, 'bead' type of models. There anions remained to be spherical beads of a defined size, but several cases of different cations were separately considered: (i) cations made of beads of the same size as anions, (ii) cations modeled as dumbbells in which one of the beads is charged and the other one is neutral, and (iii) cations modeled as triple-bead structures with one bead charged and two neutral. That was the way to capture the generic effects associated with anisotropy of the shape of RTIL ions and unequal intramolecular charge distribution. The neutral beads were imitating 'fatty' neutral counterparts ('tails') typical for many RTIL cations. The density of the mixture was relatively large, and so was the value of the compacity, γ.

Using these three models of cations, a bell shape capacitance was recovered for one bead model but a camel shape for both two- and three-bead models (see Figure 8). The latter was shown to be a consequence of the following effect: the neutral beads play the role of latent voids that can be replaced by charges thereby allowing to increase the local concentration of charges providing the growth of capacitance at small and intermediate voltages. This is schematically shown in the cartoon of Figure7; in Ref.[322] this picture is justified by the plots of the distribution of the neutral beads near the electrode surface as a function of the charge of the electrode. More details revealed by this model are presented in Ref.[47] For instance it has been shown that the onset of the lattice saturation manifested in the inverse-square-root capacitance scaling is shifted towards higher negative potentials for cations with longer tails.

It is important to emphasize that had the compacity, γ, been sufficiently small in these
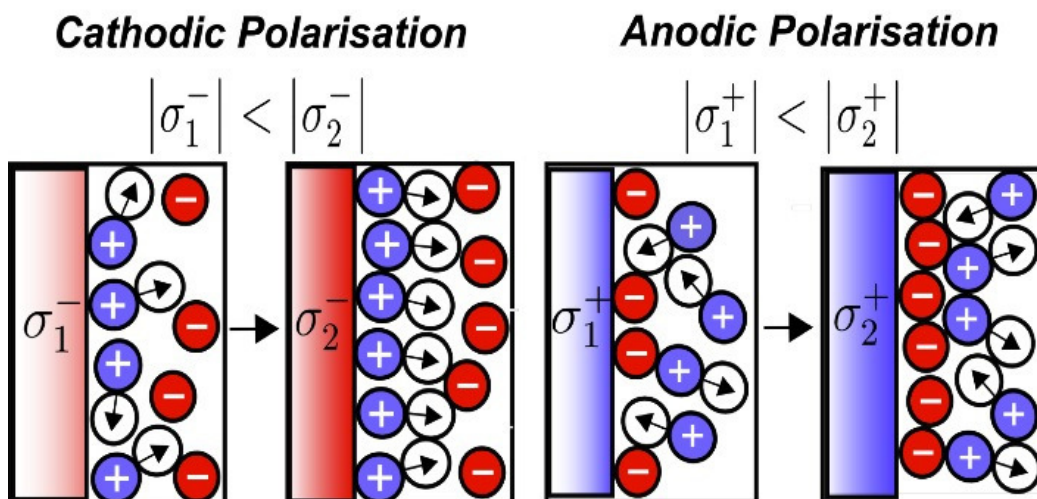
Figure 7: A cartoon showing how (i) increasing negative (cathodic) polarization of the electrode, the neutral tails of cations are got expelled from the electrode vicinity, in favour of the charged cation heads; (ii) increasing positive (anodic) polarization the neutral tails are expelled in favor of anions. The figure is reproduced with permission from Ref.[322] Copyright 2010, Elsevier.

simulations this would have inevitably led to the camel shape even for the one bead model. Thus the conclusion of Refs.[47,322] must not be misinterpreted (as e.g. it has been done for unknown reason in Ref.[382]). In fact, the camel shape is not exclusively conditioned by the existence of neutral tails of ions. As mentioned, the latter simply play the role of latent voids, allowing for a compression of the charge even in a very dense liquid. Free voids, if in abundance, or a sufficient amount of solvent will do this even better – they will cause the capacitance to display the initial Gouy-Chapman-like at small voltages changed by the saturation wings at large voltages overall warranting the double hump camel shape (see also discussion above in subsection 4.3).

With an intention to build a phenomenological theory that will incorporate ion exclusion effect and strong short-range-Coulomb correlations, Bazant et al[321] have constructed a
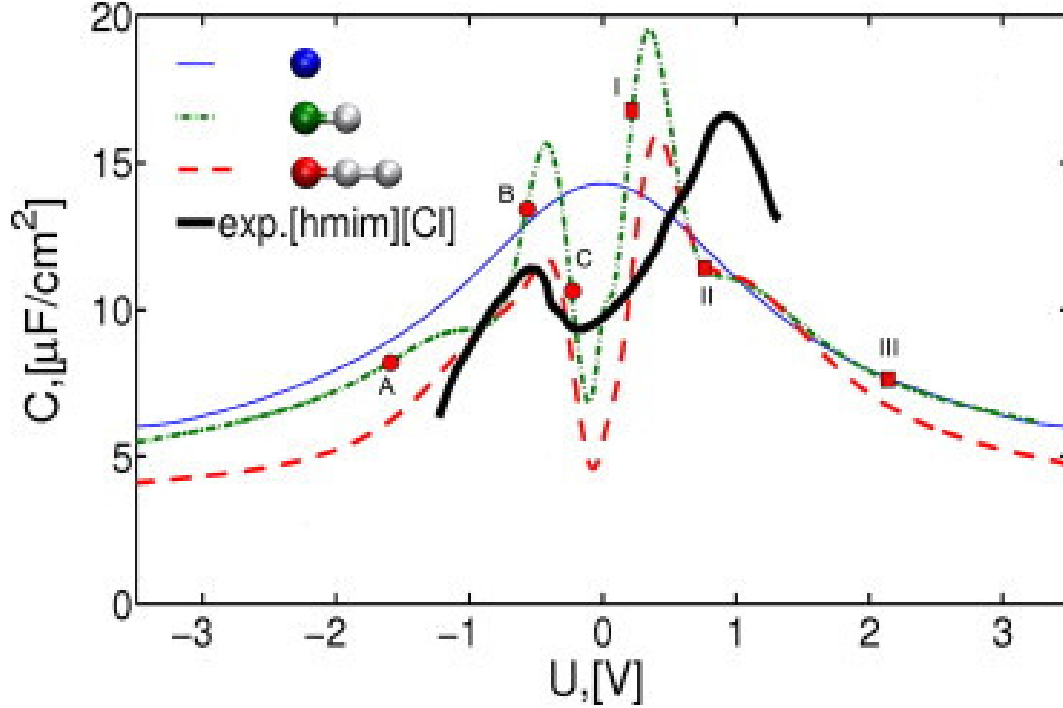
Figure 8: Differential capacitance simulated in Ref.[322] for the electroneutral mixture of charged beads, with single bead anions, and single-, double- and triple bead cations where only the coloured beads are charged, the grey beads representing neutral tails of cations. The black solid line shows an experimental capacitance curve from Ref.[398] The figure is reproduced with permission from Ref.[322] Copyright 2010, Elsevier.

phenomenological free energy functional. It reflects the latter correlations through a term providing a propensity for oscillating profiles in the charge and potential distribution near the interface (in the spirit of the works of Santangelo[399]). At the same time, it incorporates the exclusion-volume effect through the lattice gas type entropy (in a simplified form, as used in Ref.[52]). The analysis of this model that could be performed to a high degree in analytical terms, has shown the interplay between overscreening and crowding, showing how the former has got destroyed by large external fields (electrode polarization) in favor of lattice saturation. The inverse square root law for capacitance was recovered only at very large electrode polarizations; interestingly an intermediate asymptotic law of slower capacitance decay, was revealed at intermediate voltages. With essentially just one fitting parameter (the correlation length standing as a coefficient in the term favouring the oscillating patterns) this theory, continuously covering both the overscreening and covering regimes, almost quantitatively reproduced the simulations of Ref.[362] This was an unexpected success, and encouragement

for developing more sophisticated theories.

Recently Dean, Horgan, Podgornik et al[400,401] reported a Coulomb gas model that has allowed them to obtain an exact solution of the problem of the double layer near the charged electrode, however, under one condition: the model is one dimensional. That means that all the properties of each ionic layer near the surface were averaged in the plane parallel to the interface. Each layer was represented by a point on a 1D lattice, which could be occupied with a spin $s = 1$ (cations), $s = -1$ (anions), and $s = 0$ (voids or neutral molecules, if the ionic liquid is not pure but has 'solvent' additives.). The 1D model is an abstraction though, because it implies that that if $s = 1$ the whole layer is composed entirely of cations, $s = -1$ of anions and $s = 0$ will be a layer of neutral molecules, or even worse than that - voids. However, exactly solvable models in statistical mechanics are rare and therefore are of great value, as they allow to get results free of any approximations. Coulomb interactions in 1D are $\propto |i - j|$ where i and j are the indexes of the sites. No screening of these interactions is imposed, it emerges as a result of the solution of this many-body problem.

Arsenal of modern methods of statistical physics was invoked to get an exact solution of this model. The results of Refs[400,401] can be summarized as follows: (i) Overscreening is a typical feature for the potential and charge density distribution. (ii) The overall shape of the EDL capacitance-voltage dependence has a bell-like centre-line curve for the small number of voids (large compacity) and the camel-like one for a large number of voids (small compacity); both shapes are close to those predicted by the mean-field theory. (iii) Systematic oscillations around this centerline are the features of this solution, each peak representing the voltage induced swapping of the sign of the charge of the consecutive layers; oscillations about the centre line do not seem to visible decay at the wings.

Obviously this structure, exhibiting many peaks is an artifact of the 1D model, in which each layer must be composed of identical ions. Nevertheless this solution is valuable as it is, as it rigorously proves the emergence of overscreening as a result of Coulomb correlations.

All in all, both overscreening and lattice saturation in ionic systems of such density as in RTILs are seem to be established facts. The physical nature of the lattice saturation is straightforward: counterions have no room to accumulate in one layer and they start to line up, forming a queue in front of the electrode, increasing the thickness of the double layer

and thereby decreasing the capacitance. The nature of the overscreening is less obvious. There were many debates about it in the context of dipolar liquids such as water, where overscreening is the typical feature of the dielectric response.[355,358,359] The rationale of this phenomenon is as follows. There is a strong motif for charge alternation in dense ionic (or zwitterions/dipolar) systems with a wavelength comparable with the nearest neighbour distance between opposite charges (of ions or inside the dipoles). Small charge on the electrode cannot change this propensity and the charge distribution will oscillate with that wave length. However to conserve the charge the net charge in the double layer must be equal (with an opposite sign) to the charge on the electrode. It is a simple mathematical exercise to show that overscreening is a prerequisite for satisfying simultaneously the two requirements.

4.4.2 The forest is made from trees. From physics to chemistry: fully atomistic models

'There could be no theory of liquids because every liquid will have to be described by its own theory' - this sentence is often attributed to theoretical physicist L.D. Landau. We could not find documented records of this saying, propagated by a word of mouth. However, fortunately, the conservative opinion of one of the most bold and innovative theorists of the XX Century (who had published ground-breaking works not only in pure physics but also in physical chemistry and chemical physics, see[402]) was not shared by everyone in the theoretical community. The theory of liquids had been actively developed during the last century starting from pioneering works of Ornstein and Zernike[403] followed by fundamental works of Frenkel,[404] Yvon,[405] Bogolyubov,[406] Kirkwood[407,408] Born and Green[409] as well as many others (for the history of the subject see e.g. Refs[410,411]).

The theory of liquids started systematically from the theory of *simple* liquids, such as liquid noble gases of liquid metals.[410,411] Within each of the two classes, there was no need to build for every particular substance 'its own theory'. What it required, was heuristic assumptions on the *closure* of an infinite chain of nonlinear integro-differential Bogolyubov-Born-Green-Kirkwood-Yvon (BBGKY) equations[405–407,409] that could be in principle verified by comparison with computer simulations or various scattering experiments.[411] Taking-off

from the classical pioneering works on simple liquids the theory moved to simple dipolar fluids and then to more complicated, hydrogen bonded liquids, such as water and alcohols and then even to complex fluids (for an overview see[410–413]). Different advanced methods were developed such as the Reference Interaction Site Model (RISM) for homogeneous[414–417] and inhomogeneous[418] liquids, complex bridge closures of extension of the nonlinear integro-differential equations for the correlation functions[419–422] or approximations for free energy functionals[423,424] in the classical DFT.[425–427] The theories were originally targeted to describe equilibrium properties but later were expanded to describe liquid dynamics.[428–430] Most importantly, certain routines for building these closures or the forms of DFT were developed, linked to the molecular structure of the liquids.[431,432]

Is the situation with RTILs different, where we can potentially deal with an unlimited number of liquids? *Must every ionic liquid have its own theory?* There is not enough history of RTIL-focused research in the theory of molecular liquids to answer this question unambiguously. It is clear, however, that the main principles of building approximate bridge functions in molecular theories as well as forms of classical DFT theory can be applied to various RTILs, based on understanding of atomic/electronic structure of the ions (see e.g. the pioneering work of Malvaldi et al on modeling solvation effects in methyl-methylimidazolium chloride by a combination of quantum DFT with three-dimensional RISM[433]); however, as in the case of simpler liquids, those approximations must be checked via diffraction experiments and/or computer simulations. The situation with dynamics is less clear due to slow relaxation processes and mysterious glassy-like mesophases in RTILs,[434] posing questions, whether one can ever reach equilibrium simulating RTILs...

We note that molecular theories were successfully applied to different kinds of EIs with polar solvents and diluted electrolytes, from flat solid/liquid interfaces[371,435–437] to electrolyte solutions sorbed in nanoporous carbon electrodes.[438,439] However, somehow, in the double layer theory of RTILs the progress on developing *molecular-scale* theories was not that advanced. To our opinion, this is partially due to the relatively short history of the subject and partially due to an easy access to supercomputer resources these days and a number of well-developed molecular modeling packages available for researchers. Therefore, in view of the first model theories, which bypassed the level of sophistication of the descrip-

tion of ordinary liquids, the next step was to proceed straightaway to computer simulations that use sophisticated models of ions of RTIL, i.e. realistic force-fields representing interionic interactions. Indeed there are many phenomena (e.g. ion interfacial orientation) that require more detailed description of molecular structure of RTIL ions than it is provided by the course grain models. Generally, the response of real RTILs to the electrostatic field of the electrode is affected by rearrangements of non-spherically shaped ions and more complex structure of force fields acting between them. Every ionic liquid is then expected to display "individual" EDL structure and capacitance features.

However, most of the generic qualitative effects discussed in the previous sections have been reproduced in those computer simulations. Furthermore, by comparing the results with the above described 'physical' toy-model simulations, those 'molecular' simulations were able to reveal, which features of EDL are generic and which are specific for particular liquids.

Due to various interesting molecular-scale phenomena in RTILs at EIs and their importance for different applications there has been published a considerable number of molecular simulations works in the area during the last several years.[208,352,353,387,388,440–456] Molecular modelling techniques were used to study not only neat RTILs at different EIs but also behaviour of RTIL mixtures with polar solvents.[205,457–460] We have opted to discuss here in details only some of the molecular simulation papers, most closely related to the main line of this article.

The role of surface chemistry has been emphasized in the study of Feng, Zhang and Qiao,[389] who have studied the properties of [BMIM][NO$_3$] confined between oppositely charged walls, each imitated by α-quartz like slabs oriented in [100] direction. The distance between the walls was substantial, 6.63 nm for the EDLs on the opposing electrodes not to overlap, so that unlike the pioneering paper of the Belfast group[440] in which the ion distribution profiles of [DMIM][Cl] were studied in a much narrower gap (that led to a partial overlap of the cathodic and anodic EDLs), Feng et al[389] were able to study the properties of individual EDLs. They performed simulations for different fixed charges on the wall. The proximity to chemical reality in this work was not through the description of electrodes, but through the force-fields-based description of the liquid.

Feng et al showed local density of ions depicting the localization of the center of immi-

dazolium ring for cations and the geometrical center of the anion. With increasing surface charge positively, they saw a dramatic increase of the density of $[NO_3]-$ ions near the electrodes. Simultaneously they see a significant accumulation of $[BMIM]+$ ions in 'next' layer. However, since the cations are larger than anions, these two first layers partially overlap. Overall the authors see several layers both of cations and anions. Polarizing the electrodes negatively the two (overlapping) layers swap. With further increase of negative polarization the maxima in the cationic density profiles, move away from the first peak, at the cost of the increase of its height; the first peak for anions substantially moves away from the surface, but more distant peaks are only slightly affected. Interestingly, the first peak moving away becomes in the end higher. The analysis of overscreening (using diagrams of the kind suggested in Refs[322,328,362] was not performed here, but such character of the curves is typical for overscreening. In addition they have encountered with the phenomenon, already noticed in the simulations of Ref.:[353] $[BMIM]+$ cations are persistently adsorbed on the surface; their presence in the first layer is substantial even for mildly positive electrode polarization. The authors explain these effects by enhanced van der Waals attraction between the cation and the electrode, much less pronounced for anions. Differential capacitance here was rather featureless, constant for cathodic polarization and growing monotonously in the anodic range.[462]

Lynden-Bell, Frolov and Fedorov[208] studied the same [DMIM][Cl] but in a wider gap and analysing the EDL molecular structure in detail. In addition to certain findings potentially important for electrode kinetics in RTILs (that we will touch later in the review), they have obtained a number of results that are similar to those of Feng et al.[389] Namely, they detected significant changes in the structure of the ionic profiles as a function of electrode charge. They found that with positive charging of the electrode, anions substitute cations in the first layer that at neutral polarizations are preferentially adsorbed; at negative charges the anions are expelled from the first layer to form a new second layer. The cations in the first layer at low electrode charges are oriented predominantly parallel to the electrode surface (similar observations one can find in the simulation data of Feng et al[389]). However, at high negative charges they tend to orient perpendicular to the interface, maximizing the density of ions in the first layer. They found clear signatures of overscreening in their system. No

capacitance data were reported in their paper to compare with those puzzling data of Feng et al.[389]
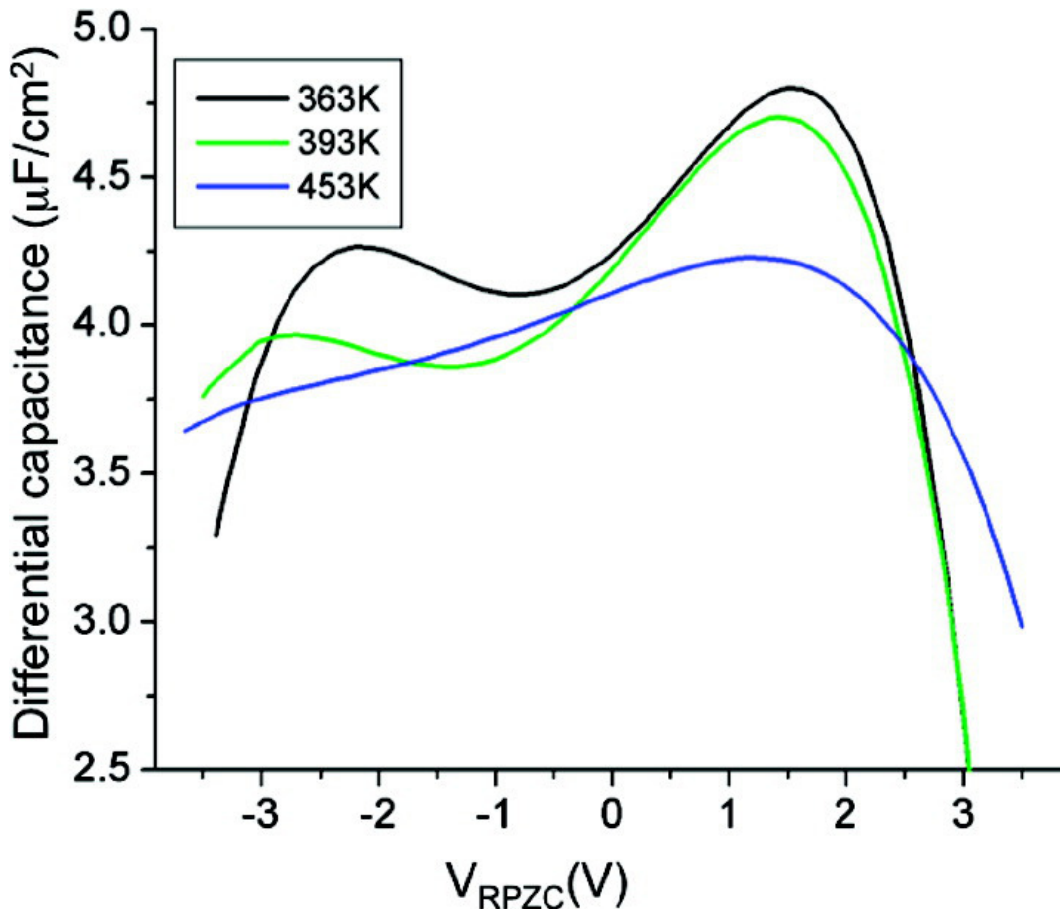
Figure 9: Differential capacitance of EDL in [Pyr$_{13}$][TFSI] simulated in Ref.[388] (the figure is reproduced from this work).

Vatamanu, Borodin and Smith,[388] performed molecular dynamic computer simulations of EDL structure and capacitance for [Pyr$_{13}$][TFSI] near a graphite electrode. Although the electrode was not described in the most primitive way, through a system of fixed charges (the electrode polarization was evaluated by minimizing the total electrostatic energy with respect to electrode charges, each graphite electrode consisting of there graphene layers), this approach could not incorporate the true electronic structure of a semi-infinite semi-metal electrode, i.e. to involve into the simulation the EDL in the graphite. We, thus, temporarily, put away Gerischer's concerns,[295,296] focusing now only the findings of this team about the EDL on the RTIL side. The calculated capacitance in this work has a camel shape structure, except for very high temperatures where the two maxima essentially

57

merge (Figure9). Within the studied broad range of potentials $(-3.5V \longleftrightarrow +3.5V)$ the lattice saturation regime, where $C \propto |u|^{-1/2}$, has not been reached, the capacitance was falling off steeper. A greater structure in the charge density profiles is observed at the positive electrode (the EDL is more compact, and this is reflected in the higher value of capacitance), as compared to negative electrode. The paper shows the density profiles for cations and anions as a function of their position to the electrode at different voltages. An innermost layer is seen 4-5.3Å away from the interface, an intermediate layer at 5.3-7.5Å, and the third layer at 7.5-9Å. At potentials near p.z.c. the cation and anion populate both the first and intermediate layers, with the majority of ion centers located in the intermediate layer. This distribution changes with increasing electrode potential, positively or negatively: the co-ion distribution in the first layer decreases and the co-ion in the intermediate layer initially increases, but only up to 1 V voltage variation (simultaneously, the counterion population in the intermediate layer decreases). At larger electrode potentials, positive or negative, the density of co-ions in the intermediate layer decreases, increasing in the third layer. These are typical signatures of overscreening, although the analysis of it in terms suggested in Refs[328,362] has not been performed.

In the next paper[387] the same group extended their investigation to [Pyr$_{13}$][FSI] comparing their results with those of [Pyr$_{13}$][TFSI]. [FSI]- is a more compact molecule than [TFSI]-. Correspondingly, with electrode polarization, the density profiles of counterions showed a stronger increase of the first peak and the sharpening of their overall distribution, while the co-ions move out of innermost layer of EDL. The first peak of [Pyr$_{13}$]+ moves closer to the electrode, as the potential becomes more negative, whereas the position of the first peak of the [FSI]- does not significantly change with the increase of the positive potential. More subtle details are revealed in the paper including the distribution of orientations of ions relative to the surface as a function of electrode potential, that demonstrated substantial differences between [FSI]- and [TFSI]-. Remarkably, in this work the authors went to much higher electrode polarizations in order to check both for [TFSI]- and [FSI]- cases the existence of the 'crowding law' - the inverse square root dependence for capacitance, $C \propto |u|^{-1/2}$. They found this regime, but only for unrealistically high voltages, about 15 V (achievable in simulations but not experiments). Close below those voltages they found the crossover between

overscreening and crowding. Of course, this is a purely academic investigation, because the decomposition of RTILs start at about 3 times lower voltages. Similarly to Georgi et al,[322] Vatamanu et al find the neutral groups of ions pointing away from the surface at large potentials, but they see it at much higher potentials than in Ref.[47] The authors explain this difference by the need to assume a stretched tail conformation first, needed to repel neutral tails from the surface, which requires higher voltages; no estimates was given, however, how large voltage it would take, to substantiate this interpretation.

A recent paper by Paek, Pak and Hwang[461] reported MD simulations of the EDL and interfacial capacitance at the interface of [BMIM+][PF$_6$-] with plane graphene. The EDL properties on the liquid side appeared to be qualitatively similar to the conclusions of other studies of this kind as discussed above. However, a dramatically new element of this work, was taking onto account the quantum capacitance of graphene in series with the EDL capacitance of the liquid half-space. This was essentially a development of Gerischer's ideas[295,296] who related the capacitance of a semi-infinite graphite with the electronic density of states and the Fermi-distribution in graphite. In Ref.[461] this has been done for a two-dimensional graphene, for which the dependence of the density of states on electric field is different. The quantum capacitance of graphene in the work of Paek et al[461] was found to be (i) smaller than the capacitance of the EDL in the liquid half-space and thus determining the overall capacitance of the two capacitors in series, and (ii) of U-shape. Having found a clear bell-shaped capacitance for the EDL in the liquid, the authors nevertheless obtain a U-shape-like results for the total capacitance, dominated by the contribution from the graphene electrode. The results of this computational study correlate well with the recent experimental work by Uesugi et al[310] in which different contributions to the EDL capacitance of the graphene-RTIL ([BMIM+][PF$_6$-]) interface were measured. We thus witness how the pioneering Gerischer's idea takes-off in the graphene era.

5 Experimental studies of EDL in RTILs at flat electrodes

5.1 EDL capacitance

Before 2000, to the authors' knowledge, the only two reports on the EDL capacitance in RTIL were two sets of curves for the salts based on a mixture of aluminum chloride with 1-butylpyridinium[88] and 1-ethyl-3-methyl imidazolium cation $[EMIM^+]$ and $[Tf^-]- = CF_3$ SO_3^-, $Me^- = (CF_3SO_2)C^-$, $[Im^-] = (CF_3SO_2)N^-$ anions[463] (in both studies a mercury electrode was used). Then in 2003 the group of Mao reported the capacitance curve for a non-chloroaluminate RTIL, $[BMIM][BF_4]$.[464] All capacitance curves reported in these works have little in common with Gouy-Chapman shapes but these publications, although pioneering, remained a scientific curiosity before the feature article[52] addressed attention to the fact that the EDL capacitance in RTILs should look different from that in diluted electrolytes and the concepts of bell and camel shape were suggested to the ionic liquid electrochemists. Since 2007 several experimental groups started to publish data on EDL capacitance in various RTILs.[398,465–477] We cannot review all of them here but stop on few milestones.

Systematic studies were undertaken by the group of Ohsaka,[465–471] take alone the article[468] in which the authors compared systematically their experimental data for a set of RTILs based on combinations of cations and anions shown in Figure 10 (and few others) at different electrodes.

$[EMI^+]$ $[BMPyr^+]$ $[TMPA^+]$ $[DMOA^+]$
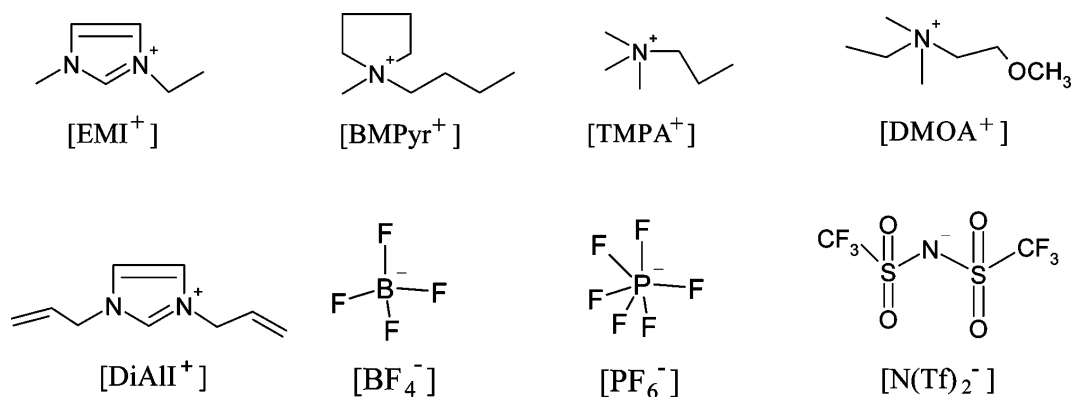
$[DiAlI^+]$ $[BF_4^-]$ $[PF_6^-]$ $[N(Tf)_2^-]$

Figure 10: Cations and anions selected in Ref.[468] for capacitance studies of RTILs at different electrodes. The figure is reproduced from Ref.[468]

That work has classified different types of capacitance curves observed, most of which were either of bell or camel shape; below, we reproduce the pertinent columns of the summary in Table 2.

Table 2: Summary of the features of the EDL capacitance for indicated electrode/RTIL combinations (reproduced from Ref.[468] with some adaptation). C_d states for differential capacitance, GC for Glassy Carbon. (note: here $N(Tf)_2^-$ states for bis(trifluoromethanesulfonyl) imide anion that is also called TFSI or TFSA in the literature (see section 10)

Results Obtained From the Differential Capacitance Curves Measured at Different Electrodes in Various RTILs

			characteristics of the capacitance curves		
RTILs	electrodes	shape	maximum (minimum) or p.z.c./V^a	hump/V^a	C_d at maximum (minimum)/ $\mu F\ cm^{-2}$
[DMOA$^+$][N(Tf)$_2^-$]	Pt	bell-like	−0.2	−	11.4
	Au	bell-like	−0.45	0.3	19.5
	GC	U-like	−0.7 (minimum)	−	9.6
[DiAII$^+$][N(Tf)$_2^-$]	Pt	bell-like	−0.25	<−1.0	11.5
[TMPA$^+$][N(Tf)$_2^-$]	Pt	bell-like	−0.78	−0.43	11.4
		(camel-like)	(−0.58) (minimum)		
[BMPyr$^+$][N(Tf)$_2^-$]	Pt	bell-like	−0.87	>0	8.7
[EMI$^+$][BF$_4^-$]	Hg		−0.23 (minimum)^b	−0.34^b	19.7
	Au		−0.51 (minimum)^b	0.45^b	12.6
	GC	U-like	0.09 (minimum)^b		12.8
[EMI$^+$][Cl$^-$]	GC	camel-like	0.32 (minimum)^c	1.0 and <0^c	23

*

$(^a)$ Value versus Ag wire.
$(^b)$ Value versus Ag/AgCl (solid).
$(^c)$ Value versus Ag/Ag/RTIL.

We note that U-like shapes were obtained on glassy carbon (GC) electrode (see Table 2). Gerischer's concerns[295,296] about a possibility of extracting information on the EDL in the liquid phase, whereas they in fact may refer to the electronic EDL on the electrode side, may be applicable to these measurements. However, the same glassy carbon electrode exhibited in another RTIL a camel shape. To rationalize generically why some of the combinations deliver a camel - and some a bell shape, is difficult, as we do not know the *real* compacities of these RTILs (that are difficult to estimate using the available theories due to the complex shapes of the ions; developing techniques for reliable estimation of real compacities is a subject of ongoing research in several theoretical groups). On the other hand, independently of the compacity, the [EMI+][Cl−] camel shape data well correspond to the effect of neutral tails unraveled in Ref.[322] However, some other of the considered cation-anion pairs could

have delivered a similar effect, but they still bring bell shapes. The treatment of the data at the wings encouragingly *supports the lattice saturation limiting law*; however, it seems to begin 'too early': no theory, and the more so no simulation predicted it for such small voltages. The molecular force-field computer simulations, as discussed above, were supposed to bring more light on the reported features, but perhaps more systematic variations, i.e. within the similar sorts of ions, might still be needed. A typical bell shape drawn in Ref.[468] is reproduced below in Figure 11.
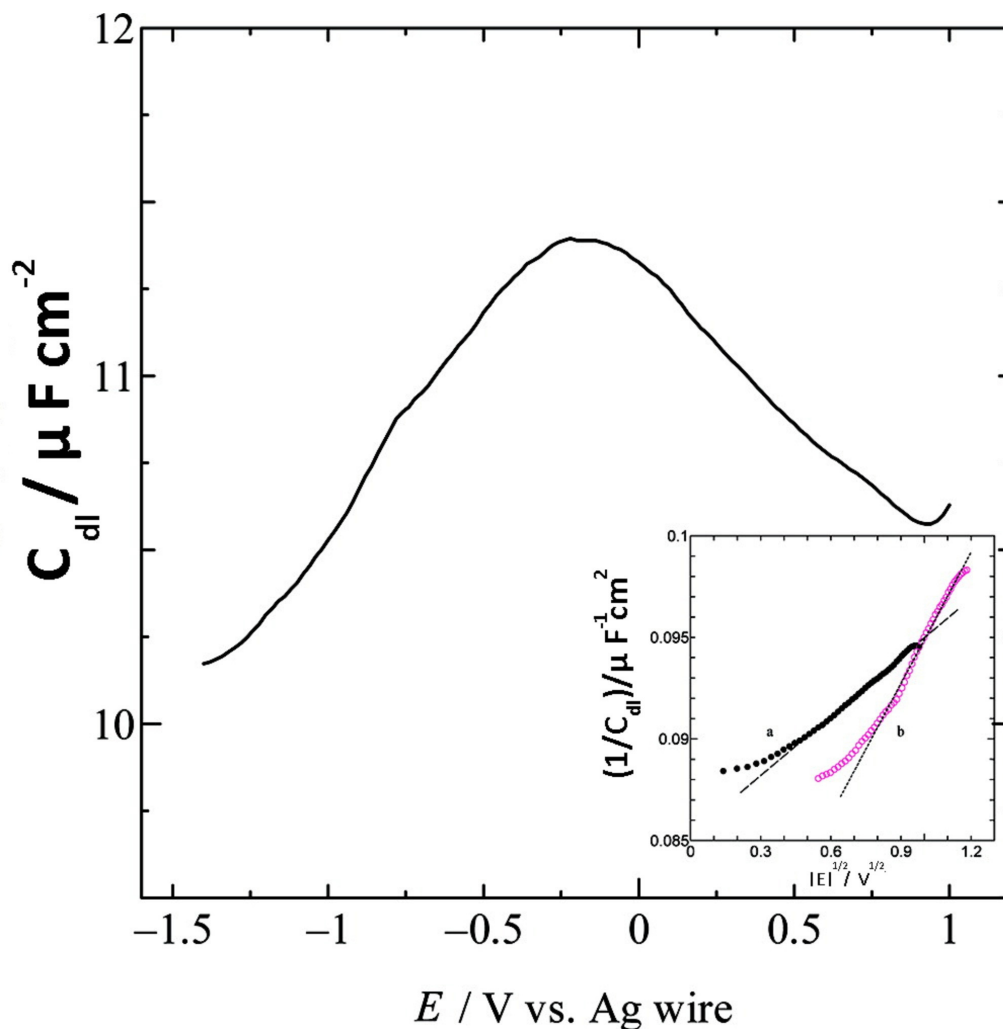
Figure 11: Typical capacitance-voltage curve measured at the platinum electrode in argon-saturated $[\text{DMOA}^+][\text{N(Tf)}_2^-]$ reproduced from Ref.[468] C_{dl} states for the measured double layer (differential) capacitance. Inset shows the plots of the inverse capacitance (in $\mu\text{F}_{-1}\text{cm}^2$) vs the square root of the absolute value of voltage drop across the EDL, in $V^{1/2}$, derived from the data of the (a) right and (b) left wings of the measured capacitance curve.

The group of Bing-Wei Mao performed measurements of the capacitive response simul-

taneously with the investigation of the structural changes of and at the interface at atomic resolution, giving new challenges for the theory. They reported capacitance data for (100) face of single crystal gold electrode[478] in [BMIM+][BF$_4$−]. A distinct peak in the measured capacitance could be classified as a bell-type behaviour, however in each marked sections of the curve the structure of the electrode surface, studied by STM, looks different, partially related with the electric-field-induced and ion-adsorption influenced surface reconstruction of Au(100), the phenomenon intensively studied earlier in ordinary electrochemical cells with aqueous electrolytes (for review see[250]). But there is in fact more to it. The work of the Mao's group revealed the richness of the structures of ions at the interface. An apparently clean bare surface of the metal is seen at -0.65 V indicating a state without specific adsorption of cations and anions. Moving the potential to -0.7 V leads to the formation of a loose layer formed by disordered adsorption of BMIM$^+$ cations. At higher negative potentials the latter undergoes a disorder-to-order transition, with BMIM$^+$ rings taking a near-parallel orientation, with a slight incline, relative to the surface. Interestingly, ordered adsorption of BMI$^+$ occurs only on Au(100) surface, but, not on Au(111). This fact reveals the necessity of some kind of structural commensurability of the surface and adsorbed BMIM$^+$. The adsorption of the of BF$_4$− anions starts at potentials positive of -0.1 V up to 0.4 V in the form of ordered $\begin{pmatrix} 3 & -1 \\ -1 & 3 \end{pmatrix}$-structure. Thus, the maximum of the bell corresponds to a potential region of a crossover from anion adsorption to cation adsorption. Changes in the lateral structure of the electrode surface or layers of adsorbed ions is not something that so far was incorporated to the theory of EDL in RTILs.

Lockett, Sedev and their collaborators[398,472] systematically studied several RTILs with different size of cations and anions, at different temperatures. All curves, as measured between -1.5 V to +1.5 V reveal camel shape curves, the qualitative features of which seemed to be in line with the results of Refs.[52,322] However, the temperature dependence looks different. Except at the wings the capacitance increases (quite substantially at maxima) with the temperature. No simple mean field theory predicts anything like that, neither coarse grain simulations mimic it.[329] The authors, however, give it an interesting interpretation. They attribute it to the presence of ion complexes in imidazolium-based ionic liquids, as was

shown by time-of-flight secondary mass spectroscopy,[479] as well as dielectric spectroscopy[480] that indicated that some 8% of all ions in RTILs may be bound in contact ionic pairs. The increase of temperature may unbind such pairs, and they may additionally contribute to the capacitance response. How, however, 8% of such releases, can contribute a two times increase in capacitance with temperature is yet unclear (we also note that the actual degree of ion association in RTILs is currently a subject of intensive debates in the literature[481–486]). It might be interesting to adopt and explore pertinent ideas of the almost forgotten Gurevich and Kharakats statistical models of adsorption,[311] an interesting option for a future investigation.

The list of further papers reporting the capacitance could be continued. It is timely, however, to refer to the work of Kolb and Paikossy.[487] They performed a detailed investigation of capacitive processes in RTILs using high resolution electrical current scale (the μA cm^{-2} scale in contrast to the mA cm^{-2} used in most of the capacitance measurements with RTILs). The conclusion of their paper was that all data reported so far should be taken with care because the electrical impedance of the interface contains a remarkable **c**onstant **p**hase **e**lement (CPE) even at atomically smooth, single crystal electrodes that they have studied, and, therefore, the capacitive element of the equivalent circuit is practically impossible to extract. Kolb and Paikossy related the observed CPE to some slow relaxation dynamics in the studied RTIL (in their case, 1-Butyl-3-methyl-imidazolium hexafluoroposphate). From that fact they came to conclusion that such equilibrium quantity like equilibrium capacitance for RTILs which behave more like glasses than equilibrium media,[434] is very difficult to achieve at realistic experimental conditions. They pointed out that earlier theories of the EDL and the double layer capacitance should be updated to take into account kinetic process in RTILs. Understanding the importance of issues raised by the authors of Ref.,[487] we note that the capacitance itself is an equilibrium quantity, which characterizes the relationship between the charge on the electrode and the voltage across the double layer. The fact that impedance measurements cannot reliably assess equilibrium characteristics is not a problem of the EDL theory that operates with equilibrium properties, but rather a problem of experimental techniques available these days.

A different way to assess the capacitance is to extract this from the plateaus of the cyclic

voltammetry curves,[488,489] that show the current, $j(t), vs$ voltage, $U(t)$. Since voltage in one sweep is varied with a constant speed: $U(t) = vt$, and current at the plateu is constant, then in principle $\frac{j}{v} = \frac{dQ}{Sdt}/\frac{dU}{dt} = \frac{d\sigma}{dU} = C$. This method of measuring the capacitance suffers from low accuracy, in particular if one wants to get not just rough estimate of it, but its voltage dependence. Recent investigation of EDL capacitance in $[\text{EMIM}^+][\text{BF}_4^-]$ and $[\text{BMIM}^+][\text{BF}_4^-]$ extracted from electrochemical impedance spectroscopy and from cyclic voltammograms has shown drastically different values and shapes of $C(V)$,[489] has led the authors to pessimistic conclusions about the reliability of assessing capacitance from impedance data, whereas frankly it is not clear which of the two methods gives poorer results.

With the due warning about possible artifacts in extraction of capacitance values from electrochemical impedance data and general scepticism about the possibility of obtaining reliable capacitance data for RTILs,[490,491] Kolb and Pajkossy estimated the capacitance from their impedance data, as being close to $6\mu F/cm^2$ and practically not varying with voltage. However, very recently a thorough investigation of Rolling and co-workers has shown that the situation may not be that hopeless, if the impedance data are properly scrutinized.[492,493] They also argued against an artifact which, to their opinion, has led[487] to the reported voltage-independent capacitance.

5.2 Molecular-level structure of the EDL

As we have earlier mentioned, the capacitance is not the only measure of EDL properties. Mezger et al[494,495] reported the synchrotron X-ray diffraction data on the structure of the distribution of cations and anions at spontaneously charged sapphire surface. Unfortunately the charge on that surface could not be independently varied, and thus no information could have been obtained how those profiles change with voltage. Nevertheless, the results were spectacular. They have unambiguously shown the oscillating patterns of charge distribution and in ionic liquids overscreening in a RTIL at an EI, subject to evaluated values of surface charge. Note that those results were published simultaneously and independently from the simulations studies of Refs.[328,362] that revealed very similar features of the overscreening but also explored the effect of the electrode polarization. In a follow up papers, Mezger at al[496] as well as Nishi et al[497,498] has shown the effect of layering near free surfaces of the

corresponding ionic liquids.

The soil was ready for X-ray studies of the structure of ionic liquids at electrodes at varied voltages and an interesting work of this kind has been recently reported.[499] X-ray reflectometry studies investigated the structure of N,N-diethyl-Nmethyl-N-(2-methoxyethyl) ammonium] [bis(trifluoromethanesulfonyl)imide] at the single crystal Au(111) electrode. Not only the overscreening was clearly demonstrated there at low voltages, but also its weakening at voltages up to ± 3 V, qualitatively in line with the simulation studies of Ref.[362] Voltages of that scale, were shown to be yet not sufficient to turn on in full the crowding effects; that is perhaps due to the effect of the tails: several simulations works show that the presence of longer neutral tails of ions shifts the onset of lattice saturation to larger voltages (c.f.[47,322,388]). The observed asymmetry in the ionic liquid response to the sign of the voltage was also not something surprising as the shape and size of the cations and anions used in this work is substantially different, consequently affecting the structure of the first layers at different electrodes depending on the electrode polarization.

Interesting attempt to perform neutron reflectometry studies of the structure of EDL as a function of electrode potential was recently reported in Ref.[273] The limited wave-vector transfer range prevented observation of cation/anion layering. Somehow, in the available Q-range only subtle differences were observed between the reflectivity data at three different applied potentials. The data analysis revealed an excess of [C4mpyr]$^+$ at the interface, with the amount decreasing at increasingly positive potentials, but a cation rich interface was found even at a positively charged electrode. Seemingly some strong chemisorption prevented dramatic changes of the content of the [C4mpyr]$^+$ cations on the gold electrode. However, the simultaneously measured capacitance curves showed signatures of a camel-shape behaviour with strong decaying wings at large and positive and negative potentials, which if our understanding of the data is correct, must indicate crowding. A dip on the capacitance curve close to the pzc (see Fig.2 in this work) is likely to indicate the role of substantial neutral tails of [C4mpyr]$^+$ cations, acting as latent voids for the local increase of the charge density and causing the initial rise of capacitance, in the spirit of the predictions of Ref.[322]

The exploration of the ionic structuring in RTILs in electrochemical environment, where

one can change the electrode potential and trace how the structure will change has been successfully pursued using other surface-specific experimental methods. Atkin and co-workers applied AFM for studying the 'layering' behavior of ionic liquids, again not in electrochemical cells.[500–502] That approach has been later extended to electrochemical interfaces.[503] The latter work has studied the interface of Au(111) with two ionic liquids, $[Py_1,4]$ [FAP] and [EMIM][FAP], by measuring AFM force-separation profiles at different electrode potentials. Figures 1 and 2 of that article had unambiguously demonstrated the layered structures of the EDL in these RTILs, revealing typically between 4 to 7 layers (signatures of layering in the force-distance curves is consistent with the diameters of ions). It was found that negative polarizations stabilize the layered structure; positive polarization has the same but a weaker effect on layering. The authors relate these differences with the difference of the molecular structure of the cations and anions in the both liquids. But the common trend is that with polarizing the electrode (negatively or positively), both the number of ionic layers and the force needed to rupture them increases. Comparing the two RTILs studied, they found that $[Py_1,4]$ [FAP] delivers more rigid structures than [EMIM][FAP], attributing it to an on-one-atom localization of charge in $[Py_1,4]^+$, as compared to more delocalized structure of charge in [EMIM]+. We believe that this was the first time when the EDL structure in RTILs was probed by 'touching the ionic layers in it one by one'.

Note that Perkin, Albrecht and Klein[66] (who used the surface force apparatus[239] technique) reported similar normal-force measurements of another RTIL, $[EMIM][EtSO_4]$, confined between two spontaneously charged mica surfaces. In that work they could distinctly detect about 3 layers. But their setup was not an electrochemical one, and the charge on the surfaces was not variable (Perkin's group is currently working on modification of the surface force apparatus techniques for in situ measurements in electrochemical environment[504]).

In their latest paper, Hayes et al[505] have studied interfacial structuring in a series of dialkylpyrrolidinium-based ionic liquids induced by confinement. They found that ionic liquids containing cations with shorter alkyl chain form alternating cation-anion monolayer structures, similar to the interfacial behavior in the liquids studied in Ref.;[66] however in a RTIL with cations having a longer alkyl chain they observed well-pronounced bilayer structures. The crossover from monolayer to bilayer type structures occurs between chain

67

lengths with the number of alkyl groups $n = 8$ and 10. The bilayer structure for $n = 10$ involves full inter-digitation of the alkyl chains. Thus the structure in such liquids appeared to be very different than in 'simple' imidazolium-based ionic liquids with short alkyl chains. Existence of the bilayer type structures was not unexpected though (c.f. Fig.6 of Ref.[52]); but the work of Perkin et al provided a solid evidence of their reality.

Inspired by the latter two papers, one may suggest conventional notions of *'simple ionic liquids'* (composed of ions with short tails) and *complex ionic liquids* (with at least one sort of ions having long tails), which are expected to display different structural behaviors in the bulk and at interfaces.

In continuation of this topic it is worth to mention that the approach of Hayes et al[503] has been extended by the group of Bing-Wei Mao[506] in which they have studied the structure of gold electrode/ 'simple ionic liquid' interface Au(111)/[BMIM][PF$_6$]. They showed, in particular, a graph with the dependence of the force at the first and the second interior layers on electrode potential. They note that the first layer always show reduced thickness regardless of the polarity of the electrode and indicated that the interaction between the surface and the ions of the first layer is the strongest and it promotes the most compact structure. Next, the force is higher at cathode polarizations (just like in Ref.[503]) than at the anode polarization of the electrode, indicating that the cation-rich layers do form more rigid structures than the anion rich layers. Hayes et al[503] suggested already that the cations of the innermost layer lie flat on the surface at large negative polarization, but neither this work or the work of Mao[506] offer a molecular-scale interpretation why this should be so. Note that in the simulations of Refs[47,322] neutral tails of cations got expelled from the electrode with increasing negative electrode polarization. This puzzle remains to be understood.

In another paper of the Mao's group, the structure of interfacial layers was studied using in situ STM.[478] That work has demonstrated a complicated interplay between building micellar vs 'worm-like' ordering of cations and the voltage affected structural transitions (surface reconstruction) of Au(111) and Au(100) electrodes. They established tricky correlations between the crystallography of gold surfaces and the lateral structures in the adsorption layers, visualized by STM. At the same time this study shows that with a target of rationalizing first the effect of electrode potential on the layered structure in RTIL, it might be better to stay

away from gold surfaces, which themselves undergo field-induced and adsorption-affected structural transitions[250] that in turn affect the structure of the ionic layers.

A complex AFM, STM and Distance Tunnelling Spectroscopy study has been reported recently as a result of collaboration between the groups of Atkin and Endres.[507] One of the conclusions of this sophisticated study was that "the electrode potential dictates the extent of multilayering, as the number of layers detected and the force required to rupture these layers increases with cathodic or anodic potential". Because the methods used in this work cannot distinguish the prevailing sign of charge accumulated in the layers, this conclusion cannot answer, do we encounter here with the onset of a crossover between overscreening and crowding (perhaps it is unlikely, as voltages had been varied here only between -2 to $+2$ V (vs. Pt reference electrode)). It is not entirely clear that the observed multilayered structures in this work are formed due to the overscreening effect, but the above mentioned X-ray reflectivity study pushes one to expect that this might be the case.

To summarize, the layered structures in RTILs observed in the works discussed are quite distinct. Their lateral structures, as well as profiles can be quite complicated though and they depend on the structure of the ions, in particular the extension of their organic un-charged tails. When these tails are not too long, normal distributions demonstrate typical overscreening profiles (*i.e.*, excessive value of the countercharge in the first-layer counterions with respect to the adjacent surface charge on the electrode), highlighting the critical role of charge-induced nanoscale correlations of the RTIL. These observations generally confirm key aspects of predicted overscreening structures in the EDL in 'plain RTILs', while revealing more intricate structures in complex RTILs. These recent experimental achievements suggest that the existing theoretical knowledge of main principles of the EDL formation in ionic liquids provide us a good baseline for understanding the fundamentals of nanoscale response of RTILs at charged interfaces.

5.3 Structural transitions in the EDL: from multilayer to monolayer structure

Although the articles discussed above provide a number of experimental and molecular modelling observations of multilayered structures formed at RTIL-solid interfaces, there is no general agreement in the literature about this. Such, Baldelli in his recent perspectives article[508] questions the formation of multilayers at the interface in ionic liquids. There is a suggestion in that work that at certain conditions the structure of the EDL in RTILs might consist of a single monolayer of counter-ions close to the electrode surface with RTIL ions further from the electrode behaving similar to the bulk liquid phase. This opinion is based on a critical review of experimental works that studied interfacial RTIL systems by the sum frequency generation (SFG) spectroscopy technique[509–512] (see also an earlier review by Baldelli on the surface structure of RTILs at electrified metal interfaces[513]). The discussed results suggest that ions at the solid-liquid interface are organized into essentially one ion-layer, a Helmholtz-like structure in which the orientational order beyond this layer is negligible.

This view on the interfacial structure of RTILs correlates with other independent experimental findings. Such, Freyland et al. reported a monolayer structure of PF_6 anions adsorbed at electrified Au(111) electrode surface.[514] This study investigated 2D phase transition of PF_6 adlayers at the electrified ionic liquid/Au(111) interface with [BMIM][PF_6] by in situ STM. They found that at potential above -0.2 V vs Pt reference, PF_6 anions form a dense monolayer with Moire-like patterns, as revealed by STM images. In most of the studied cases such patterns seemed to coexist with the uncompressed structures. The same paper reports a structural transition at the interface at more negative voltages with the structural changes occur gradually with a $(\sqrt{3} \times \sqrt{3})$ phase forming at approximate -0.45 V.

Recently, Castillo et al used the solid-state NMR techniques to investigate the structure and dynamics of [BMIM][PF_6] at the interface with silica (not charged) and laponite clay (negatively charged) surfaces.[515] They found that in the case of an uncharged amorphous support, such as silica, the ionic liquid phase behaves as an almost liquid phase but with restricted mobility. However, their results suggest that on the negatively charged layered

surface of laponite clay, the ionic liquid can form two different phases, a thin solid layer (close to a monolayer) and a truly liquid phase over the first solid layer, showing that the order imposed by the clay is not transferred beyond a few monolayers of supported solid phase. We note that there are other experimental works reporting the solid-like layer formation in RTILs, see e.g. Refs.[516,517] (these works also reported the lateral heterogeneity of the interfacial structures).

The contradiction between the different experimental observations of the EDL structure in RTILs) discussed above may be (at least partially) resolved by the results of recent modelling work of Kirchner et al[224] where the authors performed large-scale MD simulations of a coarse-grain model RTIL between two non-polarisable electrodes (the same model as in Ref.[328]). It was found in that for most charge densities studied in this work the EDL has a multilayered structure with multiple alternating layers of counter and co-ions at the electrode-RTIL interface; however, at certain charge densities the alternating multilayer structure of the electrical double layer undergoes a structural transition to a surface-frozen monolayer of densely packed counter-ions (Moire-like structure). At this point the dense ordered monolayer of counter-ions close to the electrode surface coexists with apparently non-structured RTIL further from the electrode. The points of the structural transitions are determined by the balance between the surface-counter-ion attraction and the ion-ion steric repulsion. The authors of Ref.[224] found that the multilayer to monolayer transition is directly correlated with the surface charge density, counter-ion diameter and counter-ion charge; thereby indicating that at the point of the structural transitions:

- there is total charge compensation of the electrode charge by the interfacial monolayer of counter-ions at the transition point, i.e. the phenomena of overscreening and alternating layers are almost absent at this point;

- there is dense geometric ordering of the interfacial counter-ions in a form of a dense ordered structure (so-called Moire-like structure).

We note that Ref.[224] is a pilot study that used a crude model both for the RTIL and for the electrodes. Therefore, the conclusions from this work are in no way final. More theoretical and experimental studies are necessary to explore the effects of structural transitions in the

EDL in RTIL-based interfacial systems.

5.4   EDL properties: a closer look at temperature dependence

The temperature effect on the properties of the EDL in ionic liquids is a longstanding issue. Since the 60-70s there have been intensive debates on the nature of the temperature dependence of the double layer capacitance in HTMS (e.g. molten alkali halides) within experimental[5] and theoretical & computational communities.[258,338,518] However, due to a number of experimental problems related with electrochemical measurements in high temperature molten salts, there was no general agreement in the literature about the true character of this dependence.

The recent wave of interest to electrochemical applications of RTILs at cold, room, and elevated temperatures provoked a series of new experimental[398,472,477,490,491,519,520] and computational[387,388] studies on the temperature effects on EDL properties of RTILs. Nevertheless, a review of the published results on the temperature dependence of the differential capacitance in RTILs shows that this question remains controversial.

Indeed, in several experimental studies[398,477,490,491,520] on different RTILs at different electrodes it was shown that the capacitance values increase with increasing temperature. On the other hand, Drüschler et al[519] reported new experimental results on the influence of temperature on the differential capacitance for the extremely pure ionic liquid 1-butyl-1-methylpyrrolidinium tris(pentafluoroethyl)-trifluorophosphate ([Py1,4][FAP]) at an Au(111) electrode. In this work they performed careful analysis of broadband capacitance spectra of the electrode/RTIL interface obtained by combining electrochemical impedance spectroscopy with in situ STM and in situ AFM techniques. In contrast to Refs.[398,490,491] they have shown that the capacitance for fast capacitive process decreases with increasing temperature from 30 to 90°C. Moreover, these findings correlate with molecular simulations data by Vatamanu et al,[388] who investigated the differential capacitance for N-methyl-N-propylpyrrolidinium bis(trifluoromethane)-sulfonyl imide ([pyr13][TFSI]) near a graphite electrode and also observed negative dependence of C_d from temperature. They attribute this to 'melting' of the EDL; melting of the interfacial structure at neutral graphite interface at higher temperatures was also reported in a simulation work by Dou et al;[448] this effect has been also

observed experimentally in the recent experimental work of Nishi et al (X-ray reflectivity measurements)[498] on the temperature dependence of multilayering at the free surface of an RTIL, (trihexyltetradecylphosphonium bis(nonafluorobutanesulfonyl)amide); the authors of the paper note, however, that the effect depends on the RTIL molecular structure (e.g. their results have shown little temperature dependence of the multilayer structure for another RTIL studied in this work, trioctylmethylammonium bis(nonafluorobutanesulfonyl)amide).

We already discussed above that the comparability of carbon materials with metal electrodes remains to be questionable because although carbon materials (glassy carbon, porous carbon, graphite or graphene) might reveal some metal properties they also possess semi metal properties as well. Skinner et al.[297] emphasized that the temperature-effect on the EDL capacitance at the semi metal and semiconductor electrode can be determined by the T-dependence of the Debye length in the electrode if the contribution of electronic EDL in the electrode to the total capacitance of the interface is dominating. This comes primarily from the variation of the number of charge carriers. In fact, this effect was known a while ago in electrochemistry of semiconductors.[521]

As the literature analysis shows, currently there is no commonly accepted opinion about (i) should there be any general laws for temperature-dependence of the EDL differential capacitance in RTIls, or should it be liquid-specific; (ii) how much the electrode potential should affect the temperature dependence in different potential range, except for may be the discussed weak or no dependence in the lattice saturation regime. To make things worse, not always is there an agreement about the credibility of experimental data. Furthermore, most of the experimental studies on the temperature dependence of the capacitance had been performed within a relatively narrow voltage range, $\approx \pm 1V$ interval, or even narrower.

6 Electrode reactions and their kinetics in RTILs

RTILs have attracted much of interest as 'designer solvents' for chemical reactions in the bulk- for synthesis and catalysis;[35,50] however, they are equally interesting for electrochemical reactions at electrodes, electrosynthesis and electrocatalysis due to their electrochemical and thermal stability, nonflammability/nonvolatility, electroconductivity and ability to dis-

solve different classes of substances.[17,19,24,35,50,173] During the last decade there have been published large amount of literature on the subject, covering this vast area of research in detail, take alone extraction of metals from RTILs and electrodeposition (for reviews, see e.g.[16,23–25,522–525]). We will not even try to overview this topic in full details here, referring the reader to the literature quoted above. Instead, we will just make a few brief comments on the basic principles behind electrode processes in RTILs, and how their kinetics are related with the properties of electrified interfaces and their response to charging. Dwelling on those principles, we will highlight, as we see them now, the main avenues for the development of the theory, which is here pretty much behind the existing experiments and applications.

6.1 Pros and contras for using RTILs as solvents for electrochemical reactions

Firstly, we note that by selecting a proper cation/anion combination, RTILs can solubilize many substances from metal salts to non-polar organic molecules and cellulose;[35,50,135] therefore, RTILs (as a class of compounds) can be used for a much wider range of applications than conventional solvents. However, this is not the only benefit of using RTILs as solvents for electrochemical reactions. When one chooses a solvent for electrode reaction of dissolved species of interest one wants those species to react, but not the solvent. Thus each solvent has its 'electrochemical window', i.e. the range of potentials within which it is electrochemically passive. As discussed above, the edges of that window are different for different cations and anions that at large enough voltages can themselves become the redox/oxidation species.[16,26,107,170,211] Within those windows, however, many inorganic ions can undergo reduction/oxidation reactions, depending on the electrode polarization, without unwanted secondary Faraday processes involving the electrochemical transformations of the ions of the 'solvent' RTIL. The anodic potential edge may not vary much when dealing with most 'popular' ions such as BF_4- , PF_6- , and TFSA-, but the cathodic limit is more variable depending on the identity of the cation, normally increasing with its size (see also recent review by Lane[212] that presents the specific reduction reactions that may occur at the negative electrode in commonly used RTILs).

The possible breadth of 3-5 V of that window for a considerable number of known RTILs is their substantial advantage, because the electrode polarization has an exponential effect on driving the reaction, and being able to increase the overvoltage, say twice, may results in orders-of-magnitude increase of the reaction rate. We recap on it in a more detailed discussion below.

However that advantage comes at the cost of slow migration of the reactants to the electrode. The majority of RTILs have decent intrinsic ionic conductivity due to the high density of ions. However, the mobilities of ions in RTILs, including the solute, reactant ions, are inversely proportional to the viscosity, which at room temperature is typically one or even two orders of magnitude higher for some RTILs than in ordinary electrolytes.

On the other hand, in general, viscosity of RTILs decreases with the increase of temperature[184,194] (for more details and for an updated list of RTIL viscosities see Refs.[17,79,526]). Correspondingly, the mobility of ions can be greatly increased with the temperature. Due to their low vapour pressures, RTILs as solvents can be operated at elevated temperatures overcoming the viscosity problem and related transport limitations.[222]

6.2 Electrochemical reactions in RTILS: electron transfer limited or ion transport limited?

If the reactions are reactant transport limited, we should observe the diffusion limiting current $J_{lim} \approx e z_{tr} D_{reac} \frac{c_{reac}}{L_{dif}}$ where D_{reac} is the diffusion coefficient of the reactant, c_{reac}, is the concentration of reactants in the bulk, L_{dif}, is the effective diffusion length, $z_t r$ is the number of transferred electrons in each elementary act of reaction. The properties of RTIL will enter through D_{reac} and L_{dif}. From the theoretical point of view it will not be very interesting. However, using the techniques of the rotating disk electrode[60,527,528] one can reduce diffusion limitations and extract the parameters of the electrochemical electron transfer rate. Recently this has been shown feasible in RTILs,[529] although it was previously considered difficult due to their high viscosity (for the discussion of factors hindering the application of this technique in RTILs, see[530]). We will therefore focus below on the current voltage characteristics limited by the electron transfer reaction, and particular by those with

75

small electron tunneling probabilities in the transitional configuration of the nuclear degrees of freedom, i.e. dwell on the case described by theory of nonadiabatic transitions.

6.2.1 Redox current in quantum electrochemistry

It will be useful to put down the most complete expression for the electrode current at a given electrode in order to illuminate the factors that may be important and specific for RTILs. In spite of generality of these expressions, they still contain a number of approximations about which one can read in Ref.[531] Hence,

$$J = J_c - J_a \qquad (24)$$

where the cathodic and anodic currents, related respectively with the electron transfer from the electrode to the oxidized acceptor of electrons and with the electron transfer from the reduced donor of electrons to the electrode, are given by

$$J_c = ec_{ox}\Delta z \int dE \rho(E) n(E) W_c\{E; V_1(V)\}, J_a = ec_{red}\Delta z \int dE \rho(E)[1-n(E)]W_a\{E; V_1(V)\}, \qquad (25)$$

with c_{ox} and c_{red} being the concentrations of oxidized and reduced species on the effective reaction plane, Δz is the effective width of the reaction zone, $\rho(E)$ and $n(E)$ are, respectively, the electron density of states and the Fermi-function at the electron energy level E, $W_c\{E; V_1(V)\}$ and $W_a\{E; V_1(V)\}$ are, respectively, the transition probabilities of the elementary acts of the cathodic and anodic processes. The latter quantities depend on the electron energy level E from which the electron is transferred to the acceptor in the cathodic transfer and to which the electron is transferred from the donor in the anodic transfer. The both transition probabilities depend on the potential drop between the electrode and the reaction plane $V_1(V)$ where the donor or acceptor are located, which generally may not be equal to the total potential drop between the electrode and the bulk of the solution, V. The

expressions for the transition probabilities read as

$$W_c\{E;V_1(V)\} = [T_{MA}(E,V)]^2 \exp\left(-\frac{w_{ox}(V)}{k_BT}\right) \sqrt{\frac{\pi}{E_r^{(c)}k_BTh^2}} \exp\left\{-\frac{[E_r^{(c)}+\Delta G_c(E,V)]^2}{4E_r^{(c)}k_BT}\right\}$$

(26)

and

$$W_a\{E;V_1(V)\} = [T_{DM}(E,V)]^2 \exp\left(-\frac{w_{red}(V)}{k_BT}\right) \sqrt{\frac{\pi}{E_r^{(a)}k_BTh^2}} \exp\left\{-\frac{[E_r^{(a)}+\Delta G_a(E,V)]^2}{4E_r^{(a)}k_BT}\right\}.$$

(27)

Here $T_{MA}(E,V)$ and $T_{DM}(E,V)$ are the matrix elements of transition (overlap integrals between the wave-functions of the electron states of the electrode and the acceptor, and the donor and electrode, respectively. Determination of these factors is a special task of quantum chemistry. To the accuracy of the effects considered in Ref.[532] they may be assumed, in the first approximation, to be independent of voltage. The second factor in these expressions is the Boltzmann probability for the acceptor or donor to set on the reaction plane, with w_{ox} and w_{red}, being their energies, generally potentially dependent. $E_r^{(c)}$ and $E_r^{(a)}$ are the reorganization energies which may generally be different for the cathodic and anodic transfers (the quantities in the Marcus theory[533] generally denoted by the symbol λ). $\Delta G_c(E,V)$ and $\Delta G_a(E,V)$ are the Gibbs free energy change on single electron transfer from the electron energy level E to equilibrated level of the acceptor and from the equilibrated level of donor to the electron energy level E:

$$\Delta G_c = V_1(V) - V_1^{(0)} - (E - E_F) + w_{red}(V) - w_{ox}(V) - k_BT\ln\frac{c_{ox}}{c_{red}}$$

(28)

$$\Delta G_a = V_1(V) - V_1^{(0)} + (E - E_F) + w_{ox}(V) - w_{red}(V) + k_BT\ln\frac{c_{ox}}{c_{red}}$$

(29)

The last terms in these two equations are the Nernst term with c_{red} and c_{ox} being the concentrations of donors and acceptors. $V_1^{(0)}$ is the equilibrium potential drop between the electrode and the reaction plane defined in such a way that ; it is easy to see that when $V_1(V) = V_1^{(0)}$, $J_c = J_a$, and $J = 0$ (the definition of equilibrium).

Introducing the notion of overpotential, one can reduce the expression for the current to a much more compact form,[531] but for us it was important to keep it as it is, in order to

reveal microscopic effects that the medium of reaction, in our case RTIL, can contribute. Looking at these equations we see that many terms depend here on the electrode potential, in the first place the driving force of reaction $V_1(V)$.

6.3   What will matter in RTILs?

The key factors here are the reorganization energy, the work terms, the driving force, and the overlap integral. Let us comment on each of them separately.

6.3.1   Reorganisation Energy

Let us assume that for a single electron cathode and anode transfer the reorganization energies are the same. $E_r^{(c)} = E_r^{(a)} = E_r$ This is usually estimated using the Marcus formula,[534] which near the electrode with account of image forces reads

$$E_r = e^2 \left(\frac{1}{\epsilon_\infty} - \frac{1}{\epsilon} \right) \left(\frac{1}{2a} - \frac{1}{4d} \right) \tag{30}$$

where a is the effective radius of the oxidized and reduced forms of the reactant (assumed to be the same in both cases) and d is the distance to the reaction plane; ϵ_∞ and ϵ are, respectively, the high and low frequency dielectric constants of the liquid. ϵ_∞ is due to the contribution of the polarizability of internal electrons of ions of the liquid, the quantity usually close to 2. ϵ is the 'static' dielectric constant; the latter stands in the quotes because, as emphasized earlier in this review, there is no such thing as static dielectric constant of ionically conducting liquid. We mean here the measured 'intermediate' dielectic constant due to vibrations and librations of ionic pairs, or more generally the strongly dissipating polar-phonon-like modes of the ionic liquid, the quantity of the order of 10 (see subsection 2.2.3).

This formula was the Marcus-derived[535] extension of the Pekar-Marcus (formula for the reorganization energy of the electron exchange between the ions of radii a in the bulk of a dielectric medium).[535–537]

$$E_r = e^2 \left(\frac{1}{\epsilon_\infty} - \frac{1}{\epsilon} \right) \left(\frac{1}{a} - \frac{1}{d} \right). \tag{31}$$

The reorganization energy in the bulk is larger because the electric field of ions near the electrode is image-screened by the metal. Generally both formulae are expected to give rough estimates of the corresponding reorganization energies, because they do not take into account the short range structure of the liquid, neither the electric field penetration into the electrode. There were various attempts to take both effects into account through the spatial dispersion of dielectric permittivity of the liquid and the metal in various approximations of the latter for these two phases, done in the context of reactions in ordinary polar liquids.[538–543] These studies used a number of approximations; most importantly they are built on a linear response theory of the medium to the reorganizing charge of the reactant. The study in Ref.[357] has shown, however, that the mere presence of the solute as well as the nonlinear electrostatic effects can perturb the environment and substantially distort the nononlocal electrostatics effects[544,545] washing out some of the fine structural effects that are predicted by the linear response nonlocal electrostatic theory. In view of such situation the simple formulae of Marcus type remain to be a good orientation point. How much this should be applicable for RTILs? First studies for an electron transfer in the bulk[546–548] and at electrodes[397] has shown substantial deviations of the estimates due to the short range structure, although as an 'order of magnitude estimate' the Marcus formulae can still be used.

One of the sources of the deviation can be actually traced, if we go back to more general expression for the reorganization energy,[549–551] which, if we do not take into account spatial dispersion of the dielectric permittivity, reads

$$E_r = e^2 \left(\frac{1}{a} - \frac{1}{d} \right) \frac{2}{\pi} \int\limits_0^{k_B T/4h} d\omega \frac{Im\,\epsilon(\omega)}{\omega|\epsilon(\omega)|^2}, \tag{32}$$

where $\epsilon(\omega)$ is the complex frequency dependent dielectric permittivity of the liquid. The exact Kramers-Kroenig (KK) relation expresses the integral over all frequencies with the static dielectric constant ϵ, if $\epsilon(0) = \epsilon$

$$\frac{2}{\pi} \int\limits_0^\infty d\omega \frac{Im\,\epsilon(\omega)}{\omega|\epsilon(\omega)|^2} = 1 - \frac{1}{\epsilon(0)}. \tag{33}$$

For the integral in eq 33 there is an approximate KK-relation if the frequency $k_B T/4h$ lies in the transparency band between the electronic excitations in the liquid and the vibrational modes[550] and if $\epsilon(\omega \to 0) = \epsilon = const.$

$$\frac{2}{\pi} \int\limits_0^{k_B T/4h} d\omega \frac{Im \, \epsilon(\omega)}{\omega |\epsilon(\omega)|^2} = \left(\frac{1}{\epsilon_\infty} - \frac{1}{\epsilon} \right). \tag{34}$$

With this equation valid, we recover expression of eq 32 for the reorganization energy. However, in RTILs we do not know whether any of the two assumptions hold. In particular in view of the very slow relaxation in ionic liquid (low frequency tail of, $\epsilon(\omega)$, where should we truncate the integration in eq 34? So the best strategy would be, if we have experimental data for $\frac{Im \, \epsilon(\omega)}{|\epsilon(\omega)|^2}$ to keep the integral form for the reorganization energy. Even better, had we had information not only about frequency-, but also the wave-vector-dependence of the dielectric response function $\frac{Im \, \epsilon(k,\omega)}{|\epsilon(k,\omega)|^2}$ (say, from computer simulations, such as e.g. obtained for water[356] we could use then even more general equations for the reorganization energy,

$$E_r = e^2 \frac{2}{\pi} \int\limits_0^\infty dk \left\{ \frac{1}{2} \left[\frac{(\sin ka_1)^2}{(ka_1)^2} + \frac{(\sin ka_2)^2}{(ka_2)^2} \right] - \frac{\sin ka_1}{ka_1} \frac{\sin ka_2}{ka_2} \frac{\sin kd}{kd} \right\} \frac{2}{\pi} \int\limits_0^{k_B T/4h} d\omega \frac{Im \, \epsilon(k,\omega)}{|\epsilon(k,\omega)|^2} \tag{35}$$

drawn here for a single electron exchange between two 'spherical ions of radii' a_1 and a_2, the centers of which are separated by a distance $d(a_1 + a_2)$. In the case of k-independent dielectric-response function,

$$\frac{Im \, \epsilon(k,\omega)}{|\epsilon(k,\omega)|^2} \approx \frac{Im \, \epsilon(k=0,\omega)}{|\epsilon(k=0,\omega)|^2} = \frac{Im \, \epsilon(\omega)}{|\epsilon(\omega)|^2} \tag{36}$$

the two integrals in eq 35 are decoupled and eq 35 reduces to eq 33 (if we put there $a_1 = a_2 = a$). For RTILs such assumption in the range of wave numbers $k : (2\pi/a)$, important in the integral eq 35, will unlikely be realistic. Thus eq 35 suggests an interesting scheme for future calculation of the reorganization energy and comparison of the results with the direct simulation of the latter.[547,548]

This expression however would only be applicable for the electron transfer between donor and acceptor ions in the bulk. How it should look for the electrochemical electron transfer

reactions at electrodes? This is generally a difficult problem, c.f. Refs.,[538–541,552] which is yet to be solved. Such enterprise, however, would only make sense if such approach showed good results in the bulk; the studies in Ref.[357] performed for water, suggest that this may not be the case. However, a priori we do not know, whether this would be the same for RTILs.

6.3.2 Work terms

These tell us what will be the concentrations of oxidized (for the cathodic current) and reduced (for the anodic current) species at the reaction plane, the factors also determining the currents. The probability to find there those species will depend on their charge and the potential of the plane. The latter is very much an issue of the potential distribution near the electrode, and the effects of overscreening can contribute new interesting effects here (but see a discussion below). They may be particularly important for electrodeposition reactions with a slow adsorption stage.

6.3.3 The Driving force and the potentially new form of the Frumkin correction

One of the functions of electrolyte in electrode kinetics is to provide the most compact localization of the electrostatic potential drop between the electrode and the reaction plane, to utilize the strongest drive for the reaction. In diluted electrolyte solution the potential drop between the electrode and the bulk will be spread over the diffuse double layer and only a small portion of this drop will be localized between the electrode and the reaction plane. Hence polarizing the electrode will be majorly wasted for the electrode kinetics. The correction to the expressions for the electrode current which takes into account this effect is known as the Frumkin correction.[553,554] This we symbolically incorporated in the expression for $V_1(V)$, with $V_1(V) \approx V$ only if total potential drop is fully localized between the electrode and the reaction plane. With the effect of overscreening in place in RTILs, one may expect to encounter something completely new, different from the case of diluted electrolytic solutions, where $V_1(V) < V$. Here, in the overscreening regime, $V_1(V)$ may quite easily become substantially larger than V.

To our knowledge this opportunity was first noticed and investigated in molecular dy-

namic simulations in Ref.[397] The result was however negative: manifestation of overscreening in the driving force were not found. The authors concluded that the potential distribution near the electrode averaged in the lateral plane in the absence of the reactant in question is not what actually counts in the driving force. They write: "Rather we should be considering the potential at the ion's center due only to the other charged present in the system: this might be better called a Madelung potential." This question requires further detailed investigation. If we try to translate that conclusion into the necessity to take into account what is called in electrochemistry the effect of micropotential,[555] in order to corroborate the conclusion of Ref.[397] we should assume that such effects should be abnormally high in strong correlated Coulomb systems, such as RTILs. Recent studies of Ref.[208] has shown that electrostatic potential experienced but a solute ions in RTIL is substantially different from the one that sets in the absence of such ion. However, this difference was not to the degree that the effect of oscillating overscreening patterns fully disappear.

Last but not least, in the regime of very large electrode polarization where the lattice saturation effects (crowding) might be expected,$V_1(V) \propto \sqrt{V}$.[556] This can result in a current-voltage law qualitatively different (c.f.[556]) from the Bulmer-Volmer's.[555] This is a whole new area for future investigations, where, however, experiments should first set the scene.

6.3.4   Matrix element of transition (overlap integral)

Evaluation of this quantity requires extension of modern methods of quantum chemistry with account of dense ionic environment of RTIL. In a simplified version[531,532] this may take a combination of electron density functional theory and molecular dynamics, in the spirit of ab initio Car-Parinello schemes.[557] Will that be worth the effort? The question is, indeed, justified as it refers to the calculation of the pre-exponential factor in the expression for the electrode current, whereas so many issues are yet unclear about the exponential factors! The importance of the overlap integrals is, however, obvious when they are vanishingly small, as then they substantially affect the scale of the electrode current. They are certainly important for tuning the optimal parameters of the electrodeposition reactions. Next, if they also become voltage dependent[531,532] the matrix element of transition can contribute corrections to the current voltage plot. To our knowledge, for RTILs no detailed studies in

this direction have yet been reported.

6.4   Experiments: examples of few case studies

We did not intend to go into the review of any particular published papers on the electrode
kinetics of RTILs, having focussed the previous sections of this chapter on certain general
features of the most elementary electron transfer processes at electrodes, as such 'quantum
electrochemistry' might appear to be useful in rationalization of the simplest electrochemical
reactions in RTILs. We nevertheless will briefly discuss below a very limited selection of
published, predominantly experimental papers.

Lagrost et al[558] have studied four different ionic liquids, based on
1-alkyl-3-methylimidazolium or quaternary ammonium cations as reaction media for several
typical electrochemical reactions of oxidation of organic molecules (anthracene, naphthalene,
durene, 1,4-dithiafulvene, and veratrole). They recover the reaction mechanisms from the
analysis of cyclic voltammetry curves and determine the thermodynamic and kinetics pa-
rameters of the corresponding reactions. Most strikingly they come to a conclusion that
the uncovered mechanisms seem to be almost unchanged in ionic liquids, as compared with
conventional organic media. However, the overall one order of magnitude decrease of the
electron-transfer rates between the studied aromatic molecules and the electrode, observed
for all the studied molecules, indicated at a higher solvent reorganization energy than they
could be in ordinary organic solutions. Reorganization of dense ionic atmospheres in RTILs
can indeed be larger than the reorganization in a polar solvent, so these results are quite
encouraging for application of the theory. These reactions, however, are certainly needed but
not the simplest one as they involve both first and second order reactions of cation radicals.

Interesting results were obtained for oxidation of dissolved hydrogen gas on platinum
electrodes in different ionic liquids.[559] Studies of similar processes in protic ionic liquids
have also been reported.[560]

Matsumiya et al[561] studied electrochemical ferrocene-ferriceniurn electron transfer reac-
tions in ammonium-imide RTILs , via the analysis of cyclic voltammogrammes over a po-
tential range -0.3 to +0.5 V versus I-/I_3- reference electrode in a wide enough temperature
range of 298-373 K. The Fc/Fc+ reaction was found to be a single-electron transfer pro-

cess (as expected) and diffusion controlled. The electron transfer rate constant and transfer coefficient have been retrieved by electroanalysis.[562] Both the rate constant and the diffusion coefficients for Fc/Fc+ were studied as a function of temperature, exhibiting Arrhenius dependencies.

Efforts have been invested in optimizing reference electrodes for voltammetry in RTILs.[563] In this work both the diffusion and the kinetics of electron transfer across the ionic liquid/electrode interface were studied using cyclic voltammetry and scanning electrochemical microscopy. In another work in this area[564] the authors studied the anodic oxidation of several arenes and anthracenes in RTILs. The authors of this work made conclusion about substantial deviation from the outer-sphere Marcus-type behavior of these compounds in contrast to their behavior in traditional organic solvents, in terms of correlations of the rate constant with molecular size and solvent static dielectric constant. For a number of processes in a series of RTILs the electron-transfer kinetics was found to be independent of the solution viscosity.

In Ref.[565] ferrocene was used as a redox probe and the electrochemical properties of a series of RTILs were studied using voltammetric methods and scanning electrochemical microscopy. The effect of RTIL viscosity on mass transfer dynamics within each RTIL was studied, as well the heterogeneous electron transfer rate constant, was determined.

The classical example of rather complicated electron transfer reactions - the oxygen reduction reaction (ORR) - has been studied in Ref.[566] at Pt surfaces in a protic RTIL using the method of rotating disk electrode. Water content measurements suggested that the ORR proceeded in the ionic liquid via a 4-electron reduction to water. A Tafel analysis of the rotating disk voltammetry data revealed a change in the ORR Tafel slope which seemed to be related with the change of the exchange current density the applied potential.

The hydrogen evolution reaction has been explored at gold, molybdenum, nickel, titanium and platinum electrodes. Significant differences in electrochemical rate constants were observed between the different metals. Most importantly, the authors came to a conclusion that the reaction mechanism was consistent at all five metals in the studied RTIL, in contrast to the known variations in a series of these metals in aqueous systems.[567] Hydrogen evolution was also investigated in various RTILs in Ref.[568] at Pt electrode. This work revealed a

strong effect of the nature of anion, suggesting significant interaction between protons and anions. H+ reduction on a palladium microelectrode in RTIL was studied in Ref.[569] showing signatures of Pd/H layer formation under the studied conditions.

Kinetics of Li/Li+ was studied in Refs[570,571] for a large set of RTILs.

That list could be continued, but all in all the experiments are far ahead of a molecular level theory (which is just to be developed), and many of the drawn examples are more complicated than the simplified one-stage processes sketched in the formalism described in this chapter above. The synergy will come after theorists will be able to formulate some striking predictions of quantum electrochemistry for experimentalists to test them. It has taken many years to get such tests done for some spectacular but elementary heterogeneous electron transfer reactions in ordinary electrolytes,[554,555] and it will also probably take some time for this to happen in RTILs.

7   RTILs in confined geometry

The electrochemical performance of an electrode-RTIL interface is generally 'amplified' by its area, whether it is used for energy storage (capacitors, batteries) and generation (solar cells, fuel cells), or electrocatalysis. In this respect porous and in particular nanoporous electrodes may provide the maximal enhancement of the interfacial area, as long as the electrodes are well wetted by RTIL. This justifies the interest in understanding RTIL performance in nano-confinement.

Before we go into details of molecular-scale physical-chemical phenomena in RTILs in confined geometry, we would like to note that the phenomena discussed in this section are interesting for various applications. However, due to space limitations, we will dwell on only one of those applications, as an example, namely the EDL supercapacitors.

7.1   Electrochemical capacitors: targets and challenges

Electrochemical capacitors have a vast range of applications for electrical energy storage and its fast delivery in the form of electrical current.[73,572] Their common ground is the position of supercapacitors on the so called Ragone plot - the graph of the power vs energy stored

(Figure 12). High power density,i.e. high energy delivery in unit time per unit capacitor's mass or volume, is related to the ability of fast charging/ discharging with minimal losses for the most compact architecture.
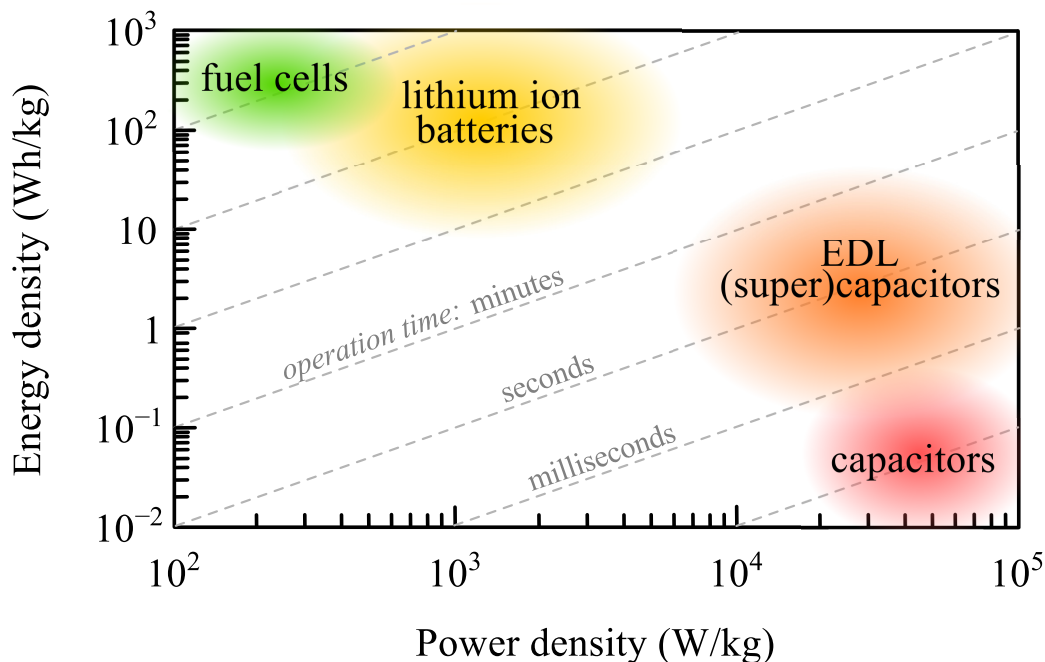

Figure 12: Ragone plot showing available energy of several types of energy storage devices. Characteristic operation times correspond to lines with unity slope.

Looking good at the Ragone plot means to possess high energy density without sacrificing power density. The supercapacitors look better in this respect than batteries, but generally they have lower energy density and higher power density, and this determines their application niche. Scientists and engineers are interested to expand the whole band to the upper-right corner; then the supercapacitors could approach the market of applications traditionally occupied by batteries. It is wanted because EDL-capacitors can be charged fast and, non-involving any electrochemical reactions, can sustain hundreds of thousands of charging-discharging cycles. But there are principle difficulties on the way of realization of this target. These difficulties are inherent to the principle of the supercapacitor.

Indeed, the way to increase the energy density is to (i) maximize the double layer capacitance per unit surface area (the 'specific capacitance'), and/or (ii) maximize the interfacial area per volume. The first option is about the best choice of the electrolyte and electrode material, underpinned by understanding the structure of the electrical double layer or empir-

ical findings, the subject of studies reviewed in the previous sections. Exploring this option one may hope to increase the specific capacitance and thereby the overall capacitance of the electrodes usually by several times. The second option, however, will allow to increase the overall capacitance by orders of magnitude. Making the surface of the electrode rough is not sufficient to reach this goal. The standard strategy here is to use 'volume-filling' interfaces typical for highly porous electrodes that are well wetted by the electrolyte. Therefore, engineering supercapacitors is often regarded synonymous to engineering the porous structure of the electrodes.[71,73,75,303] Indeed, there exist techniques for *rational design* of ordered mesoporous materials (e.g. they can be prepared by the template route; for a review see Ref.[573]).Application areas of these materials are not limited only by electrochemical capacitors; they can be also effectively exploited in other electrochemical devices (e.g. electrochemical sensors).
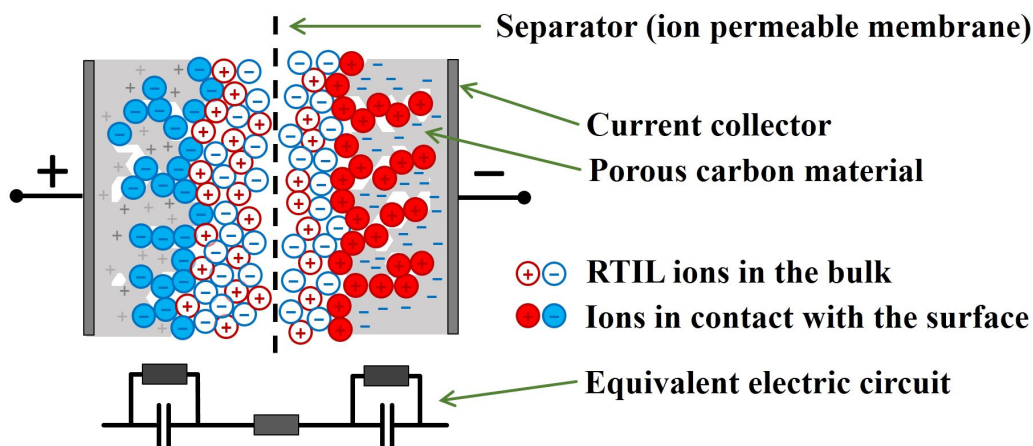

Figure 13: Electrochemical cell showing accumulation of RTIL ions at positevely and negatively charged surfaces of porous carbon electrodes.

However, using highly porous electrodes to increase capacitance automatically faces a problem. Figure 13 shows the cartoon of the cross-section of a supercapacitor with porous electrodes, from which the problem becomes clear. Separating charge, by charging the double layers on the opposing electrodes means to move anions preferentially to the left electrode (anode) and cations to the right electrode (cathode). But the higher is the porosity the longer is the way for the ions to go to reach all interior parts of the volumetric surface of the electrodes. Thus, the larger the surface, the greater the capacitances (and, consequently, the

larger is the stored charge for a given voltage), but simultaneously the greater are the ohmic losses incurred due to the transport of ions through the long pores. The slow transport of ions into the pores causes losses in the power density, as well as it slows down the overall charging-discharging rate. Hence the trade-off between the energy density and the power density/speed of the charging cycles becomes inevitable.

Next, not only the length of the pores may be a problem but the ionic conductivity inside of them. Indeed, for wide pores the conductivity may be the same as in the bulk of electrolyte; however, for nanoscale pores, it may be different for a number of reasons. Firstly, the ions will experience additional friction due to collision with the walls (the so called Knudsen diffusion.[50]) Secondly, the confinement may impose additional limitations on cations and anions, moving in opposite directions, bypassing each other. The third effect is the screening of the electrostatic interactions by the free electrons of the pore walls in the electrode, which can actually, be beneficial for charging the pore (see below).

The issue of the stored energy itself is not concerned with kinetic limitations, and we concentrate on it first. Note that as long as the characteristic pore radius (width) is much greater than the thickness of the electrical double layer, no new physics of the double layer and the energy stored in it will need to be invoked: the energy will just scale up with the interfacial area. This is no longer true when the two length scales become comparable. This fact was known already from the theory of mildly rough electrodes, where the modification of the double layer theory was needed.[574,575] For nanoporous electrodes entirely new theory had to be developed to describe the dependence of the stored charge and energy on voltage, and this development is reviewed below.

7.2 The superionic effect in narrow nanopores: experiments vs theory

Before describing the theory, we should highlight the most striking experimental facts that challenged our understanding of EDL properties in nanoconfinements.

The story of nanoporous electrodes for electrochemical capacitors is closely related with the new round of development of porous carbon materials.[74,303] This is because (i) the

porous structure of carbon is relatively easy to fabricate and control on industrial scale, (ii) the material is light-weighted, (iii) and is relatively cheap, (iv) it is a sufficiently electronic conductor ('current collector') for a system in which the kinetic limitations are determined by the transport of ions, and, finally, (v) it is electrochemically inert at higher voltages than most of the metallic electrodes.

The most popular types of porous carbon materials used as electrodes for electrochemical capacitors are: (i) **a**ctivated **c**arbon (AC), **c**arbide-**d**erived **c**arbon (CDC), and **t**emplated **c**arbon (TC); (ii) nanotube 'forests', based on single wall, double wall, or multi-wall nanotubes; (iii) the structures based on graphene sheets; (iv) onion like, and (v) nanohorn structures.[74,222,303]

It is not the task of this article to review all these structures, but we will stop on one of them which is most easy to fabricate on an industrial scale, namely the CDC. Porous carbon is produced from carbide in reactions of the following kind: $SiC(s) + 2Cl_2(g) \rightarrow SiCl_4(g) + C(s)$, leaving, after evaporation of the gas, structures like shown in Figure 14.[222,576–582]
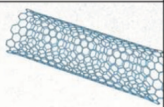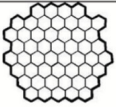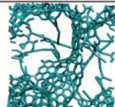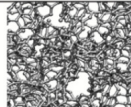
Material	Carbon onions	Carbon nanotubes	Graphene	Activated carbon	Carbide derived carbon	Templated carbon
Dimensionality	0-D	1-D	2-D	3-D	3-D	3-D
Conductivity	High	High	High	Low	Moderate	Low
Volumetric Capacitance	Low	Low	Moderate	High	High	Low
Cost	High	High	Moderate	Low	Moderate	High
Structure						

Figure 14: Different carbon material structures that are commonly used in EDL capacitors: onion-like carbon, carbon nanotubes, graphene, activated carbons, and carbide-derived carbons. Reproduced from Ref.[222]

Most importantly, the average pore size can be finely tuned by controlling the derivation temperature: between 600 and 1200 °C it monotonously grows from rougly 0.45 nm to 1.7 nm. Although there are debates in the literature how accurate the pore size distributions have been assessed,[584,585] various methods of assessing the porosity have been shown to give close results.[586]

With that technology in hands, a French-US team led by P.Simon and Y.Gogotsi has discovered a striking effect, which they have obtained for both electrolyte solution with

organic solvent[587] and a pure RTIL – (EMI$^+$-TFSI$^-$) as an electrolyte.[588] We focus on the latter. Using several methods for assessing the surface of the open pore space, they have found that for nano and sub-nano sized pores the capacitance per unit surface area grows monotonously with the decrease of the pore size, reaches maximum when the average diameter of the pores becomes equal to the characteristic size of the ions, and then sharply drops down (see Figure15).[583]
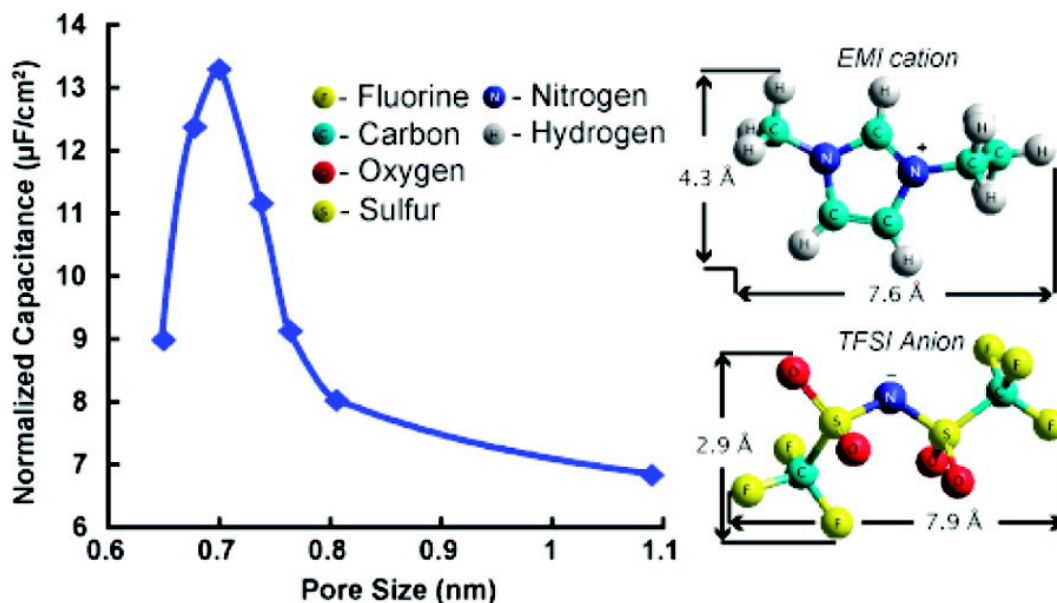

Figure 15: Depedence of the normalized capacitance on the pore size; the figure is reproduced from Ref.[588]

The drop-down itself raises no questions: the ions cannot get inside such narrow pores and the overall capacitance stops being proportional to the surface of the whole volume of the pores, but only to the surface available to ions. When nevertheless scaled to the whole surface area, it becomes vanishingly small. It does not drop down to zero step-wise, as ions do not have just one size (as well as pores!): the involved ions are elongated and their diameter of rotation about the long axis is smaller than the diameter of the average pore; ions can get squeezed into the pore but this is entropically more difficult, and the capacitance drops down. Note that it is very difficult to measure capacitance for smaller pores, because of the inaccuracies of measurements caused by impeded transport of ions (they are definitely beyond reach for impedance measurements). However why the capacitance rises with the decrease of the pore size till the ions can still get into the pore?

This fact was first rationalized in Ref.[372] where the concept of a 'superionic state' of ions inside nanoscale pores was suggested. The term 'superionic' may sound too flashy but this is debatable. The term has been used to label a speculative phase of superionic water under extreme heat and pressure, which may be natural for giant planets.[589] This phase has properties of both a solid and a liquid, where the molecules break down into a structure made of hydrogen and oxygen ions, in which oxygen crystallises but the hydrogen ions float around freely within the oxygen lattice. The term superionic is also widely familiar in a different context, as the one that describes fast ion conductivity of one sort of ions (typically cations) in solid electrolytes; in this sense superionic water is a superionic protonic conductor. In the context of electrochemical capacitors, the term reflects the idea, described in Figure 16.

When the ions get into a conductive pore, their electrostatic pair interactions are no longer given by Coulomb's law, because they are screened by free electrons of the electrodes. The screening will be maximal in a pore of an ideal metal. For such system, in a slit pore, electrostatic interaction energy between two elementary charges scaled to thermal energy at large distances from each other,

$$R >> L/\pi, \tag{37}$$

is given by the following equation:[372,590]

$$\frac{U(R, z, z_1)}{k_{\mathrm{B}}T} = \pm 2\sqrt{2}\frac{L_B}{\sqrt{RL}}\exp\left\{-\frac{R}{L/\pi}\right\}\sin\left\{-\frac{z}{L/\pi}\right\}\sin\left\{-\frac{z_1}{L/\pi}\right\}. \tag{38}$$

Here $+$ and $-$ signs stand for charges of the same and opposite signs, respectively, L_B is the Bjerrum length (see eq 2). The effective dielectric constant of the interior, ϵ, should vary between the vacuum's $\epsilon = 1$ and the optical dielectric constant of the ionic liquid, responsible for the electronic polarizability of ions, $\epsilon \approx 2$ (if no solvent additives are involved); for the latter case $L_B \approx 28$ nm. Applying this equation to the electrostatic interaction of ions of RTIL we must keep in mind that R cannot be smaller than the sum of ionic radii, roughly $\approx$ ion diameter, if the ions are of similar size; this also will be the smallest value for the gap width, L, for the ions to get there. For the gap just about to accommodate one layer of ions, the criterion in eq 37 is warranted even at closest separation between the ions; the interaction potential is exponentially screened with the decay length L/π, about three times

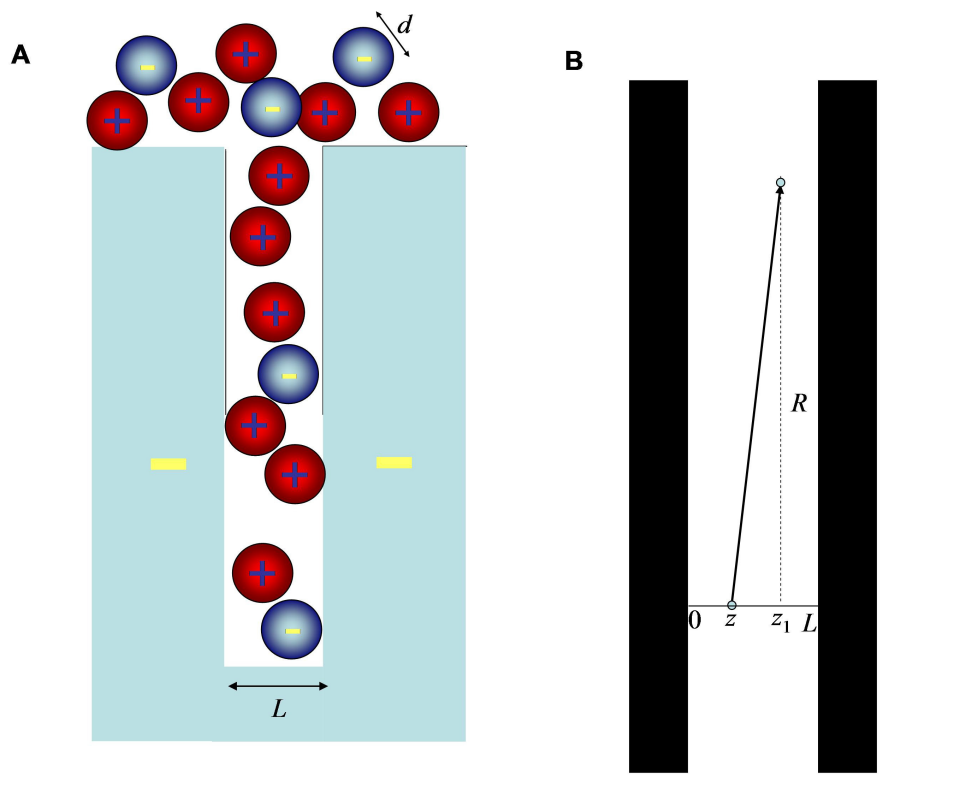shorter than the distance of the closest approach of ions.

Figure 16: (A) A cartoon of filling a slit pore with ions, the interaction between which is screened by conductive electrons of the electrode. (B) The geometry of two interacting point charges in a gap between two conductive plates, as described by eq 38.

Hence the ions inside the pore do interact but rather weakly. For instance, ions 0.7 nm in diameter within a pore of the same size at close contact with each other will interact within the energy of 1.2 k_BT. This value will increase with increasing the size of the pore, but will however similarly *decrease* with further increase of the distance between the ions. If the ions do interact weakly with each other, it will be much easier to pack inside the pore the ions of the same sign, counterions, in response to electrode polarization, and therebye create what was called the *superionic* state inside the pore.[372] With the pore increase, the repulsion between the ions of the same sign and attraction between the ions of opposite sign becomes stronger. Hence, the wider the pore, the more difficult it will be to pack there counterions. The latter explains why the specific capacitance of a pore gets larger with the decrease of its size, as long as the ions can fit it.

Another consequence of the contribution of free electrons is image force attraction of

ions to the conducting walls. Again assuming perfect metallic conductance, the reduction of the electrostatic energy of an ion, if it is moved from a bulk of the medium with dielectric constant ϵ into metallic slit pore filled with the substance of the same ϵ, is given by this equation:[372]

$$\frac{W_{im}}{k_{\mathrm{B}}T} = -\frac{L_B}{L} \cdot \ln 2 \cdot \chi(\delta), \tag{39}$$

where $\delta = z/L$ is the position of the charge from the wall in the units of the total width of the gap and $\chi(\delta)$ is a function defined as an integral,

$$\chi(\delta) = \frac{1}{2\ln 2} \int\limits_0^\infty dt \frac{e^{2\delta t} + e^{2(1-\delta)t} - 2}{e^{2t} - 1}, \tag{40}$$

when the charge is in the middle of the pore, $\delta = 1/2$, the integral can be exactly integrated to give $\chi(1/2) = 1$, otherwise it can be obtained numerically, see the graph in Figure 17.
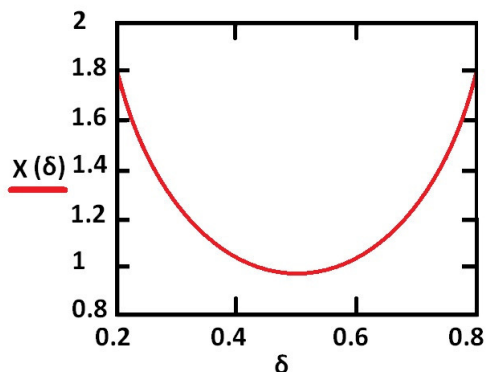

Figure 17: Function $\chi(\delta)$, eq 40.

Assuming that the center of an ion is in the middle of the pore, we can estimate the energy of transfer of the ion from hypothetic medium of dielectric constant $\epsilon \approx 2$ into 0.7 nm wide pore at room temperature to be 27.7 $k_{\mathrm{B}}T = 0.7$ eV.

However, ions get into the pore coming not from such dielectric continuum, in the bulk they are strongly solvated by other ions. We know that the ion-ion cohesion energy as well as self-solvation free energy in RTILs must be negative (and rather large) as RTILs are non-volatile. With the move of the ion into the pore, that free energy gain will be lost. The electrostatic contribution to the free energy of transfer can roughly be estimated as the energy of transfer of an ion from the bulk of dielectric constant $\epsilon \approx 2$ into highly

concentrated electrolyte in 'the solvent' of that dielectric constant, $W_{solv} \approx -(L_B/4R)k_{\mathrm{B}}T$. This estimate tells us that this energy is roughly $2\ln 2$ times smaller than the energy of electrostatic interaction of ion with the pore walls. More sophisticated calculations, may likely give larger solvation energies but the most important issue lies elsewhere: the question whether the ions would like to go inside the pore or not would be also influenced by the entropic contribution to the free energy of transfer. Indeed, the motion of ions in the pore will be confined at least in the perpendicular direction, which would cause an unfavourable loss of entropy. How substantial is the latter term is quite difficult to assess because in the bulk of an RTIL its ions are also not entirely free to move (at high frequencies the ions in RTIL experience the environment similar to that of an ionic solid[591]). Therefore, the entropic contribution may actually be relatively small. On the other hand, ions may have additional attraction to the walls due to the Van der Waals forces or in some cases even covalent interactions.

Thus *a priori*, we do not know will the ions have a propensity to fill the pores when the pore is not charged or they will have to climb a free energy step to get inside the pore; however, the crude estimates above suggest that they would rather be spontaneously filling the pore. Under such circumstances a wise strategy would be to keep the free energy of transfer as a free parameter of the theory waiting for accurate independent experiments that will answer this question. The answers may be different for different ions and different pore materials as the specific interaction of ions with the walls can make some ions 'wall-phillic' and some 'wall-phobic'. Thus, generally, we can speak about ionophillic or ionophobic pores.

Here we should recall again, as already mentioned above, that carbon materials are not ideally metallic. Electric field of ions will penetrate inside the pore walls. This is expected to slightly weaken the screening of interionic interactions and image attraction of ions to the walls.[592,593] 'Ideal metal' kind estimates are the upper estimates, corresponding to the strongest screening. We will not go into further details of this question, as investigations along these lines are currently in progress. In particular, it is interesting to know how much different will be the screening between the two sheets of graphene, as such nanotemplated structures for supercapacitors are currently under study;[143,144,305,572] similarly they could illuminate what will be the screening of ionic interactions in between single wall nanotubes

in a carbon nano-forest electrode.

We thus now discuss the results obtained within the ideal metal approximation. The first proposed theory[372] which rationalized these ideas was based on an effective medium theory, in which the electrochemical potential of an ion inside the pore was calculated with account for screened electrostatic interactions with other ions and the electrostatic potential created by the electrode, steric excluded volume effects, entropy of mixing, self energy and entropy; for details see Ref.[372]
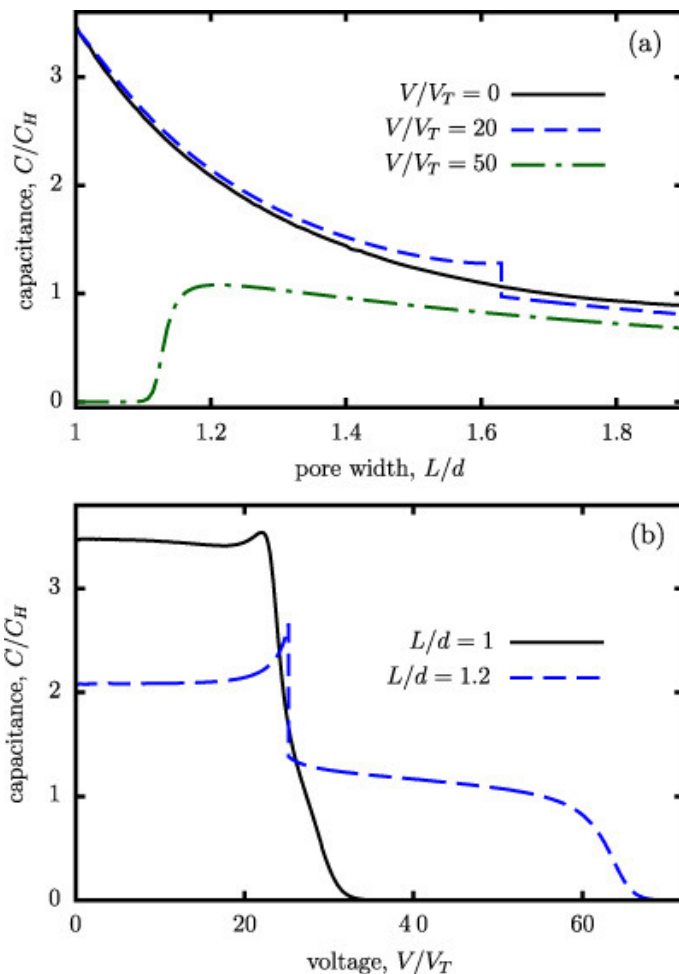
Figure 18: The capacitance of a slit pore scaled to Helmholtz capacitance shown as a function of pore width, scaled to the characteristic diameter of ions, d, for several values of the voltage drop between the electrode and the bulk of ionic liquids [given in the units of the thermal voltage, $V_T = k_B T/e$] (the upper graph), and as a function of voltage for two different pore widths (lower graph). The figure is reproduced from Ref.[372]

Importantly, this theoretical work limited the analysis to narrow pores into which only

one complete layer of ions can fit; this was needed for the quasi-two-dimensional description of the layer of ions inside the pore. The effect of the pore width was thus studied in the range from the one equal to the characteristic diameter of the ion, 1.0 d, to 1.9 d, which is perhaps a bit too far for this approximation, but the theory can safely be applied up to 1.5 d (just like in the experiments of the Gogotsi-Simon groups.[588] The main message from that work is seen from the two plots that we reproduced here in Figure 18.

The upper plot on Figure 18 displays the effect of pore width for fixed values of voltage. Unless for large electrode polarizations, the capacitance of the pore monotonously increases with the decrease of the pore width, approving the nature of the 'Simon-Gogotsi' effect. For substantially large voltage values the capacitance vanishes at yet larger pore width than the ion diameter. This is not because the ions cannot get inside the pore – they still can, but because at such voltages the pore is already fully occupied by the counterions (here anions), and the differential capacitance response to further electrode polarization is zero.

The lower plot on Figure 18, displaying the voltage dependence of capacitance for different pore sizes, shows three new features. This is the saturation of pores at large voltages, when no further counterions can be accommodated into the pores, mentioned in the previous paragraph. Next, in smaller pores the saturation starts at smaller voltages. Finally, for larger pores saturation takes place in two steps, preceded by the field-induced phase transition. That transition, as predicted, is responsible for an abrupt expulsion of the cations form the pore of the positively charged electrode, passing the phase poor in cations, but in which the amount of anions can still grow till the saturation, and hence the 'step' preceding the complete vanishing of the capacitance. This effect is weaker for narrower pores: it practically disappears for $L/d = 1$, but it emerges already for $L/d = 1.08$ (not shown above but displayed in the last figure of that paper, which investigates the possible phases and the nature of that first order transition).

All the calculations in that work have been performed under an assumption that the ions have a propensity to fill in nonpolarized pores, i.e. there is a substantial reduction in free energy of individual ions when they are transferred from the bulk into the pore. Under an opposite assumption, Monte Carlo simulations have been performed by Kiyohara et al.[594] They also predicted a field-induced transition but of a different kind: at low voltages the

pore resists to being filled by ions and the response to charging of the electrode is very minor (capacitance is close to zero); however, at some critical voltage the counterions abruptly enter the pore.
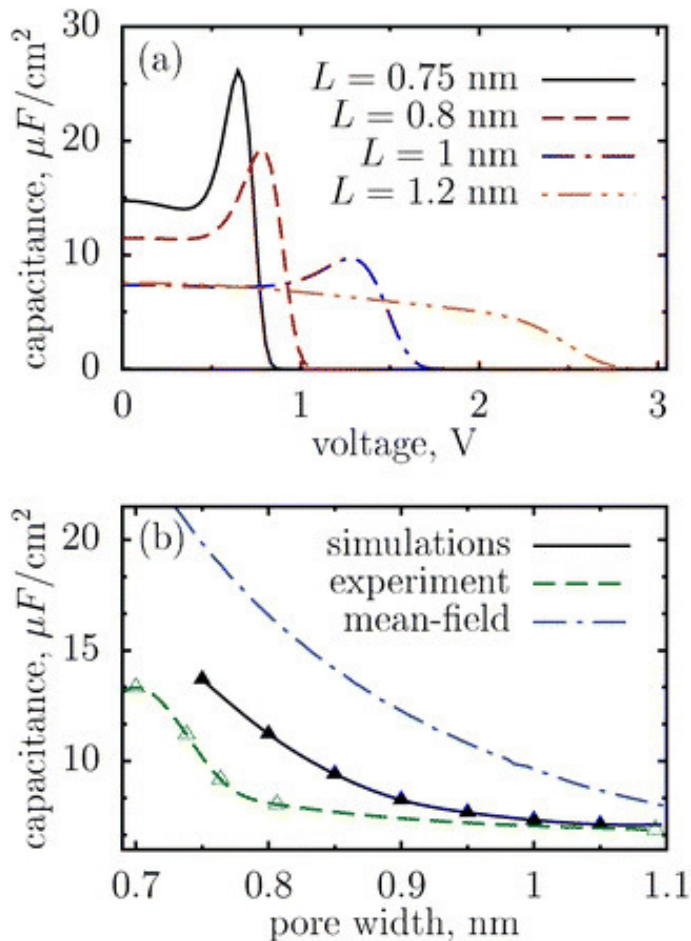
Figure 19: Differential capacitance per surface area as a function of voltage, in volts, for a few values of the pore width, as obtained in the simulations of Ref.[595] The figure is reproduced from Ref.[595]

Leaving aside the question whether the pores of a nonpolarized electrode are filled or empty (which, as discussed, is to be answered experimentally) let us concentrate on the mere existence of the phase transition considering the situation of an initially filled pore. This issue was addressed in Ref.[595] generally aimed on the verification of the predictions of the effective medium theory of Ref.[372] These article reported grand canonical Monte Carlo simulations, performed for a restrictive primitive model of ionic liquid (charged hard spheres, 0.7 nm in diameter). The screening of electrostatic interactions between the ions by the elec-

trons of the electrode was described exactly as in Ref.[372] and equal propensity was assumed for each individual cation and anion to get into the interior of a nonpolarized pore. This simulation has again shown the anomalous capacitance effect, although the enhancement of the capacitance with the decrease of the pore size was weaker than in the effective medium theory.[596] Typical voltage dependent capacitance curves reproduced the general character of the capacitance curves, but not all of its features. First of all, no phase transition was observed in the simulations, i.e. no jump-wise expulsion of co-ions (cations), or alike at a 'critical' voltage. Consequently, no intermediate co-ion (cation)-depleted phase was detected, within which further increase of the counterion (anion) concentration would have been possible with the capacitance vanishing only at larger voltages, after the pore is completely occupied by the counterions. Instead, the capacitance vanishes immediately after a critical value of the voltage preceded by a peak that characterises the voltage-induced replacement of co-ions by counterions, accompanied in the range of the peak by 'electrostriction' (the increase of the overall density of the ions in the pore).[372]

To distinguish these fine details experimentally is not easy, due to a complicated structure of the electrodes, pore size distribution, more complicated shape of ions in reality, etc, and generally difficulties of measuring the capacitance in porous systems. There, impedance measurements are highly problematic, whereas extraction of equilibrium capacitance from cyclic voltamogram is prone to inaccuracies.[597] Some comparison has been made, however, in Ref.[598] in the context of optimization of energy storage. We underline however that under such circumstances theoretical understanding of the capacitance-voltage and capacitance-pore size dependencies may be pivotal for development future nanoengineering strategies.

In this context it is worth to dwell on one more lessening example studied in Ref.[599] Let us consider a cylindrical nanopore in, again, an ideally conductor. Assume that there is a strong propensity for both cations and anions to be there, when the pore is not polarized, and all what happens when it gets polarized, is that the co-ions get replaced by counterions. How this occurs, kinetically, is another question, we just assume that the swapping is possible due to some degrees of freedom that we do not consider explicitly, such as phonons in the wall, fluctuations of orientations of intrinsically anisotropic ions, internal conformations of ions, etc.

Electrostatic interaction energy of two charges lying on an axis of a cylindrical pore of radius a at a distance R from each other is given by an expression:[590]

$$\frac{eU(R)}{k_{\mathrm{B}}T} = \pm\frac{L_B}{R}\left\{1 - \int_0^\infty \frac{dx}{I_0(x)^2}\frac{\sin[(R/a)x]}{x}\right\} = \pm 2\frac{L_B}{a}\sum_{m=1}^\infty \frac{\exp\left\{-\frac{k_m R}{a}\right\}}{k_m[J_1(k_m)]^2} \tag{41}$$

where k_m are the zeros of Bessel function of the of zero order, $J_0(k_m) = 0 : k_1 = 2.4$, $J_1(y_1) = 0.52$; $k_2 = 5.52$, $J_1(y_1) = -0.35,\ldots$ But for the purpose of describing interionic interactions, practically for all relevant values of interionic separations, R, one may keep only the first term in the sum, using the expression

$$\frac{eU(R)}{k_{\mathrm{B}}T}\underset{R>a}{\approx} \pm 3.082\frac{L_B}{a}e^{-2.4R/a} \tag{42}$$

Thus, electrostatic interaction is again exponentially screened, but stronger than in a slit pore, as the decay range is roughly $1/4.8$ of the pore diameter, whereas in a slit pore the decay range is $1/3.14$ of the pore width. This is understandable, because in a cylindrical pore the interacting charges are surrounded by metal 'from all sides'.

Assuming again the propensity of both ions to occupy a nonpolarized pore, and considering for simplicity the cations and anions to be of the same size, the Hamiltonian of such system (in the units of $k_{\mathrm{B}}T$) can be written[599] in terms of a 1-dimensional 'Ising model with nearest neighbour interaction in external field':

$$\frac{H}{k_{\mathrm{B}}T} = \sum_i \left\{\frac{\alpha}{2}(S_i S_{i+1} + S_i S_{i-1}) + uS_i\right\}, \tag{43}$$

where

$$\alpha = eU(d)/k_{\mathrm{B}}T, \tag{44}$$

and d is the 'lattice constant' $\approx$ diameter of the ions. In this description each site of the lattice is occupied either by the cation $S_i = 1$ or by the anion $S_i = -1$. Since $U(2d) \approx U(d)\exp\left\{-2.4\frac{d}{a}\right\}$, and in this model $2a < 2d$ (so that only one row of ions can fit the pore), the assumption of only the nearest neigbour interaction is justified. The first term under the sum in eq 43 favours cations to neighbour anions. The last term in that sum, in which u

is the electrostatic potential drop between the electrode and the bulk of electrolyte given in the units of 'thermal voltage' $k_\text{B}T/e$, the quantity which is constant inside the pore, favours occupation of each site by a counterion.[600]

Luckily, the 1D Ising model in an external field has a well known exact solution, and no extra work is needed to obtain the result. Namely, the thermally averaged value of 'spin' is given by[601]

$$\langle S_i \rangle = -\frac{\sinh u}{\sqrt{(\sinh u)^2 + e^{4\alpha}}}. \tag{45}$$

An important response function is the derivative:

$$\chi(u) = \frac{d\langle S_i \rangle}{du}. \tag{46}$$

In the Ising model of magnetism the latter is proportional to magnetic susceptibility, whereas in our problem this derivative characterizes the system response to the polarization of the electrode, represented by the capacitance per unit surface area of the pore:[599]

$$C = \frac{\epsilon L_B}{2\pi a d} \chi(u). \tag{47}$$

Differentiating $\langle S_i \rangle$ over u one gets a simple formula for the capacitance of a single pore:[599]

$$\chi(u) = e^{-2\alpha} \frac{\cosh u}{\{1 + [\sinh(u)]^2 e^{-4\alpha}\}^{3/2}}. \tag{48}$$

Assuming that the capacitance of the electrode is dominated by the capacitances of its long pores, for an electrode with a system of identical pores this will be the expression for the specific capacitance of the electrodes calculated per its surface area in which the internal surface area dominates.

One may also be interested in the volumetric capacitance, i.e. the capacitance per total volume of the electrodes including its pore volume:

$$C_v = \frac{\epsilon L_B P}{\pi a^2 d} \chi(u). \tag{49}$$

The capacitance per mass of the electrode is given by:

$$C_m = \frac{\epsilon L_B P}{\pi a^2 d \rho_m (1-P)} \chi(u),$$

(50)

where ρ_m is the mass density of the bulk electrode material.

According to these equations, the voltage dependence of the capacitance is entirely determined by one parameter - the coupling constant α. How strong is the latter? Following eq 41 and eq 42, for d = 0.7 nm, and a =0.35 nm, $\alpha = 2.033$, but when the pore radius becomes just 0.2 nm larger, $\alpha = 4.622$. All in all the interaction energy of neighbouring ions in the pore is larger, but not much larger, than the thermal energy. Had it been much greater, it would have been difficult to charge the pore and the latter would have taken place only for large voltages. The graphs in Figure20 shows eq 47 and eq 48 in action: they demonstrate how the capacitance-voltage plots depend on the coupling constant affected by the increase of the pore radius at a constant packing of ions on the axis. We see that when the pore diameter is just a tiny bit larger that the diameter of an ion, the capacitance becomes almost zero for small voltages and it takes some voltage to start accepting the charge into the pore; the position of the maxima is roughly at $u_{max} \approx 2\alpha + \ln 2$ and after this voltage the pore admits about 70% of the counter charge, and further charging becomes increasingly difficult. The capacitance peak has a 'resonance' nature. One needs to apply that much voltage that will 'crash' the propensity for cations and anions to pair, i.e. the reduction of the free energy gained by getting only counterions into the polarized pore must beat the energy of cation and anion interactions.

The effect of temperature is tricky because temperature enters both u and α, we refer the reader to Ref.[599] for details.

However, such sharp pictures refer to the capacitance of a single pore. Even a minor dispersion of pore sizes will cause a dramatic change on the capacitance-voltage plot. This is not surprising because Figure20 shows a very strong, resonance-kind effect even for a small variation of the pore size. Figure21 shows the capacitance per unit surface area averaged with a Gaussian distribution of pore sizes for different dispersion of the pore sizes (note that the same averaging procedure for the volumetric capacitance or gravimetric capacitance, will
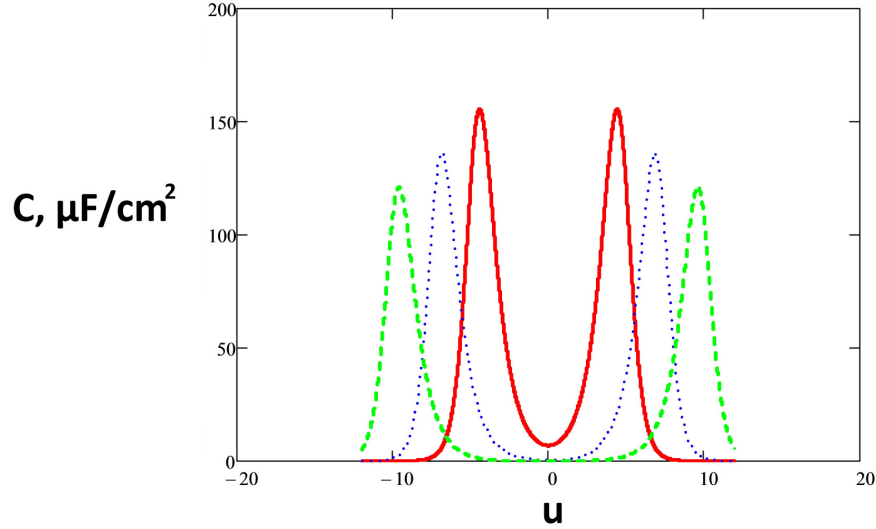
Figure 20: Ising model results for the capacitance-voltage dependence[599] (voltage given in the units of 'thermal voltage' $k_B T/e \sim \text{Volt}/40$) – the effect of the diameter of the pore. Calculated using eq 47 and eq 48 for the ions of diameter 0.7 nm. Curves: $2a = 0.7$ nm $[\alpha = 2.033]$, red/solid; 0.8 nm $[\alpha = 3.249]$, blue/dotted; 0.9 nm $[\alpha = 4.622]$, dashed/green.

lead to slightly different shape of the curves than for the specific capacitance, because of the different power of the pore radius in the denominator).
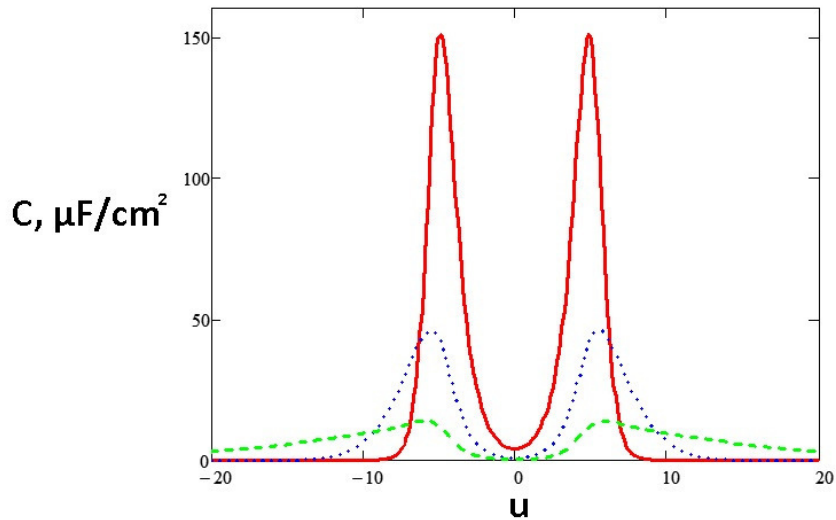

Figure 21: Capacitance of a narrow cylindrical pore at dense packing of ions, just about to accommodate one row of ions on its axis weighted over Gaussian pore radius distribution (for details see Ref.[599]). Ion diameter $d = 0.7$ nm, pore diameter $2a = 7.2$ nm; the curves correspond to dispersion of pore radii: 0 (red/solid); 0.05 nm (blue/dotted), 0.2 nm (green/dashed).

The main lesson from the results of Ref.[599] (some of these results we have reproduced in Figure 20 and Figure 21) is that the voltage dependence becomes milder (peaks becomes much less sharp) with inclusion of the pore radius distribution, and the overall value of capacitance becomes smaller except for at large voltage wings. This 'toy' model allows to parameterize and 'visualize' these complicated effects in most simple terms.

Note that these graphs were plotted under an assumption of dense packing of cations and anions (no vacancies in the lattice, i.e. the free energies of transfer of ions from the bulk of the solution into the interior of the pore is negative and much greater in the absolute value than the thermal energy), and more specifically, for the same propensity for the cations and anions to enter the pore.

The account for the latter effect is trivial:[599] a difference in the free energy of transfer between cations and anions will cause a shift of the curves along the voltage axis. For instance if the absolute value of the free energy of transfer of anions into the pore is larger than for cations by the value of ΔW (even if they are of the same size, but because of some specific interaction with the walls), this would be equivalent to subtracting half of that difference (scaled to $k_\mathrm{B}T$) from u in the expression for the Hamiltonian.[35] The minimum of the capacitance curves will then be shifted to $u = e\Delta W/2k_\mathrm{B}T$, and the whole curve will be shifted to the right by that value.

However, when the unpolarized pores prefer to stay empty, or the free energy of transfer is not much greater than the thermal energy, the Ising model will be inapplicable. Voids in the lattice must be considered statistically and on the same footing as ions. The account for the presence of voids requires a more sophisticated, three-state model, where the new state $S_i = 0$ means that the site is occupied by the void. Such three-state model, an analogue of the so called Blum-Every-Griffith (BEG) model, is currently under investigation. It should show richer behavior of charging and the capacitance-voltage dependence in a situation when the competition in filling the pore is not only between cations and anions but also between ions and vacancies.

The consequences of the effects of the size of the pore and of the pore size distribution – (the latter have been studied by averaging the results of Monte Carlo simulations in slit pores using pore size distributions extracted from experimental data) have been analyzed in Ref.[598]

The results have been compared with specially performed measurements of the capacitance and the pore size distribution assessed by using established porosimetry techniques.[598] Most importantly, that work addressed attention to the question of the optimal size of the pore for the maximal energy storage; we think that it is worth to dwell on the question here.

7.3 Energy storage in nanoporous electrodes: what is the optimal size for the pores?

Continuing the discussion of ultraporous electrodes, in which the pores can accommodate only one layer (in slit pores) or one row (in cylindrical pores) of ions, we can ask ourselves a question, what should be the optimal size of the pore for the maximal energy storage? Let us stick for definiteness to a slit pore, as was studied in Ref.;[598] however, we note that similar analysis can be performed for cylindrical pore geometry using the equations presented above[601] or of any more general model, such as e.g. the Blum-Emery-Griffith model.

The volumetric density of electrical energy stored in a sample composed from an array of slit pores of width L with the thickness of the walls, W, reads as:[598]

$$E(V) = \int_0^V dv \, vC_v(v) = \frac{2}{W+L} \int_0^U dv \, vC(v).$$ (51)

In all the curves for the differential capacitance shown above, the latter term vanishes after a certain value of voltage because the pore cannot accommodate more charge after some point. It is therefore becoming a question of finding an optimum, what should be the best pore size for the largest energy density for a given voltage, particularly because (c.f. Figure 22) those capacitance curves that 'survive' at larger voltages lie majorly lower than the 'nonsurvivors' at smaller voltages. Integration in eq 51 and the maximalization of the result for the stored energy with respect to the pore size for a given voltage gives graphs of the kind, shown in Figure 22.[598]

This is just a snapshot from a larger number of results of Ref.:[598] there one can find other lessening curves as well as those demonstrating the role of pore size distribution. But the main message is that for a given operating voltage the energy density is a non-monotonic
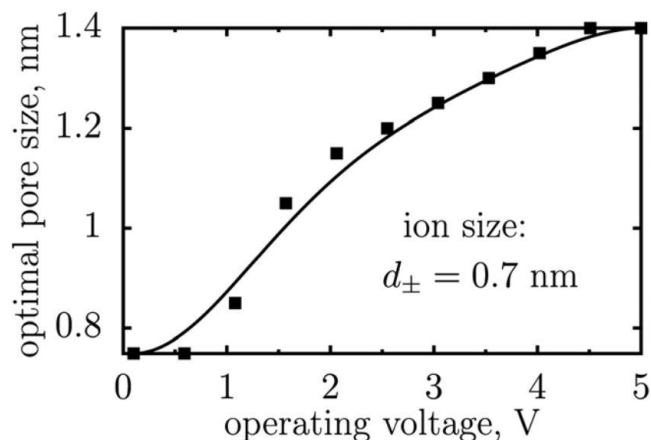
Figure 22: Optimal pore width of a porous supercapacitor as a function of the applied voltage. The symbols are obtained from the integration of MC simulation results for the differential capacitance, and the line using the spline curve that approximates them. The figure is reproduced from Ref.[598]

function of the pore width and its maximum depends on the voltage. To instruct a material engineer one needs to know the capacitance-voltage dependence which can be identified by theory, simulation[366] or, of course best of all, measurements. Narrowing the pore size distribution leads to the increase in the stored energy density (i.e. a monodisperse electrode with a carefully selected pore size) may be ideal for the energy storage in a nanoporous supercapacitor (c.f. Fig 6b in Ref.[598]). Note that the optimization that we were talking about so far was for 'ultra-narrow pores' that can accommodate just one row or one layer of ions. Larger nanopores would require different treatment.

7.4 Larger nanopores and the capacitance oscillations

A lesson how intensive is research in this area these days is given by the following story. On 24 August 2011, two papers were received – one by ACS Nano[449] and one by Nano Letters,[383] and a month later by Physical Chemistry Letters,[602] all published in October 2011! All three papers highlighted the phenomenon inherent to their titles: oscillatory behaviour of capacitance as a function of pore size, when the pore size is increasing from an ultra small value where the anomalous capacitance effect is observed 0.7-1 nm to the value of several ion diameters. Although different methods as well as different levels of description of the

molecular structure of RTIL ions were used in these papers (classical DFT of a restricted primitive model in Ref.,[383] MD simulations of an assembly of charged spheres in Ref.,[449] and fully atomistic MD simulations for model EMIM+ and TFSA− ions in Ref.,[602] all performed for model carbon slit pores), the results were qualitatively similar. The work[383] was later extended to the case of an RTIL-(organic)solvent mixture in a pore.[384]

The common conclusion of these works was that the capacitance undergoes 'oscillations' with the pore size; this effect was interpreted by the layering effect. As long as only one layer of ions can fit the gap, the smaller the gap, the higher the capacitance, but when the increase of the gap will allow to accommodate the second layer the capacitance again increases, just because more charge can be accommodated there. And off it goes, because when we further slightly increase the gap size, not yet allowing for the third layer, the capacitance will go down again due to weakening of the screening of interionic interactions, but with the accommodation of the fourth layer it will start growing again, and so on. Ref.[383] has reported data for pore width up to 12 ionic diameters (it was more difficult to simulate such large system by MD, so that Refs.[449] and[602] have limited their consideration by a couple of ionic diameters), with decaying oscillations extending in this ideal system up to 8 ionic diameters.

Although these predictions have not yet been experimentally verified, we believe that the effect might be real. According to the concept of the superionic state in nanopore, every time that we increase the pore size we make the, interaction between ions stronger and impede the ability to charge the pore due to the increased repulsion between counterions. But opening the possibility to fill in the next layer we double the charge and thus the capacitance per unit surface area of the pore should go up (we note that the volumetric one may not; this must be specially checked for each system). The two competing trends must provide the decaying oscillations.

None of the three mentioned papers have studied the interplay of the pore width and the voltage dependence, which must be very interesting. It would be natural to expect that vanishing the differential capacitance in wider pores will take place at much larger voltages. This was predicted for narrow pores,[372,595,598] but in wider pores the effects will be even more pronounced and interesting 'oscillatory' dependences might appear. It will be relevant

to perform investigations similar to Refs.[372,595] and in particular to Ref.[598] in terms of understanding the optima for energy storage for a wider scale of pore sizes.

7.5 'Quantized friction' in confined nanofilms of RTILs

We have already discussed above some of the papers that we are going to highlight in this section in the context of layering and overscreening in RTILs. However, the results presented in these papers have also a special value for understanding the properties of RTILs as potential lubricants,[157] with a highly relevant (for some applications, e.g. reading computer hard disks) possibility of friction control by voltage.

Ref.[66] reported high-resolution measurements of the forces between two atomically smooth surfaces across the film of the studied RTIL for film thicknesses ranging from 1 to 6 ionic diameters. Both, normal force, the so called structural force, and a shear force were measured, using the classical surface force apparatus of mica cross cylinders,[239] as a function of surface-to-surface separation. For the films thinner than 2 nm, oscillatory normal forces were observed with decreasing the surface-to-surface separation, as pairs of ionic layers were squeezed out of the film. This was very much expected, as one more evidence of the layering structure of the ionic liquid between charged walls (freshly cleaved mica surfaces are spontaneously negatively charged). However, measurements of the shear force has revealed spectacular effects. Friction appeared to be one or two orders of magnitude lower than that observed for the films of non-polar molecular liquids. Most interestingly, these studies have revealed a phenomenon of 'quantized friction'. Comparing the stable thicknesses of the film with 1 layer and 3 layers (2 layers are not stable between the identically charges surfaces for obvious reasons: the net charge in the neighboring layers should alternate, and this cannot make happy both surfaces), the friction of a 1-layer film is an order of magnitude higher than that for a three layer film, with an abrupt jump of the friction coefficient between the two states.

These fascinating results may have far leading consequences for the application of RTILs as lubricants;[157] however, qualitatively, they can be explained in a relatively straightforward way. The authors of Ref.[66] attributed these effects to "geometric and charge characteristics of ionic liquids", assuming that "the irregular shapes of the ions lead to a lower shear stress,

while the strong coulombic interactions between the ions and the charged confining surfaces leading to a robust film", when the film is one layer thick. Speaking in physical terms, the whole effect should be about the interplay between the patterns of charges on mica and those in the layers of RTIL. If those in anyway can be commensurate for a thin film, the shear resistance must be strong. However, commensurate or not, the laterally oscillating patterns of electric field created by a regular pattern of charges on the mica surfaces, with periodicity length a, will decay into the bulk of the film exponentially with a decay range a/π. This is a 'fast' decay, and the inhomogeneous component of the field crucial for shear resistance and friction will not be felt for thicker films. With that said, these phenomena certainly deserves development of a proper theory or computer simulation.

Bou-Malham and Bureau[67] investigated effects on surface charges on flow and molecular layering under nanoconfinement in two different RTILs that have the same organic cation, ([BMIM]+, and two different counterions ((i) [BF$_4$]−, and (ii) [PF$_6$]−). They also used the surface-force apparatus technique. This study has shown drastic effect of the charge surface on the layering of the RTILs in the nanoconfinement. Both ionic liquids start exhibiting strong molecular layering when confined between charge-bearing mica surfaces. The authors of Ref.[67] have shown that such layering dramatically affects the flow properties of the liquids: as confinement gets narrower, the viscosity increases over several orders of magnitude, until the liquids eventually get jammed and exhibited a solid-like response. However, the same liquids confined between *noncharged* methyl-terminated surfaces displayed no such layering and flown through the gap with their bulk-like viscosity, even when confined down to two monolayers in thickness.

The charge on the mica surface is fixed, so one cannot probe the effects of the voltage variation,which must obviously affect the structure of the RTIL film. Hence, very recently Sweeney et al[69] went farther and investigated a possibility of controlling friction by changing the voltage, using electrochemical in situ AFM configuration. They have studied gold electrode in RTIL measuring the friction by sliding the silica cantilever at nanoscale distance over the electrode surface. Friction force was recorded as a function of potential and applied load, varying normal loads up to 25 nN.

For all the probed potentials the shear resistance increased with the normal load, but

friction was shown to depend on electrode potential: the friction coefficient was found to be always higher with positive potentials. The authors interpreted it as follows. For positive potentials the probe displaces the last cation layer for normal loads greater than 2.5 nN but never displaced the last anion layer for all normal loads used. Correspondingly the last anion layer is displaced at negative potentials, but at no force it displaces the cation layer, kept solid at negative potentials. The authors of this very interesting paper consider various other features of the electric field effect on friction, stressing the importance of this work for a future 'nanotribotronics' – a science of manipulating friction at the nanoscale, in this case by using such a handy weapon as electrode potential.

8 Examples of other applications of RTILs at EIs

In this section we will briefly overview examples of other applications of RTILs at EIs such as batteries, fuel cells, solar cells and micro-actuators.

We note that, as mentioned in the introduction, there are many other application areas of RTILs at EIs such as electrodeposition, reactive media for electrosynthesis, electroanalytical and sensing applications etc. However, there are several good reviews and books on these subjects already and due to space limitations we would like to address interested readers to these essays, such as Refs[23,173,603,604] (electrodeposition), Refs[139,140] (electrosynthesis and electrochemical reactivity), Refs[17,28] (electroanalytical chemistry) and Refs[21,215] (sensors); see also Refs[33,36,79,80,522] and references therein for general information about RTIL applications.

8.1 Batteries

The main advantages of using RTILs in batteries are (i) large electrochemical window of some RTILs; (ii) nonvolatility; (iii) higher conductivity compared to standard polymer electrolytes used in commercial batteries; (iv) large operation range of temperatures; (v) most of RTILs are non-flammable.

Indeed, large EW leads to higher operation voltage of the batteries and, consequently, to higher amount of energy storage per battery mass. Batteries are meant to operate for years,

and, therefore, nonvolatility of battery electrolytes is strongly required to improve their shelf life. Therefore, for years, non-volatile polymer electrolytes were used in commercial ï£ijbatteries for electronic applications. However, the polymer electrolytes have one main drawback - their low ionic conductivity that leads to high ohmic losses in batteries.[182,605] RTILs, being also inflammable, have much higher conductivity that the polymer electrolytes. At the same time, they can operate in a large range of temperatures. Because they furthermore are nonaggressive to metals and other substances, that makes them an attractive alternative electrolytes for large-scale commercial use in batteries and there is an ongoing research on studying properties of new battery systems based on RTILs.[113,118,145,146,320,606]

Most of this research is focused on applications of RTILs in lithium-based batteries.[607] Recent review by Lewandowski and Swiderska-Mocek[107] overviews properties of room temperature ionic liquids (RTILs) as electrolytes for lithium and lithium-ion batteries. They point to the critical importance of the formation of the solid electrolyte interface (SEI) on the anode surface for correct operation of secondary lithium-ion batteries based ionic liquids as electrolytes. The authors conclude that SEI layer may be formed by electrochemical transformation of (i) a molecular additive, (ii) RTIL cations or (iii) RTIL anions. They argue that, due to the SEI formation the reference system in lithium battery-relevant electrochemical studies should be Li/SEI/Li+ rather than Li/Li+.[608] This review also discusses such properties of RTIL electrolytes as viscosity, conductivity, vapour pressure and lithium-ion transport numbers, all from the point of view of their influence on battery performance.

Primary lithium batteries that use a metal lithium electrode (Li/Li+) have higher energy densities compared to the secondary lithium batteries that use a carbon negative electrode which works as a host for Li+ ions by intercalation.[3,605,609] However, one of the main problems with the development of rechargeable primary lithium batteries is that the metallic lithium electrode used in these batteries quickly loses its smoothness during the repeated charging/discharging cycles with consequent forming of dendritic deposits on the electrode surface.[3,320,607] These deposits may cause an internal electrical short-circuit between the cathode and anode that would quickly deteriorate the battery properties. The deterioration of the electrode surface is the main reason of why despite of the inversible character of the reaction on the Li/Li+ electrode, the number of battery charging/recharging cycles is limited

that has negative effect on the shelf-life of the batteries. Another problem is safety issues related with dangerous reactions of metallic lithium and its alloys with water and other commonly used solvents.[607]

The high potential of RTIL-based electrolytes to overcome these problems because of their high electrochemical stability and overall chemical inertness was recognized in early 2000s.[607,610–612] Such, Howlett et al reported high lithium metal cycling efficiency in RTILs (made from N-methyl, N-alkyl pyrrolidinium cations with TFSA anion).[612] Shin et al suggested to incorporate of RTILs into polymer electrolytes to develop safe and stable battery electrolytes with higher conductivity than the 'dry' polymer electrolytes.[609]

To increase conductivity, RTILs in battery applications can be mixed with organic solvents.[319,613,614] Schweikert et al[614] investigated formation of lithium dendrites in lithium/$Li_4Ti_5O_{12}$ battery cells with different electrolytes by using a combination of different experimental techniques such as electrochemical impedance spectroscopy, scanning electron microscopy and in situ 7Li nuclear magnetic resonance spectroscopy. They demonstrated that the growth of lithium dendrites is significantly correlated to the electrolyte employed. All electrolytes used in this work, based on the ionic liquid 1-ethyl-3-methylimidazolium bis(trifluoromethane-sulfonyl)azanide (EMIM-TFSA) (either neat EMIM-TFSA or a mixture of EMIM-TFSA with ethylene carbonate or propylene carbonate), show reduced dendrite growth in comparison to the standard electrolyte for Li-ion batteries, lithium hexafluorophosphate ($LiPF_6$) in ethylene carbonate/dimethyl carbonate (EC/DMC). In the same work it has also been shown that $LiPF_6$ in EMIM-TFSA and $LiPF_6$ in EMIM-TFSA/propylene carbonate efficiently suppress lithium dendrites.

Even higher energy storage than in Li-ion batteries can be achieved in Li-O2 and Li-S batteries.[615] However, these devices currently exist only as prototypes because there are still a number of problems to overcome before development of commercially suitable Li-O2 and Li-S batteries such as safety, stability, cycling efficiency, formation of insulation layers on the electrode etc.[613] Use of RTILs as working electrolyte in Li-O2 and Li-S batteries is discussed as one of possible solutions to overcome these problems.[616,617]

In all the battery applications understanding the nanoscale structure of RTILs at electrodes is crucial for developing theoretical concept of their performance. It is important to

achieve a microscopic level of understanding the formation of dendrites and the elementary act of electrode kinetics, if electron transfer limited.

8.2   Fuel Cells

Protic ionic liquids are used as proton conducting media in fuel cells due to their high proton conductivity, low water sorption, thermal stability and low viscosity.[152,618] Such, recently, van de Ven et al used the ionic liquid 1-H-3-methylimidazolium bis(trifluoromethanesulfonyl) imide ([HMIM][TFSI]) as conductive filler in a tailor-made porous, polymeric polybenzimidazole (PBI) support as proton conductive membrane for high temperature (>100 °C) fuel cell applications.[152] They have shown that the fuel cell performance of this membrane clearly exceeds that of Nafion 117 at temperatures above 90 C. A power density of 0.039 Wcm^{-2} was obtained at the intended operation temperature of 150 °C proved that such PBI/RTIL membranes can be considered as a serious candidate for low temperature fuel cell applications.

The role of the interface between the porous electrodes and the electrolyte is complicated here by the fact that electrolyte is imbedded into the membrane, and the interface contains usually three phase boundaries.

8.3   Solar Cells

RTILs has been actively used for as electrolytes in dye-sensitized solar cells (DSSCs) that have attracted much attention as low-cost alternatives to conventional inorganic photovoltaic devices.[147,148,150,306,619] Liquid-state DSSCs with standard electrolytes have stability issues due to volatility of electrolytes; however, these drawbacks can be overcomed by using non-volatile and electrochemically stable RTILs[150,151,620–622] (for an overview of recent developments in this area see Ref.[151]).

8.4   Flexible energy storage devices

It has been shown that RTIL-nanocarbon composites can be used as soft functional materials for different applications including electronics and energy.[300,306,623,624] Such, Pushparaj et

al demonstrated in their paper[623] the possibility of development of energy-storage devices such as supercapacitors, Li-ion batteries, and their hybrids based on flexible nanocarbon-cellulose-RTIL sheets. As they write in their paper "selfstanding flexible paper devices can result in unprecedented design ingenuity, aiding in new forms of cost-effective energy storage devices that would occupy minimum space and adapt to stringent shape and space requirements".[623] Tamailarasan and Ramaprabhu in their recent paper[220] performed thorough analysis of several factors influencing performance of hybrid electrode materials based on carbon nanotubes-graphene-RTIL composites for high performance supercapacitors.[220] For an overview of nano-carbon composites for capacitive energy storage see also the recent review of Simon and Gogotsi.[222]

8.5 Miniaturized nanocarbon based electronics

Due to the low volatility of RTILs they can be used on a very small scale, i.e. at very high surface to volume ratios. This makes them very attractive as electrolytes for nano-scale electronic components such as microsupercapacitors[309] electrolyte-gated field-effect-transistors[162,164] and polymer semiconductors.[163] Understanding the structure of electrical double layer at micro and nano electrodes is crucial for understanding the operation of these devices.

8.6 Polymer electrolyte composite electroactuators

The main principle of EDL-based electroactuators is relatively simple, as such electroactuators are nothing else than plane capacitors with electrodes attached to bendable metallic plates.[625–628] Electrolyte here is impregnated into the polymer matrix, separating these plates. If the sizes of cations and anions are dramatically different, by applying voltage between two electrodes one redistributes ions between them. The region near the electrode rich in larger ions gets swollen and strained, whereas the region at the other electrode, rich in smaller ions, gets shrunk and relaxed. Correspondingly, the two plates bend in the latter direction. Changing the sign of the voltage between such electrodes will change the direction of bending. Ideally, if there is no trapping of ions and hysteresis, this process will be fully

reversible (which of course rarely happens in real systems).

This principle lies in the basis of a voltage-controlled 'micro-muscle'. Just a few volts are typically needed to achieve substantial actuation, making such systems prime candidates in applications to smart robotics and prosthetics.[77,629] Equally the forced bending of such beam generates voltage, which may be used for sensing beam bending fluctuations in turbulent flows, where local pressure and fluid-velocity fluctuations will generate alternating voltage, of special importance for hydraulics and aeronautics.[630,631] As transducers, one can envisage their applications as motion detectors and high performance sensors in artificial organs.[632–635] Last but not least, engineers think about using such electroactuators for generating electricity from ocean waves, coastal surf, and river white waters.[636,637]

The largest effect on bending is when only ions of one sign can move (can be of several sorts), the other is attached to the side chains of the polymer. Such system is realized when exchanging protons of Nafion by - as large as possible- ionic liquid cations, which have an ability to move, with terminal SO_3- groups immobile residing on the side chains.[638,639] In addition to the EDL-formation-induced swelling strain, there is also an 'electrostatic' stress on the polymer backbone due to the Coulomb repulsion of the net local unbalanced charge in the cation-depleted regions consisting predominantly of immobile anions. Depending on the average concentration of charge carriers, the latter effect can amplify the -swelling-induced bending or compete with it.[640] To avoid high friction and achieve faster electroactuator response organic solvent additives are often used to 'lubricate' the movement of cations.

Practically *analytical* theory of such systems have been recently developed which formulates the laws of equilibrium bending and bending dynamics;[640,641] for review of previous theories see these last works. However, that theory has been developed for electrode surfaces with a mild roughness (with the correlation length of roughness much larger than the characteristic thickness of the EDL (c.f.[574]). In reality, the trend is to maximalize the surface area, in order to amplify the the electroactuator's bending response. Similar to supercapacitors, porous electrodes are used, down to nanoscale porosity, e.g. by using nanotemplated structures such as carbon nanoforest rooted into the current collector beams. There was yet no theory adapted to such more complicated confinement.

Going back to the classical flat plate geometry EDL-based electroactuators, we note that

the description of the EDL here is somewhat different from the case of RTIL structures at other liquid-solid flat interfaces. First we note that here we deal with only one sort of mobile ions (cations) that rearrange upon building the EDL at the anode side consequently leaving behind almost bare anode layer at the cathode. All ions in electroactuators are imbedded in the polymer matrix with average ≈ 1 nm distance between the side-chain-anions, and thereby the distance between the ions is (on average) also ≈ 1 nm. There could be also some solvent molecules added to widen and lubricate pores of the membrane. All in all, concentrations of ions might be somewhat lower in the electroactuator membrane than in neat RTILs. For such systems, the theoretical framework developed for solid electrolytes with single mobile charge carriers[556] seems to serve its purpose as demonstrated in Refs.[372,598,642]

9 Conclusions

This review discussed principles of the theory of the EDL in RTILs at flat interfaces, the characteristics of RTILs in electrified nanoconfinement, and manifestations of these properties in various experimentally observed phenomena potentially important for generation and storage of electrical energy, information transduction and sensing, electrode kinetics and metal processing, as well as (nano)mechanical applications of RTILs (lubrication, electroactuators etc.). It was centred on the topics that have recently received some understanding (through the theory, reasonable models, simulations, and experiments) and those where new pressing questions still await answers could be formulated.

There is no easy way to end a review of the area where new important papers appear almost every day and the total number of publications reached (according to the ISI WoS) some 2,500, with >300 published in just 2012. We, therefore, terminate it with several remarks intended to sketch the big picture.

It is now commonly accepted that the EDL structure in RTILs is principally different from that of diluted electrolytic solutions, due to the effects of ion packing and strong Coulomb correlations ('lattice saturation' vs 'overscreening'). Both kinds of these effects become crucial due to high ionic densities of pure RTILs, remaining important in RTILs with minor addition of neutral organic molecules. However, the sterical effects gradually

become less and less important with dilution. Theoretical methods for the description of EDL on ideally flat surfaces have been developed and the basic laws of EDL response to electrode polarization (the crossover between 'overscreening' and 'lattice saturation') have been uncovered. Some progress towards understanding of the effects of surface roughness have been made.

Combination of the currently developed models of EDL with more involved models of the electronic double layer in the electrode remains to be the most pressing issue for the theory development, particularly in view of using various forms of carbon for which the ideal conductor approximation may not be adequate.

The ideas about EDL in semi-infinite RTILs could not be directly transferred to the polarization of RTILs in nanoconfinement. In narrow nanopores of the electrode the role of screening of interionic interactions by the electronic polarizability of the conducting walls appears crucial, as it renormalizes the ion-ion interactions. If pores are ideally metallic, the ions inside the pores will interact with each other via attractive/repulsive Yukawa-like short-range potentials, which will change dramatically the statistical mechanics of the ionic assembly there and its response to the electrode polarization. Within reasonable approximations these effects have been described both theoretically and through simulations. Deviation from ideal metallic screening in nanopores of carbon materials may change the character of ion-ion interactions, although the strength of the interactions will be in any case reduced and should become short range, because these materials are electronic conductors. The investigation of these effects is in progress.

Both, at flat interfaces and in nanoconfinement, the new theories predict strong dependence of the electrical capacitance of the interfaces on voltage. For flat interfaces it is not a Gouy-Chapman like dependence in defined cases; in nanoconfinement completely new laws come out. These show nonmonotonic voltage dependence, the shape of which is very sensitive to the pore size. Strong pore size dependence of capacitance at a given voltage was predicted explaining experimental observations. When pores get larger, interesting oscillating patterns of the capacitance pore-size-dependence were predicted theoretically and by simulations; these predictions are yet to be experimentally approved. However, in porous electrodes used for practical applications there are pores of different sizes. The pore-size distributions

116

'average out' and suppress many of the sharp features of the capacitance voltage-dependence.

Overscreening and layering phenomena play an important role not only in the formation of EDL in RTILs, but also in formation of normal and shear forces between surfaces separated by RTILs. Those observations resulted in the experimentally discovered phenomenon of quantized friction, the theory of which remains to be built.

Overscreening may appear to be very important in electrochemical kinetics through the so-called Frumkin correction effect. In RTIL-based electrolytes this may become not a correction at all, but something that fully renormalizes the driving force for electron transfer reactions at electrodes, at low and moderate voltages. At large voltages, lattice saturation effect may cause non-Tafel current-voltage characteristics. The theory and understanding of these effects are still at their infancy.

The effects of surface roughness and chemical inhomogeneity of electrode surfaces on the overscreeing and layering remain to be theoretically investigated. If the correlation length of roughness (or chemical inhomogeneity) and the mean height of roughness are of the order of the characteristic correlation lengths in RTILs, the layering and overscreening (which are some kind of resonance phenomena) can get smeared out. This will not happen, however, if the roughness/inhomogeneity scales are much larger, because for the structure of EDL the interface will locally look smooth and homogeneous.

RTILs in elastic media and the role of excluded volume effects there is another interesting area for future development. Progress has been made in the theory, understanding, and experimental characterization of electroactuation with RTILs using mildly rough electrodes. In nanoporous electrodes of supercapacitors and electroactuators, the effects of ion-induced stress and strain remain to be understood and quantitatively investigated.

Many interesting effects of ion molecular shape have been studied in the EDL at flat electrodes, but this remains to be explored in nanoconfinement.

Some first steps towards rationalyzing the differences between the laws of energy storage in porous electrodes with RTILs and with ordinarily organic or aqueous solutions have been made. In the latter case the counterions, drawn by voltage, are to replace not only the co-ions, but also the solvent molecules. Theoretical analysis has revealed the differences in the energy storage capacity between the cases of ionophobic and ionophillic, solvophobic

117

and solvophillic pores. The predictions of the theory remain to be experimentally approved. Once established, they may appear to be lessening for energy storage technologies.

Recall that most of the interest to RTILs, in terms of their applications, is due to their low volatility and wider electrochemical stability compared to most standard electrolytes. The low volatility makes the large surface-to-volume ratio to be not a problem for applications in various nanodevices. As for the electrochemical stability, not in every RTIL it is as good as one may wish it. Establishing the voltage-windows within which electrochemical reactions that may cause degradation of the electrodes do not take place is a subject of many experimental studies. These have been and are being performed for various RTILs and their mixtures at various electrodes. For a practitioner in energy storage, one of the most important requirements is that RTIL, as an electrolyte, would provide the maximal number of charging cycles without the onset of the degradation. In particular, such high-tech devices as supercapacitors are very expensive, and currently the primary target is not only their price, but also durability and a warranted and largest return on investment during its life-time. This aspect has to be kept in mind when formulating the tasks for chemical theory and computations in RTIL electrodics. For instance, one of the important physical effects here may be the distribution of impurities near the interface. As many RTILs are generally sorbing water from the air and easily dissolving organic additives, it remains to be understood how much of these polar or polarizable molecules will get sucked into the inhomogeneous electric field of the EDL and how they will be distributed there. A legitimate question is, how rich-in-water the EDL might become (an undesirable feature in the most cases), even at negligible concentrations of water in the bulk?

One of the possible central subjects for future studies is the dynamics of the double layer charging and relaxation in RTILs. The mysteriously slow 'glassy-like' relaxation of ionic liquids in the bulk is still not well understood, the more so the fast and slow dynamic components of charging at interfaces. Investigation of transport dynamics in nano-scale pores has just started. Note that studying the dynamics is not only about the time dependence and charging-discharging rates: it is about energy losses and, thereby, power delivery. In the context of forces between solids, it is crucial for the dissipation and dynamic friction. These will likely soon become the subject of many publications.

10   Nomenclature

$$\begin{aligned}
\text{AC} &= \textbf{a}\text{ctivated } \textbf{c}\text{arbon} \\[4pt]
\text{AFM} &= \text{atomic force microscopy} \\[4pt]
\text{BASIL} &= \text{Biphasic Acid Scavenging Utilizing Ionic Liquids}[104] \\[4pt]
\text{BBGKY} &= \text{Bogolyubov-Born-Green-Kirkwood-Yvon (equations)} \\[4pt]
\text{BEG} &= \text{Blum-Every-Griffith (model)} \\[4pt]
\text{CDC} &= \textbf{c}\text{arbide-}\textbf{d}\text{erived } \textbf{c}\text{arbon} \\[4pt]
\text{CPE} &= \textbf{c}\text{onstant } \textbf{p}\text{hase } \textbf{e}\text{lement} \\[4pt]
\text{CS} &= \text{Charged-Sheet (correction)} \\[4pt]
\text{DFT} &= \text{density functional theory} \\[4pt]
\text{DSSC} &= \text{dye-sensitized solar cell} \\[4pt]
\text{EDL} &= \text{electrical double layer} \\[4pt]
\text{EI} &= \text{electrified interface} \\[4pt]
\text{EW} &= \text{electrochemical window} \\[4pt]
\text{GC} &= \text{glassy carbon} \\[4pt]
\text{GCh} &= \text{Gouy-Chapman (theory)} \\[4pt]
\text{HTMS} &= \text{high temperature molten salt} \\[4pt]
\text{IL} &= \text{ionic liquid} \\[4pt]
\text{KK} &= \text{Kramers-Kroenig (relation)} \\[4pt]
\text{MD} &= \text{Molecular Dynamics (simulations)} \\[4pt]
\text{MIES} &= \text{metastable induced electron spectroscopy}
\end{aligned}$$

MSA = mean spherical approximation

NICISS = neutral-impact-collision ion scattering spectroscopy

ORR = oxygen reduction reaction

PME = Particle Mesh Ewald

p.z.c. = potential of zero charge

RISM = Reference Interaction Site Model

RTIL = room temperature ionic liquid

SEI = solid electrolyte interface

SFG = sum frequency generation (spectroscopy)

STM = scanning tunneling microscopy

TC = **t**emplated **c**arbon

TGA = thermogravimetric analysis

VTF = Vogel-Tammann-Fulcher (equation)

XPS = X-ray photoelectron spectroscopy

3D-EWC = 3D Ewald correction (method)

Ionic Liquids

Cations

BMIM = 1-butyl-3-methylimidazolium

BMMIM = 1-butyl-2,3 dimethylimidazolium

BMPy = N-Butyl-3-methyl-pyridinium

BMPyr = N-n-butyl-N-methylpyrrolidinium

BTM = butyltrimethylammonium

C_nMIM = 1-alkyl-3-methylimidazolium

DiAlI = 1,3-diallylimidazolium

DMOA = N,N-Diethyl-N-methyl-N-(2-methoxyethyl)ammonium

EMI = EMIM = 1-ethyl-3-methylimidazolium

HMIM = 1-H-3-methylimidazolium

HMPyr = HMPyrr = 1-hexyl-1-methyl-pyrrolidinium

HTE = hexyltriethylammonium

MOEMMor = 4-(2-Methoxyethyl)-4-methylmorpholinium

MOPMPip = 1-(3-methoxypropyl)-1-methylpiperidinium

$N_{112,102}$ = N-Ethyl-N,N-dimethyl-2-methoxyethylammonium

Pyr_{13} = N-methyl-N-propylpyrrolidinium

$P_{4,666}$ = Trihexyl(tetradecyl) phosphonium

TMPA = N,N,N-trimethyl-N-propylammonium

S222 = Triethylsulfonium

Anions

DCA = dicyanamide [FAP] = tris(pentafluoroethyl)-trifluorophosphate

FSI = bis(fluorosulfonyl)imide

OAc = acetate

TFA = trifluoroacetate

TfO = OTf = trifluoromethanesulfonate (triflate), $[CF_3SO_3]$-

TFSA = bis(trifluoromethanesulfonyl)azanide, $[(CF_3SO_2)_2N]$-, (this anion has ambiguous naming and it also named in the literature as TFSI, bis(trifluoromethanesulfonyl)imide) or bis(trifluoromethanesulfonyl)imidide), or bistriflamide or bis(trifluoromethylsulfonyl)amide, NTf_2 (or $N(Tf)_2$))

TFSI = bis(trifluoromethanesulfonyl)imide=bis(trifluoromethanesulfonyl)imidide (see also the comment above)

TPTP = tris(pentafluoroethyl)trifluorophosphate

11   Acknowledgment

References

(1) Bockris, J. O.; Khan, S. U. M. *Surface Electrochemistry: A Molecular Level Approach*; Springer: New York, 1993.

(2) Kornyshev, A. A.; Spohr, E.; Vorotyntsev, M. A. *Electrochemical Interfaces: At the Border line*; Wiley-VCH, 2002.

(3) Izutsu, K. *Electrochemistry in Nonaqueous Solutions*; Wiley-VCH, 2009.

(4) Schmickler, W.; Santos, E. *Interfacial Electrochemistry*; Springer: New York, 2010.

(5) Graves, A. D.; Inman, D. *J. Electroanal. Chem.* **1970**, *25*, 357.

(6) Rovere, M.; Tosi, M. P. *Rep. Prog. Phys.* **1986**, *49*, 1001.

(7) Bockris, J.; Reddy, A. K. N. *Modern electrochemistry. 1*; Kluwer Academic Publishers: New York, 2002.

(8) Hurley, F. H.; WIer, T. P. *J. Electrochem. Soc.* **1951**, *98*, 207.

(9) Ford, W. T. *Anal. Chem.* **1975**, *47*, 1125.

(10) Welch, B.; Osteryoung, R. *J. Electroanal. Chem.* **1981**, *118*, 455.

(11) Galiński, M.; Lewandowski, A.; Stępniak, I. *Electrochim. Acta.* **2006**, *51*, 5567.

(12) Liu, Q.; El Abedin, S. Z.; Endres, F. *Surf. Coat. Tech.* **2006**, *201*, 1352.

(13) Bonhote, P.; Dias, A. P.; Papageorgiou, N.; Kalyanasundaram, K.; Gratzel, M. *Inorg. Chem.* **1996**, *35*, 1168.

(14) Earle, M. J.; Seddon, K. R. *Pure. Appl. Chem.* **2000**, *72*, 1391.

(15) Endres, F. *ChemPhysChem* **2002**, *3*, 144.

(16) Buzzeo, M.; Evans, R.; Compton, R. *ChemPhysChem* **2004**, *5*, 1106.

(17) Ohno, H., Ed. *Electrochemical Aspects of Ionic Liquids*; Wiley & Sons, 2005.

(18) Silvester, D.; Compton, R. *Z. Phys. Chem.* **2006**, *220*, 1247.

(19) MacFarlane, D. R.; Forsyth, M.; Howlett, P. C.; Pringle, J. M.; Sun, J.; Annat, G.; Neil, W.; Izgorodina, E. I. *Accounts. Chem. Res.* **2007**, *40*, 1165.

(20) El Abedin, S. Z.; Polleth, M.; Meiss, S. A.; Janek, J.; Endres, F. *Green. Chem.* **2007**, *9*, 549.

(21) Wei, D.; Ivaska, A. *Anal. Chim. Acta.* **2008**, *607*, 126.

(22) Armand, M.; Endres, F.; MacFarlane, D. R.; Ohno, H.; Scrosati, B. *Nat. Mater.* **2009**, *8*, 621.

(23) Su, Y. Z.; Fu, Y. C.; Wei, Y. M.; Yan, J. W.; Mao, B. W. *Chemphyschem* **2010**, *11*, 2764.

(24) MacFarlane, D. R.; Pringle, J. M.; Howlett, P. C.; Forsyth, M. *Phys. Chem. Chem. Phys.* **2010**, *12*, 1659.

(25) Liu, H.; Liu, Y.; Li, J. *Phys. Chem. Chem. Phys.* **2010**, *12*, 1685.

(26) Barrosse-Antle, L. E.; Bond, A. M.; Compton, R. G.; O'Mahony, A. M.; Rogers, E. I.; Silvester, D. S. *Chem-Asian. J.* **2010**, *5*, 202.

(27) Opallo, M.; Lesniewski, A. *J. Electroanal. Chem.* **2011**, *656*, 2.

(28) Siangproh, W.; Duangchai, W.; Chailapakul, O. In *Handbook of Ionic Liquids: Properties, Applications and Hazards*; Mun, J., Sim, H., Eds.; Nova Science Publishers, Inc.: New York, 2012; p 79.

(29) Abbott, A. P.; Frisch, G.; Ryder, K. S. *Annu. Rev. Mater. Res.* **2013**, *43*.

(30) Plechkova, N. V.; Seddon, K. R. *Chem. Soc. Rev.* **2008**, *37*, 123.

(31) Wishart, J. F. *Energ. Environ. Sci.* **2009**, *2*, 956.

(32) Giernoth, R. *Angew. Chem. Int. Edit.* **2010**, *49*, 2834.

(33) Werner, S.; Haumann, M.; Wasserscheid, P. *Annu. Rev. Chem. Biomol. Eng.* **2010**, *1*, 203.

(34) Torimoto, T.; Tsuda, T.; Okazaki, K.-i.; Kuwabata, S. *Adv. Mater.* **2010**, *22*, 1196.

(35) Hallett, J. P.; Welton, T. *Chem. Rev.* **2011**, *111*, 3508.

(36) Seddon, K. R.; Plechkova, N. V. *Ionic Liquids UnCOILed: Critical Expert Overviews*; John Wiley & Sons, 2012.

(37) Lin, R.; Taberna, P.-L.; Fantini, S.; Presser, V.; Pérez, C. R.; Malbosc, F.; Rupesinghe, N. L.; Teo, K. B. K.; Gogotsi, Y.; Simon, P. *J. Phys. Chem. Lett.* **2011**, *2*, 2396.

(38) Freire, M. G.; Santos, L. M.; Fernandes, A. M.; Coutinho, J. A.; Marrucho, I. M. *Fluid. Phase. Equilibr.* **2007**, *261*, 449.

(39) Niedermeyer, H.; Hallett, J. P.; Villar-Garcia, I. J.; Hunt, P. A.; Welton, T. *Chem. Soc. Rev.* **2012**, *41*, 7780.

(40) Hunt, P. A.; Kirchner, B.; Welton, T. *Chem-Eur. J.* **2006**, *12*, 6762.

(41) Kossmann, S.; Thar, J.; Kirchner, B.; Hunt, P. A.; Welton, T. *J. Chem. Phys.* **2006**, *124*, 174506.

(42) Lehmann, S. B. C.; Roatsch, M.; Schöppke, M.; Kirchner, B. *Phys. Chem. Chem. Phys.* **2010**, *12*, 7473.

(43) Kurig, H.; Vestli, M.; Tõnurist, K.; Jänes, A.; Lust, E. *J. Electrochem. Soc.* **2012**, *159*, A944.

(44) Rigby, J.; Izgorodina, E. I. *Phys. Chem. Chem. Phys.* **2013**, *15*, 1632.

(45) Krossing, I.; Slattery, J. M.; Daguenet, C.; Dyson, P. J.; Oleinikova, A.; Weingärtner, H. *J. Am. Chem. Soc.* **2006**, *128*, 13427.

(46) Hayyan, M.; Mjalli, F. S.; Hashim, M. A.; AlNashef, I. M.; Mei, T. X. *J. Ind. Eng. Chem.* **2013**, *19*, 106.

(47) Georgi, N.; Kornyshev, A. A.; Fedorov, M. V. *J. Electroanal. Chem.* **2010**, *649*, 261.

(48) We note, however, that although the vapour pressure of most RTILs is very small, it is, nevertheless, *measurable* for most of RTILs.[36,49] Moreover, as it was shown in Refs,[49,112] high-vacuum and ultra-high vacuum (UHV) distillation of ionic liquids and separation of ionic liquid mixtures are, in principle, possible; UHV distillation can be used for obtaining high purity ionic liquids for analytical applications.[112] .

(49) Earle, M. J.; Esperança, J. M. S. S.; Gilea, M. A.; Lopes, J. N. C.; Rebelo, L. P. N.; Magee, J. W.; Seddon, K. R.; Widegren, J. A. *Nature* **2006**, *439*, 831.

(50) Welton, T. *Chem. Rev.* **1999**, *99*, 2071.

(51) Marinescu, M.; Urbakh, M.; Barnea, T.; Kucernak, A. R.; Kornyshev, A. A. *J. Phys. Chem. C.* **2010**, *114*, 22558.

(52) Kornyshev, A. A. *J. Phys. Chem. B.* **2007**, *111*, 5545.

(53) Hansen, J. P.; McDonald, I. R. *Phys. Rev. A* **1975**, *11*, 2111.

(54) Rosenfeld, Y. *J. Chem. Phys.* **1993**, *98*, 8126.

(55) Freyland, W. *Coulombic fluids: bulk and interfaces*; Springer series in solid-state sciences; Springer: Berlin, 2011; p 168.

(56) Levin, Y. *Rep. Prog. Phys.* **2002**, *65*, 1577.

(57) Schröer, W.; Weingartner, H. *Pure. Appl. Chem.* **2004**, *76*, 19.

(58) Schröer, W. *NATO Sci. Ser. II Math.* **2005**, *206*, 143.

(59) Bockris, J. O.; Reddy, A. K. N.; Gamboa-Aldeco, M. *Modern electrochemistry. 2A*, 2nd ed.; Kluwer Academic Publishers: New York, 2002 .

(60) Brett, C. M.; Oliveira Brett, A. In *Comprehensive Chemical Kinetics*; Bamford, C., Compton, R. G., Eds.; Elsevier B.V.: Amsterdam, 1986 .

(61) Endres, F.; Hofft, O.; Borisenko, N.; Gasparotto, L. H.; Prowald, A.; Al-Salman, R.; Carstens, T.; Atkin, R.; Bund, A.; El Abedin, S. Z. *Phys. Chem. Chem. Phys.* **2010**, *12*, 1724.

(62) Monroe, C. W.; Daikhin, L. I.; Urbakh, M.; Kornyshev, A. A. *J. Phys-Condens. Mat.* **2006**, *18*, 2837.

(63) Monroe, C. W.; Daikhin, L. I.; Urbakh, M.; Kornyshev, A. A. *Phys. Rev. Lett.* **2006**, *97*, 136102.

(64) Girault, H.; Kornyshev, A. A.; Monroe, C. W.; Urbakh, M. *J. Phys-Condens. Mat.* **2007**, *19*, 370301.

(65) Monroe, C. W.; Urbakh, M.; Kornyshev, A. A. *J. Electrochem. Soc.* **2009**, *156*, P21.

(66) Perkin, S.; Albrecht, T.; Klein, J. *Phys. Chem. Chem. Phys.* **2010**, *12*, 1243.

(67) Bou-Malham, I.; Bureau, L. *Soft. Matter.* **2010**, *6*, 406.

(68) Perkin, S. *Phys. Chem. Chem. Phys.* **2012**, *14*, 5052.

(69) Sweeney, J.; Hausen, F.; Hayes, R.; Webber, G. B.; Endres, F.; Rutland, M. W.; Bennewitz, R.; Atkin, R. *Phys. Rev. Lett.* **2012**, *109*, 155502.

(70) Li, H.; Rutland, M. W.; Atkin, R. *Phys. Chem. Chem. Phys.* **2013**,

(71) Vol'fkovich, Y. M.; Serdyuk, T. M. *Russ. J. Electrochem+.* **2002**, *38*, 935.

(72) Mastragostino, M.; Soavi, F. *J. Power. Sources.* **2007**, *174*, 89.

(73) Simon, P.; Gogotsi, Y. *Nat. Mater.* **2008**, *7*, 845.

(74) Beguin, F.; Frackowiak, E. *Carbons for Electrochemical Energy Storage and Conversion Systems*; CRC Press, 2010.

(75) Conway, B. E. *Electrochemical supercapacitors: scientific fundamentals and technological applications*; Springer, 1999.

(76) Bar-Cohen, Y. In *Compliant structures in nature and engineering*; Jenkins, C. H., Ed.; WIT: Southampton; UK, 2005.

(77) Bar-Cohen, Y.; Zhang, Q. *MRS. Bull.* **2008**, *33*, 173.

(78) Xiong, L.; Fletcher, A. M.; Ernst, S.; Davies, S. G.; Compton, R. G. *Analyst* **2012**, *137*, 2567.

(79) Wasserscheid, P., Welton, T., Eds. *Ionic Liquids in Synthesis*; Wiley-VCH, 2003.

(80) Gaune-Escard, M.; Seddon, K. R. *Molten Salts and Ionic Liquids: Never the Twain?*; John Wiley and Sons, 2009.

(81) Cao, Y.; Yao, S.; Wang, X.; Peng, Q.; Song, H. In *Handbook of Ionic Liquids: Properties, Applications and Hazards*; Mun, J., Sim, H., Eds.; Nova Science Publishers, Inc.: New York, 2012; p 145–172.

(82) Wilkes, J. S. *Green. Chem.* **2002**, *4*, 73–80.

(83) Walden, P. *Bull. Russ. Acad. Sci. Phys.* **1914**, 405.

(84) Gabriel, S.; Weiner, J. *Ber. Dtsch. Chem. Ges.* **1888**, *21*, 2669.

(85) Graenacher, C. Cellulose Solution. U.S. Patent 1,943,176, Jan 9, **1934** .

(86) Chum, H. L.; Koch, V. R.; Miller, L. L.; Osteryoung, R. A. *J. Am. Chem. Soc.* **1975**, *97*, 3264.

(87) Mirnaya, T. A.; Prisyazhnyi, V. D.; Shcherbakov, V. A. *Russ. Chem. Rev.* **1989**, *58*, 821.

(88) Gale, R. J.; Osteryoung, R. A. *Electrochim. Acta.* **1980**, *25*, 1527.

(89) Hussey, C. L.; King, L. A.; Nardi, J. C. AlCl3 /1-alkyl pyridinium chloride room temperature electrolytes. U.S. Patent US4122245 A, Aug 19, **1977**.

(90) Wilkes, J.; Levisky, J.; Wilson, R.; Hussey, C. *Inorg. Chem.* **1982**, *21*, 1263.

(91) Fannin, A.; King, L.; Stech, D.; Vaughn, R.; Wilkes, J.; Williams, J. *J. Electrochem. Soc.* **1982**, *129*, C122.

(92) Wilkes, J.; Levisky, J.; Pflug, J.; Hussey, C.; Scheffler, T. *Anal. Chem.* **1982**, *54*, 2378.

(93) Wilkes, J.; Frye, J.; Reynolds, G. *Inorg. Chem.* **1983**, *22*, 3870.

(94) Fannin, A.; Floreani, D.; King, L.; Landers, J.; Piersma, B.; Stech, D.; Vaughn, R.; Wilkes, J.; Williams, J. *J. Phys. Chem* **1984**, *88*, 2614.

(95) Hussey, C.; Scheffler, T.; Wilkes, J.; Fannin, A. *J. Electrochem. Soc.* **1986**, *133*, 1389.

(96) Dymek, C.; Hussey, C.; Wilkes, J.; Oye, H. *J. Electrochem. Soc.* **1987**, *134*, C510.

(97) Øye, H.; Jagtoyen, M.; Oksefjell, T.; Wilkes, J. *Mater. Sci. Forum.* **1991**, *73-75*, 183.

(98) Elias, A.; Wilkes, J. *J. Chem. Eng. Data.* **1994**, *39*, 79.

(99) Poole, C. F. *J. Chromatogr. A.* **2004**, *1037*, 49.

(100) Gale, R.; Osteryoung, R. *Inorg. Chem.* **1979**, *18*, 1603.

(101) Price, D.; Copley, J. *Phys. Rev. A* **1975**, *11*, 2124.

(102) Copley, J.; Rahman, A. *Phys. Rev. A* **1976**, *13*, 2276.

(103) Wilkes, J.; Zaworotko, M. *J. Chem. Soc. Chem. Comm.* **1992**, 965.

(104) Maase, M.; Massonne, K. In *Ionic Liquids Iiib: Fundamentals, Progress, Challenges and Opportunities: Transformations and Processes*; Rogers, R. D., Seddon, K. R., Eds.; Amer Chemical Soc: Washington, 2005; Vol. 902; p 126.

(105) Tang, S.; Baker, G. A.; Zhao, H. *Chem. Soc. Rev.* **2012**, *41*, 4030.

(106) Stark, A. *Top. Curr. Chem.* **2009**, *290*, 41.

(107) Lewandowski, A.; Świderska-Mocek, A. *J. Power. Sources.* **2009**, *194*, 601.

(108) Armstrong, J. P.; Hurst, C.; Jones, R. G.; Licence, P.; Lovelock, K. R. J.; Satterley, C. J.; Villar-Garcia, I. *J. Phys. Chem. Chem. Phys.* **2007**, *9*, 982.

(109) Ludwig, R.; Kragl, U. *Angew. Chem. Int. Edit.* **2007**, *46*, 6582.

(110) Rocha, M. A. A.; Lima, C. F. R. A. C.; Gomes, L. R.; Schröder, B.; Coutinho, J. A. P.; Marrucho, I. M.; Esperança, J. M. S. S.; Rebelo, L. P. N.; Shimizu, K.; Lopes, J. N. C.; Santos, L. M. N. B. F. *J. Phys. Chem. B.* **2011**, *115*, 10919–10926.

(111) Zaitsau, D. H.; Fumino, K.; Emel'yanenko, V. N.; Yermalayeu, A. V.; Ludwig, R.; Verevkin, S. P. *ChemPhysChem* **2012**, *13*, 1868.

(112) Taylor, A. W.; Lovelock, K. R. J.; Deyko, A.; Licence, P.; Jones, R. G. *Phys. Chem. Chem. Phys.* **2010**, *12*, 1772.

(113) Borgel, V.; Markevich, E.; Aurbach, D.; Semrau, G.; Schmidt, M. *J. Power. Sources.* **2009**, *189*, 331.

(114) Rogers, E. I.; Šljukić, B.; Hardacre, C.; Compton, R. G. *J. Chem. Eng. Data.* **2009**, *54*, 2049.

(115) Lu, X.; Burrell, G.; Separovic, F.; Zhao, C. *J. Phys. Chem. B* **2012**, *116*, 9160.

(116) Tian, Y.-H.; Goff, G. S.; Runde, W. H.; Batista, E. R. *J. Phys. Chem. B.* **2012**, *116*, 11943.

(117) Olson, E. J.; Bühlmann, P. *J. Electrochem. Soc.* **2013**, *160*, A320.

(118) Xiang, J.; Wu, F.; Chen, R.; Li, L.; Yu, H. *J. Power. Sources.* **2013**, *233*, 115.

(119) Freire, M. G.; Carvalho, P. J.; Gardas, R. L.; Marrucho, I. M.; Santos, L. M. N. B. F.; Coutinho, J. A. P. *J. Phys. Chem. B.* **2008**, *112*, 1604.

(120) Chaban, V. V.; Prezhdo, O. V. *J. Phys. Chem. Lett.* **2011**, *2*, 2499.

(121) Wypych, G., Ed. *Handbook of solvents*; ChemTec Publishing, Toronto, Kanada, 2001.

(122) Cho, C. W.; Pham, T. P. T.; Jeon, Y. C.; Vijayaraghavan, K.; Choe, W. S.; Yun, Y. S. *Chemosphere* **2007**, *69*, 1003.

(123) Stephens, G.; Licence, P. *Chim. Oggi.* **2011**, *29*, 72.

(124) McCrary, P. D.; Rogers, R. D. *Chem. Commun.* **2013**,

(125) Czerwicka, M.; Stolte, S.; Muller, A.; Siedlecka, E. M.; Golebiowski, M.; Kumirska, J.; Stepnowski, P. *J. Hazard. Mater.* **2009**, *171*, 478.

(126) Ventura, S. P. M.; Gonçalves, A. M. M.; Sintra, T.; Pereira, J. L.; Gonçalves, F.; Coutinho, J. A. P. *Ecotoxicology* **2013**, *22*, 1.

(127) Docherty, K. M.; Kulpa, C. F. *Green. Chem.* **2005**, *7*, 185.

(128) Ranke, J., Stolte, S., Stormann, R., Arning, J., Jastorff, B. *Chem. Rev.* **2007**, *107*, 2183.

(129) Swatloski, R. P.; Holbrey, J. D.; Rogers, R. D. *Green. Chem.* **2003**, *5*, 361.

(130) Siedlecka, E. M.; Czerwicka, M.; Stolte, S.; Stepnowski, P. *Curr. Org. Chem.* **2011**, *15*, 1974.

(131) Fernandez, J. F.; Neumann, J.; Thoming, J. *Curr. Org. Chem.* **2011**, *15*, 1992.

(132) Steinruck, H. P.; Libuda, J.; Wasserscheid, P.; Cremer, T.; Kolbeck, C.; Laurin, M.; Maier, F.; Sobota, M.; Schulz, P. S.; Stark, M. *Adv. Mater.* **2011**, *23*, 2571.

(133) Stojanovic, A.; Keppler, B. K. *Separ. Sci. Tech.* **2012**, *47*, 189.

(134) Kilpelainen, I.; Xie, H.; King, A.; Granstrom, M.; Heikkinen, S.; Argyropoulos, D. S. *Jour. Agr. Food. Chem.* **2007**, *55*, 9142.

(135) Wang, H.; Gurau, G.; Rogers, R. D. *Chem. Soc. Rev.* **2012**, *41*, 1519.

(136) Freyland, W.; Zell, C.; Abedin, S. E.; Endres, F. *Electrochim. Acta.* **2003**, *48*, 3053.

(137) Zhang, M. M.; Kamavaram, V.; Reddy, R. G. *JOM* **2003**, *55*, A54.

(138) El Abedin, S. Z.; Endres, F. *Chemphyschem* **2006**, *7*, 58.

(139) Yoshida, J.-i.; Kataoka, K.; Horcajada, R.; Nagaki, A. *Chem. Rev.* **2008**, *108*, 2265.

(140) Hapiot, P.; Lagrost, C. *Chem. Rev.* **2008**, *108*, 2238.

(141) Balducci, A.; Bardi, U.; Caporali, S.; Mastragostino, M.; Soavi, F. *Electrochem. Commun.* **2004**, *6*, 566.

(142) Frackowiak, E. *J. Braz. Chem. Soc.* **2006**, *17*, 1074.

(143) Vivekchand, S. R. C.; Rout, C. S.; Subrahmanyam, K. S.; Govindaraj, A.; Rao, C. N. R. *J. Chem. Sci.* **2008**, *120*, 9.

(144) Liu, C.; Yu, Z.; Neff, D.; Zhamu, A.; Jang, B. Z. *Nano Lett.* **2010**, *10*, 4863.

(145) Sakaebe, H.; Matsumoto, H.; Tatsumi, K. *Electrochim. Acta.* **2007**, *53*, 1048.

(146) Quartarone, E.; Mustarelli, P. *Chem. Soc. Rev.* **2011**, *40*, 2525.

(147) Wang, P.; Zakeeruddin, S. M.; Moser, J.-E.; Grätzel, M. *J. Phys. Chem. B.* **2003**, *107*, 13280.

(148) Li, B.; Wang, L.; Kang, B.; Wang, P.; Qiu, Y. *Sol. Energy Mater. Sol. Cells* **2006**, *90*, 549.

(149) Zistler, M.; Wachter, P.; Schreiner, C.; Fleischmann, M.; Gerhard, D.; Wasserscheid, P.; Hinsch, A.; Gores, H. J. *J. Electrochem. Soc.* **2007**, *154*, B925.

(150) Hagfeldt, A.; Boschloo, G.; Sun, L.; Kloo, L.; Pettersson, H. *Chem. Rev.* **2010**, *110*, 6595.

(151) Lee, C.-P.; Ho, K.-C. In *Handbook of Ionic Liquids: Properties, Applications and Hazards*; Mun, J., Sim, H., Eds.; Nova Science Publishers, Inc.: New York, 2012; p 173.

(152) van de Ven, E.; Chairuna, A.; Merle, G.; Benito, S. P.; Borneman, Z.; Nijmeijer, K. *J. Power. Sources.* **2013**, *222*, 202.

(153) Millefiorini, S.; Tkaczyk, A. H.; Sedev, R.; Efthimiadis, J.; Ralston, J. *J. Am. Chem. Soc.* **2006**, *128*, 3098.

(154) Nanayakkara, Y. S.; Moon, H.; Payagala, T.; Wijeratne, A. B.; Crank, J. A.; Sharma, P. S.; Armstrong, D. W. *Anal. Chem.* **2008**, *80*, 7690.

(155) Zhang, X.; Cai, Y. *Angewandte Chemie* **2013**, *125*, 2345.

(156) Zhou, F.; Liang, Y.; Liu, W. *Chem. Soc. Rev.* **2009**, *38*, 2590.

(157) Palacio, M.; Bhushan, B. *Tribol. Lett.* **2010**, *40*, 247.

(158) Garcia-Etxarri, A.; Aizpurua, J.; Molina-Aldareguia, J.; Marcilla, R.; Adolfo Pomposo, J.; Mecerreyes, D. *Front. Phys. China* **2010**, *5*, 330.

(159) Albrecht, T.; Moth-Poulsen, K.; Christensen, J. B.; Hjelm, J.; Bjørnholm, T.; Ulstrup, J. *J. Am. Chem. Soc.* **2006**, *128*, 6574.

(160) Chen, F.; Qing, Q.; Xia, J. L.; Li, J. H.; Tao, N. J. *J. Am. Chem. Soc.* **2009**, *131*, 9908.

(161) Xie, W.; Frisbie, C. D. *J. Phys. Chem. C.* **2011**, *115*, 14360.

(162) Thiemann, S.; Sachnov, S.; Porscha, S.; Wasserscheid, P.; Zaumseil, J. *J. Phys. Chem. C.* **2012**, *116*, 13536.

(163) Paulsen, B. D.; Frisbie, C. D. *J. Phys. Chem. C.* **2012**, *116*, 3132.

(164) Kim, S. H.; Hong, K.; Xie, W.; Lee, K. H.; Zhang, S.; Lodge, T. P.; Frisbie, C. D. *Adv. Mater.* **2013**, *25*, 1822.

(165) Ye, J. T.; Inoue, S.; Kobayashi, K.; Kasahara, Y.; Yuan, H. T.; Shimotani, H.; Iwasa, Y. *Nat. Mater.* **2010**, *9*, 125.

(166) Silvester, D. S. *Analyst* **2011**, *136*, 4871.

(167) Rehman, A.; Zeng, X. *Accounts. Chem. Res.* **2012**, *45*, 1667.

(168) Ionic Liquids Database - ILThermo. http://ilthermo.boulder.nist.gov/ILThermo/, 2013; `http://ilthermo.boulder.nist.gov/ILThermo/`.

(169) Aparicio, S.; Atilhan, M.; Karadas, F. *Ind. Eng. Chem. Res.* **2010**, *49*, 9580.

(170) Zhang, S.; Lu, X.; Zhou, Q.; Li, X.; Zhang, X.; Li, S. *Ionic Liquids: Physicochemical Properties*; Elsevier Science, 2009.

(171) Zhang, S. J.; Sun, N.; He, X. Z.; Lu, X. M.; Zhang, X. P. *J. Phys. Chem. Ref. Data* **2006**, *35*, 1475.

(172) A quotation from the back-cover of this book reads: *"This comprehensive database on physical properties of pure ionic liquids (ILs) contains data collected from 269 peer-reviewed papers in the period from 1982 to June 2008. There are more than 9,400 data points on the 29 kinds of physicochemical properties for 1886 available ionic liquids, from which 807 kinds of cations and 185 kinds of anions were extracted. This book includes nearly all known pure ILs and their known physicochemical properties through June 2008. In addition, the authors incorporate the main applications of individual ILs and a large number of references."* .

(173) Endres, F., MacFarlane, D., Abbott, A., Eds. *Electrodeposition from ionic liquids*; Wiley-VCH, 2008.

(174) Kobrak, M. N. *Green. Chem.* **2008**, *10*, 80.

(175) Huang, M.-M.; Jiang, Y.; Sasisanker, P.; Driver, G. W.; Weingartner, H. *J. Chem. Eng. Data* **2011**, *56*, 1494.

(176) Choi, U.H.; Mittal, A.; Price, T.L.; Gibson, H.W.; Runt, J.; Colby, R.H. *Macromolecules* **2013**, *46*, 1174 .

(177) Kosower, E.M. *J. Am. Chem. Soc.* **1958**, *80*, 3253.

(178) Kamlet, M.J., Abboud, J.L.M., Abraham, M.H., Taft, R.W. *J. Org. Chem.* **1983**, *48*, 2877.

(179) Borges, R. S.; Ribeiro, H.; Lavall, R. L.; Silva, G. G. *J. Solid State Electrochem.* **2012**, *16*, 3573.

(180) We note that in such devices the temperature can increase spontaneously via Joule heat; in this case such systems would need external cooling. .

(181) Holbrey, J. D.; Seddon, K. R. *J. Chem. Soc., Dalton Trans* **1999**, 2133.

(182) Jayaraman, S.; Maginn, E. J. *J. Chem. Phys.* **2007**, *127*, 214504.

(183) Lei, Z.G., Chen, B.H., Li, C.Y., Liu, H. *Chem. Rev.* **2008**, *108*, 1419 .

(184) Coutinho, J. A. P.; Carvalho, P. J.; Oliveira, N. M. C. *RSC Adv.* **2012**, *2*, 7322.

(185) Sillars, F. B.; Fletcher, S. I.; Mirzaeian, M.; Hall, P. J. *Phys. Chem. Chem. Phys.* **2012**, *14*, 6094.

(186) Sánchez, L. G.; Espel, J. R.; Onink, F.; Meindersma, G. W.; Haan, A. B. d. *J. Chem. Eng. Data* **2009**, *54*, 2803.

(187) Tokuda, H.; Hayamizu, K.; Ishii, K.; Susan, M. A. B. H.; Watanabe, M. *J. Phys. Chem. B.* **2005**, *109*, 6103.

(188) Maginn, E. J. *Accounts. Chem. Res.* **2007**, *40*, 1200.

(189) Weingärtner, H. *Angew. Chem. Int. Edit.* **2008**, *47*, 654.

(190) Turton, D. A.; Hunger, J.; Stoppa, A.; Hefter, G.; Thoman, A.; Walther, M.; Buchner, R.; Wynne, K. *J. Am. Chem. Soc.* **2009**, *131*, 11140.

(191) Okoturo, O.; VanderNoot, T. *J. Electroanal. Chem.* **2004**, *568*, 167.

(192) Kowsari, M. H.; Alavi, S.; Ashrafizaadeh, M.; Najafi, B. *J. Chem. Phys.* **2008**, *129*, 224508.

(193) Tsuzuki, S. *ChemPhysChem* **2012**, *13*, 1664.

(194) Liu, Q.-S.; Yan, P.-F.; Yang, M.; Tan, Z.-C.; Li, C.-P.; Welz-Biermann, U. *Acta Phys.-Chim. Sin.* **2011**, *27*, 2762.

(195) Krossing, I.; Slattery, J. M. *Z. Phys. Chem.* **2006**, *220*, 1343.

(196) Slattery, J. M.; Daguenet, C.; Dyson, P. J.; Schubert, T. J. S.; Krossing, I. *Angew. Chem. Int. Edit.* **2007**, *46*, 5384.

(197) Vila, J., Varela, L.M., Cabeza, O. *Electrochim. Acta.* **2007**, *52*, 7413 .

(198) Tsuzuki, S.; Tokuda, H.; Hayamizu, K.; Watanabe, M. *J. Phys. Chem. B.* **2005**, *109*, 16474.

(199) Tsuzuki, S.; Shinoda, W.; Saito, H.; Mikami, M.; Tokuda, H.; Watanabe, M. *J. Phys. Chem. B.* **2009**, *113*, 10641.

(200) Eiden, P.; Bulut, S.; Köchner, T.; Friedrich, C.; Schubert, T.; Krossing, I. *J. Phys. Chem. B.* **2011**, *115*, 300.

(201) Tsuda, T.; Imanishi, A.; Torimoto, T.; Kuwabat, S. In *Ionic Liquids: Theory, Properties, New Approaches*; Kokorin, A., Ed.; InTech, 2011.

(202) Zheng, Y.; Dong, K.; Wang, Q.; Zhang, J.; Lu, X. *J. Chem. Eng. Data* **2013**, *58*, 32.

(203) Salanne, M.; Siqueira, L. J. A.; Seitsonen, A. P.; Madden, P. A.; Kirchner, B. *Faraday Discuss.* **2011**, *154*, 171.

(204) Segalini, J.; Daffos, B.; Taberna, P. L.; Gogotsi, Y.; Simon, P. *Electrochim. Acta.* **2010**, *55*, 7489.

(205) McDonough, J. K.; Frolov, A. I.; Presser, V.; Niu, J.; Miller, C. H.; Ubieto, T.; Fedorov, M. V.; Gogotsi, Y. *Carbon* **2012**, *50*, 3298.

(206) We note that the addition of solvent can also affect the electrochemical stability of the system, see e.g.[229] However, for the sake of clarity we do not discuss this effect in this section. .

(207) Lynden-Bell, R. M. *Phys. Chem. Chem. Phys.* **2010**, *12*, 1733.

(208) Lynden-Bell, R. M.; Frolov, A. I.; Fedorov, M. V. *Phys. Chem. Chem. Phys.* **2012**, *14*, 2693.

(209) Baker, G. A.; Rachford, A. A.; Castellano, F. N.; Baker, S. N. *ChemPhysChem* **2013**, *14*, 1025.

(210) Rani, M. A. A.; Brant, A.; Crowhurst, L.; Dolan, A.; Lui, M.; Hassan, N. H.; Hallett, J. P.; Hunt, P. A.; Niedermeyer, H.; Perez-Arlandis, J. M.; Schrems, M.; Welton, T.; Wilding, R. *Phys. Chem. Chem. Phys.* **2011**, *13*, 16831.

(211) Matsumoto, H. In *Electrochemical Aspects of Ionic Liquids*; Ohno, H., Ed.; A John Wiley & Sons, Inc.: Hoboken, New Jersey, 2005; p 35.

(212) Lane, G. H. *Electrochim. Acta.* **2012**, *83*, 513.

(213) Fletcher, S.; Black, V. J.; Kirkpatrick, I.; Varley, T. S. *J. Solid State Electrochem.* **2013**, *17*, 327.

(214) Bernard, U. L.; Izgorodina, E. I.; MacFarlane, D. R. *J. Phys. Chem. C.* **2010**, *114*, 20472.

(215) Shiddiky, M. J.; Torriero, A. A. *Biosens. Bioelectron.* **2011**, *26*, 1775.

(216) Romann, T.; Oll, O.; Pikma, P.; Lust, E. *Electrochem. Commun.* **2012**, *23*, 118.

(217) Wang, J. *Electroanalysis* **2005**, *17*, 1341.

(218) Ismail, A. S.; El Abedin, S. Z.; Hofft, O.; Endres, F. *Electrochem. Commun.* **2010**, *12*, 909.

(219) Kurig, H.; Jänes, A.; Lust, E. *J. Electrochem. Soc.* **2010**, *157*, A272.

(220) Tamailarasan, P.; Ramaprabhu, S. *J. Phys. Chem. C.* **2012**, *116*, 14179.

(221) Wei, Y.; Liu, H.; Jin, Y.; Cai, K.; Li, H.; Liu, Y.; Kang, Z.; Zhang, Q. *New J. Chem.* **2013**,

(222) Simon, P.; Gogotsi, Y. *Accounts. Chem. Res.* **2013**, *46*, 1094.

(223) Vivek, J. P.; Burgess, I. J. *Langmuir* **2012**, *28*, 5040.

(224) Kirchner, K.; Kirchner, T.; Ivaništšev, V.; Fedorov, M. *Electrochim. Acta.* **2013**,

(225) Gnahm, M.; Müller, C.; Répánszki, R.; Pajkossy, T.; Kolb, D. M. *Phys. Chem. Chem. Phys.* **2011**, *13*, 11627.

(226) Costa, R.; Pereira, C. M.; Silva, F. *RSC Adv.* **2013**,

(227) Schlegel, M. L.; Nagy, K. L.; Fenter, P.; Cheng, L.; Sturchio, N. C.; Jacobsen, S. D. *Geochim. Cosmochim. Acta* **2006**, *70*, 3549.

(228) Zhou, H.; Rouha, M.; Feng, G.; Lee, S. S.; Docherty, H.; Fenter, P.; Cummings, P. T.; Fulvio, P. F.; Dai, S.; McDonough, J.; Presser, V.; Gogotsi, Y. *ACS Nano* **2012**, *6*, 9818.

(229) O'Mahony, A. M.; Silvester, D. S.; Aldous, L.; Hardacre, C.; Compton, R. G. *J. Chem. Eng. Data* **2008**, *53*, 2884.

(230) Zhao, C.; Bond, A. M.; Lu, X. *Anal. Chem.* **2012**, *84*, 2784.

(231) Ridings, C.; Lockett, V.; Andersson, G. *Phys. Chem. Chem. Phys.* **2011**, *13*, 21301.

(232) Liu, Z.; El Abedin, S. Z.; Endres, F. *Electrochim. Acta.* **2013**, *89*, 635.

(233) Helmholtz, H. *Ann. Phys.* **1853**, *89*, 211, 353.

(234) Cohen, E. R.; Cvitaš, T.; Frey, J. G.; Holmstrőm, B.; Kuchitzu, K.; Marquardt, R.; Mills, I.; Pavese, F.; Quack, M.; Stohner, J.; Strauss, H. L.; Takami, M.; Thor, A. J. *Quantities, units and symbols in physical chemistry, 3rd edition*; International Union of Pure and Applied Chemistry, The Royal Society of Chemistry: Cambridge, 2007.

(235) Gouy, L. G. *C. R. Seances Acad. Sci.* **1909**, *149*, 654.

(236) Gouy, L. G. *J. Phys. Theor. Appl.* **1910**, *9*, 457.

(237) Debye, P. J. W.; Hückel, E. A. A. J. *Phys. Z.* **1923**, *24*, 185.

(238) Stern, O. *Z. Elektrochem. Angew. Phys. Chem.* **1924**, *30*, 508.

(239) Israelachvili, J. N. *Intermolecular and Surface Forces*; Academic Press: Boston, 1992.

(240) Price, N. C.; Dwek, R. A.; Wormald, M.; Ratcliffe, G. R. *Principles and problems in physical chemistry for biochemists*; Oxford University press, 2001.

(241) Bard, A. J., Stratmann, M., Wilson, G. S., Eds. *Encyclopedia of Electrochemistry: Bioelectrochemistry*; Wiley VCH: Weinheim, 2002; Vol. 9.

(242) Scholz, F. *Electroanalytical Methods: Guide to Experiments and Applications*; Springer, 2002.

(243) Neves-Petersen, M. T.; Petersen, S. B.; El-Gewely, M. R. *Protein electrostatics: A review of the equations and methods used to model electrostatic equations in biomolecules - Applications in biotechnology*; Elsevier, 2003; Vol. Volume 9; p 315.

(244) Wu, J.; Hu, Z. B. In *Encyclopedia of Nanoscience and Nanotechnology*; Schwarz, J., Contescu, C., Putyera, K., Eds.; Marcel Dekker, Inc„ 2004; p 1967.

(245) Frumkin, A. *Potencialy nulevogo zarjada*; Nauka: Moskva, 1982.

(246) Bockris, J. O. *Comprehensive treatise of electrochemistry*; Plenum Press: New York, 1980.

(247) Parsons, R.; Zobel, F. *J. Electroanal. Chem. (1959)* **1965**, *9*, 333.

(248) Dogonadze, R. R., Kalman, E., Kornyshev, A. A., Ulstrup, J., Eds. *The Chemical Physics of Solvation. Part C*; Elsevier: Amsterdam, 1988.

(249) Fawcett, W. *Isr. J. Chem.* **1979**, *18*, 3.

(250) Kornyshev, A.; Vilfan, I. *Electrochim. Acta.* **1995**, *40*, 109.

(251) Grahame, D. C. *J. Am. Chem. Soc.* **1958**, *80*, 4201.

(252) Parry, J. M.; Parsons, R. *Trans. Faraday Soc.* **1963**, *59*, 241.

(253) Vorotyntsev, M. A. In *Modern Aspects of Electrochemistry*; Bockris, J. O., Conway, B. E., White, R. E., Eds.; Modern Aspects of Electrochemistry 17; Springer US, 1986; p 131–222.

(254) Kornyshev, A. A.; Schmickler, W.; Vorotyntsev, M. A. *Phys. Rev. B* **1982**, *25*, 5244.

(255) Kornyshev, A.; Vorotyntsev, M. *Can. J. Chem.* **1981**, *59*, 2031.

(256) Blum, L.; Henderson, D.; Parsons, R. *J. Electroanal. Chem.* **1984**, *161*, 389.

(257) Fawcett, W. R. *Liquids, solutions, and interfaces: from classical macroscopic descriptions to modern microscopic details*; Oxford Univ. Press: Oxford, 2004.

(258) Schmickler, W.; Henderson, D. *Prog. Surf. Sci.* **1986**, *22*, 323.

(259) Boda, D.; Henderson, D.; Chan, K. Y. *J. Chem. Phys.* **1999**, *110*, 5346.

(260) Bikerman, J. J. *Philos. Mag.* **1942**, *33*, 384.

(261) Grimley, T.; Mott, N. *Discuss. Faraday Soc.* **1947**, *1*, 3.

(262) Grimley, T. *Proc. R. Soc. London, Ser. A* **1950**, *201*, 40.

(263) Dutta, M.; Bagchi, S. *Indian J. Phys.* **1950**, *24*, 61.

(264) Freise, V. *Z. Elektrochem.* **1952**, *56*, 822.

(265) Di Caprio, D.; Borkowska, Z.; Stafiej, J. *J. Electroanal. Chem.* **2003**, *540*, 17.

(266) Borukhov, I.; Andelman, D.; Orland, H. *Phys. Rev. Lett.* **1997**, *79*, 435.

(267) Kralj-Iglic, V.; Iglic, A. *J. Phys. II* **1996**, *6*, 477.

(268) Bazant, M. Z.; Kilic, M. S.; Storey, B. D.; Ajdari, A. *Adv. Colloid Interface Sci.* **2009**, *152*, 48.

(269) Sloutskin, E.; Ocko, B. M.; Tamam, L.; Kuzmenko, I.; Gog, T.; Deutsch, M. *J. Am. Chem. Soc.* **2005**, *127*, 7796.

(270) Jeon, Y.; Sung, J.; Bu, W.; Vaknin, D.; Ouchi, Y.; Kim, D. *J. Phys. Chem. C.* **2008**, *112*, 19649.

(271) Sloutskin, E.; Lynden-Bell, R. M.; Balasubramanian, S.; Deutsch, M. *J. Chem. Phys.* **2006**, *125*, 174715.

(272) Bowers, J.; Vergara-Gutierrez, M. C.; Webster, J. R. P. *Langmuir* **2004**, *20*, 309.

(273) Lauw, Y.; Horne, M. D.; Rodopoulos, T.; Lockett, V.; Akgun, B.; Hamilton, W. A.; Nelson, A. R. J. *Langmuir* **2012**, *28*, 7374.

(274) Kolbeck, C.; Cremer, T.; Lovelock, K. R. J.; Paape, N.; Schulz, P. S.; Wasserscheid, P.; Maier, F.; Steinruck, H.-P. *J. Phys. Chem. B.* **2009**, *113*, 8682.

(275) Lockett, V.; Sedev, R.; Harmer, S.; Ralston, J.; Horne, M.; Rodopoulos, T. *Phys. Chem. Chem. Phys.* **2010**, *12*, 13816.

(276) Iwahashi, T.; Nishi, T.; Yamane, H.; Miyamae, T.; Kanai, K.; Seki, K.; Kim, D.; Ouchi, Y. *J. Phys. Chem. C.* **2009**, *113*, 19237.

(277) Hammer, T.; Reichelt, M.; Morgner, H. *Phys. Chem. Chem. Phys.* **2010**, *12*, 11070.

(278) Ridings, C.; Lockett, V.; Andersson, G. *Phys. Chem. Chem. Phys.* **2011**, *13*, 17177.

(279) Ridings, C.; Lockett, V.; Andersson, G. *Colloids Surf., A* **2012**, *413*, 149.

(280) Endres, F.; Borisenko, N.; Abedin, S. Z. E.; Hayes, R.; Atkin, R. *Faraday Discuss.* **2012**, *154*, 221.

(281) Painter, K. R.; Ballone, P.; Tosi, M. P.; Grout, P. J.; March, N. H. *Surf. Sci.* **1983**, *133*, 89.

(282) Ballone, P.; Pastore, G.; Tosi, M. P.; Painter, K. R.; Grout, P. J.; March, N. H. *Phys. Chem. Liq.* **1984**, *13*, 269.

(283) Revere, M.; Tosi, M. P. *Rep. Prog. Phys.* **1999**, *49*, 1001.

(284) Tosi, M. P. In *Condensed Matter Physics Aspects of Electrochemistry*; Tosi, M. P., Kornyshev, A. A; World Scientific, Singapore, 1991; p. 68.

(285) Torrie, G. M.; Valleau, J. P. *J. Chem. Phys.* **1980**, *73*, 5807.

(286) Torrie, G. M.; Valleau, J. P.; Patey, G. N. *J. Chem. Phys.* **1982**, *76*, 4615.

(287) Torrie, G. M.; Valleau, J. P. *J. Phys. Chem.* **1982**, *86*, 3251.

(288) Lanning, O. J.; Madden, P. A. *J. Phys. Chem. B.* **2004**, *108*, 11069.

(289) Dogonadze, R.; Chizmadzhev, Y. *Dokl. Akad. Nauk SSSR* **1964**, *157*, 944.

(290) Weingaertner, H. *Z. Phys. Chem.* **2006**, *220*, 1395.

(291) Parsons, R. *Chem. Rev.* **1990**, *90*, 813.

(292) Kisza, A. *J. Electroanal. Chem.* **2002**, *534*, 99.

(293) Amokrane, S.; Badiali, J. In *Modern Aspects of Electrochemistry*; Bockris, J. O., Conway, B. E., White, R.; Plenum: New York, NY, USA, 1992; Vol. 22.

(294) Kornyshev, A. A. *Electrochim. Acta.* **1989**, *34*, 1829.

(295) Gerischer, H. *J. Phys. Chem.* **1985**, *89*, 4249.

(296) Gerischer, H.; McIntyre, R.; Scherson, D.; Storck, W. *J. Phys. Chem.* **1987**, *91*, 1930.

(297) Skinner, B.; Chen, T.; Loth, M. S.; Shklovskii, B. I. *Phys. Rev. E* **2011**, *83*, 056102.

(298) Luque, N.; Schmickler, W. *Electrochim. Acta.* **2012**, *71*, 82.

(299) Liu, H.; He, P.; Li, Z.; Sun, C.; Shi, L.; Liu, Y.; Zhu, G.; Li, J. *Electrochem. Commun.* **2005**, *7*, 1357.

(300) Fukushima, T.; Aida, T. *Chem-Eur. J.* **2007**, *13*, 5048.

(301) Pauliukaite, R.; Murnaghan, K. D.; Doherty, A. P.; Brett, C. M. A. *J. Electroanal. Chem.* **2009**, *633*, 106.

(302) Faridbod, F.; Ganjali, M. R.; Pirali-Hamedani, M.; Norouzi, P. *Int. J. Electrochem. Sci.* **2010**, *5*, 1103.

(303) Gogotsi, Y.; Presser, V. *Carbon Nanomater.*; CRC Press, 2010.

(304) Salimi, A.; Lasghari, S.; Noorbakhash, A. *Electroanalysis* **2010**, *22*, 1707.

(305) Miller, J. R.; Outlaw, R. A.; Holloway, B. C. *Science* **2010**, *329*, 1637.

(306) Brennan, L. J.; Byrne, M. T.; Bari, M.; Gun'ko, Y. K. *Adv. Energy Mater.* **2011**, *1*, 472.

(307) Zhang, Q.; Wu, S.; Zhang, L.; Lu, J.; Verproot, F.; Liu, Y.; Xing, Z.; Li, J.; Song, X.-M. *Biosens. Bioelectron.* **2011**, *26*, 2632.

(308) Luo, J.; Jang, H. D.; Huang, J. *ACS Nano* **2013**,

(309) Lin, J.; Zhang, C.; Yan, Z.; Zhu, Y.; Peng, Z.; Hauge, R. H.; Natelson, D.; Tour, J. M. *Nano Lett.* **2013**, *13*, 72.

(310) Uesugi, E.; Goto, H.; Eguchi, R.; Fujiwara, A.; Kubozono, Y. *Sci. Rep.* **2013**, *3*.

(311) Gurevich, Y.; Kharkats, Y. *J. Electroanal. Chem.* **1978**, *86*, 245.

(312) Gurevich, Y.; Kharkats, Y. *J. Phys. Chem. Solids* **1978**, *39*, 751.

(313) Gurevich, Y.; Kharkats, Y. *Usp. Fiz. Nauk* **1982**, *136*, 693.

(314) Scheidegger, A. E. *The physics of flow through porous media*; University of Toronto Press, 1974.

(315) Seddon, K. R.; Stark, A.; Torres, M. J. *Pure. Appl. Chem.* **2000**, *72*, 2275.

(316) Rausch, M. H.; Lehmann, J.; Leipertz, A.; Froba, A. P. *Phys. Chem. Chem. Phys.* **2011**, *13*, 9525.

(317) Coadou, E.; Timperman, L.; Jacquemin, J.; Galiano, H.; Hardacre, C.; Anouti, M. *J. Phys. Chem. C.* **2013**,

(318) Couadou, E.; Jacquemin, J.; Galiano, H.; Hardacre, C.; Anouti, M. *J. Phys. Chem. B.* **2013**, *117*, 1389.

(319) Lombardo, L.; Brutti, S.; Navarra, M. A.; Panero, S.; Reale, P. *J. Power Sources* **2013**, *227*, 8.

(320) Wang, M.; Shan, Z.; Tian, J.; Yang, K.; Liu, X.; Liu, H.; Zhu, K. *Electrochim. Acta.* **2013**, *95*, 301.

143

(321) Bazant, M. Z.; Storey, B. D.; Kornyshev, A. A. *Phys. Rev. Lett.* **2011**, *106*, 046102.

(322) Fedorov, M. V.; Georgi, N.; Kornyshev, A. A. *Electrochem. Commun.* **2010**, *12*, 296.

(323) We note that flexible non-polar functional groups of RTIL ions (e.g. alkyl chains) can also act as voids, see Refs.[47,322] .

(324) Kilic, M. S.; Bazant, M. Z.; Ajdari, A. *Phys. Rev. E* **2007**, *75*, 021503.

(325) Oldham, K. B. *J. Electroanal. Chem.* **2008**, *613*, 131.

(326) Fawcett, W. R.; Ryan, P. J. *Collect. Czech. Chem. Commun.* **2009**, *74*, 1665.

(327) Fawcett, W. R.; Ryan, P. J. *Phys. Chem. Chem. Phys.* **2010**, *12*, 9816.

(328) Fedorov, M. V.; Kornyshev, A. A. *J. Phys. Chem. B.* **2008**, *112*, 11868.

(329) Kirchner, K. A simulation study of simple ionic liquids near charged walls: The melting of the electric double layer and structural transitions at the interface. Doctoral thesis, University of Strathclyde, Glasgow, 2013.

(330) Huddleston, J. G.; Visser, A. E.; Reichert, W. M.; Willauer, H. D.; Broker, G. A.; Rogers, R. D. *Green. Chem.* **2001**, *3*, 156.

(331) Binder, K. In *Phase Transitions and Critical Phenomena*; Domb, C., Lebowitz, J. L., Eds.; Academic Press, 2000.

(332) Damaskin, B. B.; Petrii, O. A.; Batrakov, V. V.; Uvarov, E. B.; Parsons, R.; Barradas, R. G. *J. Electrochem. Soc.* **1972**, *119*, 279C.

(333) Nabutovskii, V.; Nemov, N. *J. Colloid Interface Sci.* **1986**, *114*, 208.

(334) Szparaga, R.; Woodward, C. E.; Forsman, J. *J. Phys. Chem. C.* **2012**, *116*, 15946.

(335) Sangster, M. J. L.; Dixon, M. *Adv. Phys.* **1976**, *25*, 247.

(336) Heyes, D. M.; Clarke, J. H. *J. Chem. Soc., Faraday Trans. 2* **1981**, *77*, 1089.

(337) Torrie, G.; Valleau, J. *Chem. Phys. Lett.* **1979**, *65*, 343.

(338) Boda, D.; Henderson, D.; Chan, K. Y.; Wasan, D. T. *Chem. Phys. Lett.* **1999**, *308*, 473.

(339) Boda, D.; Henderson, D. *J. Chem. Phys.* **2000**, *112*, 8934.

(340) Toukmaji, A. Y.; Board, J. A. *Comput. Phys. Commun.* **1996**, *95*, 73.

(341) Board, J. A.; Humphres, C. W.; Lambert, C. G.; Rankin, W. T.; Toukmaji, A. Y. Ewald and Multipole Methods for Periodic N-Body Problems. 1997; `http://citeseer.ist.psu.edu/500629.html`.

(342) Spohr, E. *J. Electroanal. Chem.* **1998**, *450*, 327.

(343) Spohr, E. *Electrochim. Acta.* **2003**, *49*, 23.

(344) Kornyshev, A. A.; Spohr, E.; Vorotyntsev, M. A. *Encyclopedia of Electrochemistry*; Wiley-VCH: Weinheim, 2007.

(345) Darden, T.; York, D.; Pedersen, L. *J. Chem. Phys.* **1993**, *98*, 10089.

(346) Yeh, I.-C.; Berkowitz, M. L. *J. Chem. Phys.* **1999**, *111*, 3155.

(347) Spohr, E. *J. Chem. Phys.* **1997**, *107*, 6342.

(348) Crozier, P. S.; Rowley, R. L.; Henderson, D.; Boda, D. *Chem. Phys. Lett.* **2000**, *325*, 675.

(349) Crozier, P. S.; Rowley, R. L.; Spohr, E.; Henderson, D. *J. Chem. Phys.* **2000**, *112*, 9253.

(350) Lynden-Bell, R. M. *Mol. Phys.* **2003**, *101*, 2625.

(351) Lynden-Bell, R. M.; Kohanoff, J.; Del Popolo, M. G. *Faraday Discuss.* **2005**, *129*, 57.

(352) Lynden-Bell, R. M.; Del Pópolo, M. G.; Youngs, T. G. A.; Kohanoff, J.; Hanke, C. G.; Harper, J. B.; Pinilla, C. C. *Acc. Chem. Res.* **2007**, *40*, 1138.

(353) Pinilla, C.; Del Pópolo, M.; Kohanoff, J.; Lynden-Bell, R. *J. Phys. Chem. B.* **2007**, *111*, 4877.

(354) Horn, R. G.; Evans, D. F.; Ninham, B. W. *J. Phys. Chem* **1988**, *92*, 3531.

(355) Bopp, P. A.; Kornyshev, A. A.; Sutmann, G. *Phys. Rev. Lett.* **1996**, *76*, 1280.

(356) Bopp, P. A.; Kornyshev, A. A.; Sutmann, G. *J. Chem. Phys.* **1998**, *109*, 1939.

(357) Fedorov, M. V.; Kornyshev, A. A. *Mol. Phys.* **2007**, *105*, 1.

(358) Lowen, H.; Hansen, J. P.; Madden, P. A. *J. Chem. Phys.* **1993**, *98*, 3275.

(359) Cheng, L.; Fenter, P.; Nagy, K. L.; Schlegel, M. L.; Sturchio, N. C. *Phys. Rev. Lett.* **2001**, *87*, 156103.

(360) Booth, M. J.; Haymet, A. D. J. *Mol. Phys.* **2001**, *99*, 1817.

(361) Lanning, O. J.; Shellswell, S.; Madden, P. A. *Mol. Phys.* **2004**, *102*, 839.

(362) Fedorov, M. V.; Kornyshev, A. A. *Electrochim. Acta.* **2008**, *53*, 6835.

(363) Merlet, C.; Salanne, M.; Rotenberg, B.; Madden, P. A. *J. Phys. Chem. C.* **2011**, *115*, 16613.

(364) Bhuiyan, L. B.; Lamperski, S.; Wu, J.; Henderson, D. *J. Phys. Chem. B.* **2012**, *116*, 10364.

(365) Merlet, C.; Salanne, M.; Rotenberg, B. *J. Phys. Chem. C.* **2012**, *116*, 7687.

(366) Merlet, C.; Rotenberg, B.; Madden, P. A.; Taberna, P.-L.; Simon, P.; Gogotsi, Y.; Salanne, M. *Nat. Mater.* **2012**,

(367) Ji, Y.; Shi, R.; Wang, Y.; Saielli, G. *J. Phys. Chem. B.* **2013**, *117*, 1104.

(368) Lauw, Y.; Horne, M. D.; Rodopoulos, T.; Leermakers, F. A. M. *Phys. Rev. Lett.* **2009**, *103*, 117801.

(369) Lamperski, S.; Outhwaite, C. W.; Bhuiyan, L. B. *J. Phys. Chem. B.* **2009**, *113*, 8925.

(370) Trulsson, M.; Algotsson, J.; Forsman, J.; Woodward, C. E. *J. Phys. Chem. Lett.* **2010**, *1*, 1191.

(371) Luque, N.; Woelki, S.; Henderson, D.; Schmickler, W. *Electrochim. Acta.* **2011**, *56*, 7298.

(372) Kondrat, S.; Kornyshev, A. *J. Phys-Condens. Mat.* **2011**, *23*, 022201.

(373) Henderson, D.; Lamperski, S. *J. Chem. Eng. Data* **2011**, *56*, 1204.

(374) Aoki, K. *Electrochim. Acta.* **2012**, *67*, 216.

(375) Reszko-Zygmunt, J.; Sokołowski, S.; Henderson, D.; Boda, D. *The J. Chem. Phys.* **2005**, *122*, 084504.

(376) Wu, J.; Jiang, T.; Jiang, D.-e.; Jin, Z.; Henderson, D. *Soft. Matter.* **2011**, *7*, 11222.

(377) Forsman, J.; Woodward, C. E.; Trulsson, M. *J. Phys. Chem. B.* **2011**, *115*, 4606.

(378) Jiang, D.-e.; Meng, D.; Wu, J. *Chem. Phys. Lett.* **2011**, *504*, 153.

(379) Lauw, Y.; Horne, M. D.; Rodopoulos, T.; Nelson, A.; Leermakers, F. A. M. *J. Phys. Chem. B.* **2010**, *114*, 11149.

(380) Henderson, D.; Lamperski, S.; Jin, Z.; Wu, J. *J. Phys. Chem. B.* **2011**, *115*, 12911.

(381) Henderson, D.; Wu, J. *J. Phys. Chem. B.* **2012**, *116*, 2520.

(382) Henderson, D.; Lamperski, S.; Bari Bhuiyan, L.; Wu, J. *J. Chem. Phys.* **2013**, *138*, 144704.

(383) Jiang, D.-e.; Jin, Z.; Wu, J. *Nano Lett.* **2011**, *11*, 5373.

(384) Jiang, D.-e.; Jin, Z.; Henderson, D.; Wu, J. *J. Phys. Chem. Lett.* **2012**, *3*, 1727.

(385) Szparaga, R.; Woodward, C. E.; Forsman, J. *J. Phys. Chem. C.* **2013**, *117*, 1728.

(386) Vatamanu, J.; Borodin, O.; Bedrov, D.; Smith, G. D. *J. Phys. Chem. C.* **2012**, *116*, 7940.

(387) Vatamanu, J.; Borodin, O.; Smith, G. D. *J. Phys. Chem. B.* **2011**, *115*, 3073.

(388) Vatamanu, J.; Borodin, O.; Smith, G. D. *J. Am. Chem. Soc.* **2010**, *132*, 14825.

(389) Feng, G.; Zhang, J. S.; Qiao, R. *J. Phys. Chem. C.* **2009**, *113*, 4549.

(390) Vatamanu, J.; Borodin, O.; Smith, G. D. *Phys. Chem. Chem. Phys.* **2010**, *12*, 170.

(391) Schmidt, J.; Krekeler, C.; Dommert, F.; Zhao, Y.; Berger, R.; Site, L. D.; Holm, C. *J. Phys. Chem. B.* **2010**, *114*, 6150.

(392) Dommert, F.; Wendler, K.; Berger, R.; Delle Site, L.; Holm, C. *ChemPhysChem* **2012**, *13*, 1625.

(393) Berendsen, H. J. C.; van der Spoel, D.; van Drunen, R. *Comput. Phys. Commun.* **1995**, *91*, 43.

(394) Lindahl, E.; Hess, B.; van der Spoel, D. *J. Mol. Model.* **2001**, *7*, 306.

(395) van der Spoel, D.; Lindahl, E.; Hess, B.; Groenhof, G.; Mark, A. E.; Berendsen, H. J. C. *J. Comput. Chem.* **2005**, *26*, 1701.

(396) Hess, B.; Kutzner, C.; van der Spoel, D.; Lindahl, E. *J. Chem. Theory Comput.* **2008**, *4*, 435.

(397) Reed, S. K.; Madden, P. A.; Papadopoulos, A. *J. Chem. Phys* **2008**, *128*, 124701.

(398) Lockett, V.; Sedev, R.; Ralston, J.; Horne, M.; Rodopoulos, T. *J. Phys. Chem. C.* **2008**, *112*, 7486.

(399) Santangelo, C. D. *Phys. Rev. E* **2006**, *73*, 041512.

(400) Démery, V.; Dean, D. S.; Hammant, T. C.; Horgan, R. R.; Podgornik, R. *Europhys. Lett.* **2012**, *97*, 28004.

(401) Démery, V.; Dean, D. S.; Hammant, T. C.; Horgan, R. R.; Podgornik, R. *J. Chem. Phys.* **2012**, *137*, 064901.

(402) Landau, L. D. *Collected papers of L.D. Landau*; Pergamon Press, 1965.

(403) Ornstein, L. S.; Zernike, F. *Proc. K. Ned. Akad. Wet.* **1914**, *17*, 793.

(404) Frenkel, I. I. *Kinetic Theory of Liquids*; Dover Publications, 1955.

(405) Yvon, J. *La théorie statistique des fluides et l'équation d'état*; Hermann & cie, 1935.

(406) Bogoliubov, N. *J. Phys. (Moscow)* **1946**, *10*, 265.

(407) Kirkwood, J. G. *J. Chem. Phys.* **1935**, *3*, 300.

(408) Kirkwood, J. G. *J. Chem. Phys.* **1946**, *14*, 180.

(409) Born, M.; Green, H. S. *Proc. R. Soc. A* **1946**, *188*, 10.

(410) Hansen, J.-P.; McDonald, I. R. *Theory of Simple Liquids, 4th ed*; Elsevier Academic Press, Amsterdam, The Netherlands, 2000.

(411) Barrat, J.-L.; Hansen, J.-P. *Basic concepts for simple and complex liquids*; Cambridge University Press, New York, 2003.

(412) Monson, P. A.; Morriss, G. P. *Adv. Chem. Phys.* **1990**, *77*, 451.

(413) Hirata, F., Ed. *Molecular theory of solvation*; Kluwer Academic Publishers, Dordrecht, Netherlands, 2003.

(414) Chandler, D.; Andersen, H. C. *J. Chem. Phys.* **1972**, *57*, 1930.

(415) Chandler, D.; Silbey, R.; Ladanyi, B. *Mol. Phys.* **1982**, *46*, 1335.

(416) Beglov, D.; Roux, B. *J. Phys. Chem.* **1997**, *101*, 7821.

(417) Kovalenko, A.; Ten-No, S.; Hirata, F. *J. Comput. Chem.* **1999**, *20*, 928.

(418) Ishizuka, R.; Chong, S. H.; Hirata, F. *J. Chem. Phys.* **2008**, *128*, 034504.

(419) Chandler, D.; Mccoy, J. D.; Singer, S. J. *J. Chem. Phys.* **1986**, *85*, 5971.

(420) Ichiye, T.; Haymet, A. D. J. *J. Chem. Phys.* **1990**, *93*, 8954.

(421) Perkyns, J. S.; Pettitt, B. M. *Chem. Phys. Lett.* **1992**, *190*, 626.

(422) Raineri, F. O.; Stell, G. *J. Phys. Chem. B.* **2001**, *105*, 11880.

(423) Singer, S. J.; Chandler, D. *Mol. Phys.* **1985**, *55*, 621.

(424) Ten-no, S.; Jung, J.; Chuman, H.; Kawashima, Y. *Mol. Phys.* **2010**, *108*, 327.

(425) Kierlik, E.; Rosinberg, M. L. *Phys. Rev. A* **1991**, *44*, 5025.

(426) Gendre, L.; Ramirez, R.; Borgis, D. *Chem. Phys. Lett.* **2009**, *474*, 366.

(427) Patra, C. N. *J. Chem. Phys.* **1999**, *111*, 9832.

(428) Wu, J. Z.; Li, Z. D. *Annu. Rev. Phys. Chem.* **2007**, *58*, 85.

(429) Miyata, T.; Hirata, F. *J. Comput. Chem.* **2008**, *29*, 871.

(430) Nishiyama, K.; Yamaguchi, T.; Hirata, F. *J. Phys. Chem. B.* **2009**, *113*, 2800.

(431) Llanorestrepo, M.; Chapman, W. G. *Int. J. Thermophys.* **1995**, *16*, 319.

(432) Choudhury, N.; Ghosh, S. K. *Phys. Rev. E* **2002**, *66*, 021206.

(433) Malvaldi, M.; Bruzzone, S.; Chiappe, C.; Gusarov, S.; Kovalenko, A. *J. Phys. Chem. B.* **2009**, *113*, 3536.

(434) Taylor, A. W.; Licence, P.; Abbott, A. P. *Physical Chemistry Chemical Physics* **2011**, *13*, 10147.

(435) Kovalenko, A.; Hirata, F. *J. Chem. Phys.* **1999**, *110*, 10095.

(436) Woelki, S.; Kohler, H.-H.; Krienke, H. *J. Phys. Chem. B.* **2008**, *112*, 3365.

(437) Howard, J. J.; Perkyns, J. S.; Pettitt, B. M. *J. Phys. Chem. B.* **2010**, *114*, 6074.

(438) Tanimura, A.; Kovalenko, A.; Hirata, F. *Chem. Phys. Lett.* **2003**, *378*, 638.

(439) Tanimura, A.; Kovalenko, A.; Hirata, F. *Langmuir* **2007**, *23*, 1507.

(440) Pinilla, C.; Del Pópolo, M. G.; Lynden-Bell, R. M.; Kohanoff, J. *J. Phys. Chem. B.* **2005**, *109*, 17922.

(441) Kislenko, S. A.; Samoylov, I. S.; Amirov, R. H. *Phys. Chem. Chem. Phys.* **2009**, *11*, 5584.

(442) Kislenko, S. A.; Amirov, R. H.; Samoylov, I. S. *Phys. Chem. Chem. Phys.* **2010**, *12*, 11245.

(443) Sha, M. L.; Wu, G. Z.; Dou, Q. A.; Tang, Z. F.; Fang, H. P. *Langmuir* **2010**, *26*, 12667.

(444) Wang, S.; Li, S.; Cao, Z.; Yan, T. Y. *J. Phys. Chem. C.* **2010**, *114*, 990.

(445) Shim, Y.; Kim, H. J. *ACS Nano* **2010**, *4*, 2345.

(446) Feng, G.; Huang, J. S.; Sumpter, B. G.; Meunier, V.; Qiao, R. *Phys. Chem. Chem. Phys.* **2010**, *12*, 5468.

(447) Vatamanu, J.; Cao, L.; Borodin, O.; Bedrov, D.; Smith, G. D. *J. Phys. Chem. Lett.* **2011**, *2*, 2267.

(448) Dou, Q.; Sha, M. L.; Fu, H. Y.; Wu, G. Z. *J. Phys.: Condens. Matter* **2011**, *23*, 175001.

(449) Wu, P.; Huang, J. S.; Meunier, V.; Sumpter, B. G.; Qiao, R. *ACS Nano* **2011**, *5*, 9044.

(450) Ong, S. P.; Andreussi, O.; Wu, Y.; Marzari, N.; Ceder, G. *Chem. Mater.* **2011**, *23*, 2979.

(451) Feng, G.; Qiao, R.; Huang, J.; Dai, S.; Sumpter, B. G.; Meunier, V. *Phys. Chem. Chem. Phys.* **2011**, *13*, 1152.

(452) Feng, G.; Jiang, D.-e.; Cummings, P. T. *J. Chem. Theory Comput.* **2012**, *8*, 1058.

(453) Xing, L.; Vatamanu, J.; Smith, G. D.; Bedrov, D. *J. Phys. Chem. Lett.* **2012**, *3*, 1124.

(454) Si, X.; Li, S.; Wang, Y.; Ye, S.; Yan, T.; Si, X.; Li, S.; Wang, Y.; Ye, S.; Yan, T. *ChemPhysChem* **2012**,

(455) Xing, L.; Vatamanu, J.; Borodin, O.; Bedrov, D. *J. Phys. Chem. Lett.* **2013**, *4*, 132.

(456) Kislenko, S. A.; Amirov, R. H.; Samoylov, I. S. *J. Phys.: Conf. Ser.* **2013**, *418*, 012021.

(457) Yang, L.; Fishbine, B. H.; Migliori, A.; Pratt, L. R. *J. Am. Chem. Soc.* **2009**, *131*, 12373.

(458) Feng, G.; Huang, J.; Sumpter, B. G.; Meunier, V.; Qiao, R. *Phys. Chem. Chem. Phys.* **2011**, *13*, 14723.

(459) Rodriguez, J.; Elola, M. D.; Laria, D. *J. Phys. Chem. C* **2012**, *116*, 5394.

(460) Frolov, A. I.; Kirchner, K.; Kirchner, T.; Fedorov, M. V. *Faraday Discuss.* **2012**, *154*, 235.

(461) Paek, E.; Pak, A. J.; Hwang, G. S. *J. Electrochem. Soc.* **2013**, *160*, A1.

(462) A technical note: similarly to Ref.,[390] Feng et al displayed a picture for integral capacitance which shows divergence and negative values. This was because the authors of both papers have plotted integral capacitance as net charge in the EDL divided by the overall voltage drop across the double layer, Q/U. Since $Q = 0$ at the p.z.c., equally $Q \neq 0$ at $U = 0$, unless $U_{p.z.c} = 0$ which is usually not true, particularly in the case of preferential adsorption of one sort of the ions. Hence the divergence! Had both groups evaluated integral capacitance in the right way as $Q/(U - U_{p.z.c})$, the divergence would have been removed. This minor confusion does not affect the value of the rest of the analysis in both papers, and it would not be even worth mentioning it, unless it has appeared in two different papers, somewhat puzzling readers. .

(463) Nanjundiah, C.; McDevitt, S. F.; Koch, V. R. *J. Electrochem. Soc.* **1997**, *144*, 3392.

(464) Lin, L.; Wang, Y.; Yan, J.; Yuan, Y.; Xiang, J.; Mao, B. *Electrochem. Commun.* **2003**, *5*, 995.

(465) Alam, M.; Islam, M.; Okajima, T.; Ohsaka, T. *Electrochem. Commun.* **2007**, *9*, 2370.

(466) Alam, M. T.; Islam, M. M.; Okajima, T.; Ohsaka, T. *J. Phys. Chem. C.* **2007**, *111*, 18326.

(467) Alam, M. T.; Islam, M. M.; Okajima, T.; Ohsaka, T. *J. Phys. Chem. C.* **2008**, *112*, 16600.

(468) Islam, M. M.; Alam, M. T.; Ohsaka, T. *J. Phys. Chem. C.* **2008**, *112*, 16568.

(469) Islam, M. M.; Alam, M. T.; Okajima, T.; Ohsaka, T. *J. Phys. Chem. C.* **2009**, *113*, 3386.

(470) Alam, M. T.; Islam, M. M.; Okajima, T.; Ohsaka, T. *J. Phys. Chem. C.* **2009**, *113*, 6596.

(471) Alam, M. T.; Masud, J.; Islam, M. M.; Okajima, T.; Ohsaka, T. *J. Phys. Chem. C.* **2011**, *115*, 19797.

(472) Lockett, V.; Horne, M.; Sedev, R.; Rodopoulos, T.; Ralston, J. *Phys. Chem. Chem. Phys.* **2010**, *12*, 12499.

(473) Gore, T. R.; Bond, T.; Zhang, W.; Scott, R. W.; Burgess, I. J. *Electrochem. Commun.* **2010**, *12*, 1340.

(474) Siinor, L.; Lust, K.; Lust, E. *J. Electrochem. Soc.* **2010**, *157*, F83.

(475) Siinor, L.; Lust, K.; Lust, E. *Electrochem. Commun.* **2010**, *12*, 1058.

(476) Siinor, L.; Siimenson, C.; Ivaništšev, V.; Lust, K.; Lust, E. *J. Electroanal. Chem.* **2012**, *668*, 30.

(477) Siinor, L.; Arendi, R.; Lust, K.; Lust, E. *J. Electroanal. Chem.* **2013**, *689*, 51.

(478) Su, Y.-Z.; Yan, J.-W.; Li, M.-G.; Xie, Z.-X.; Mao, B.-W.; Tian, Z.-Q. *Z. Phys. Chem.* **2012**, *226*, 979.

(479) Weingärtner, H.; Knocks, A.; Schrader, W.; Kaatze, U. *J. Phys. Chem. A.* **2001**, *105*, 8646.

(480) Smith, E. F.; Rutten, F. J. M.; Villar-Garcia, I. J.; Briggs, D.; Licence, P. *Langmuir* **2006**, *22*, 9386.

(481) Tokuda, H.; Hayamizu, K.; Ishii, K.; Susan, M. A. B. H.; Watanabe, M. *J. Phys. Chem. B.* **2004**, *108*, 16593.

(482) Lopes, J. N. C.; Gomes, M. F. C.; Padua, A. A. H. *J. Phys. Chem. B.* **2006**, *110*, 16816.

(483) Spickermann, C.; Thar, J.; Lehmann, S. B. C.; Zahn, S.; Hunger, J.; Buchner, R.; Hunt, P. A.; Welton, T.; Kirchner, B. *J. Chem. Phys.* **2008**, *129*, 104505.

(484) Fernandes, A. M.; Rocha, M. A. A.; Freire, M. G.; Marrucho, I. M.; Coutinho, J. A. P.; Santos, L. M. N. B. F. *J. Phys. Chem. B.* **2011**, *115*, 4033.

(485) Preiss, U.; Verevkin, S. P.; Koslowski, T.; Krossing, I. *Chem-Eur. J.* **2011**, *17*, 6508.

(486) Gebbie, M. A.; Valtiner, M.; Banquy, X.; Fox, E. T.; Henderson, W. A.; Israelachvili, J. N. *P. Natl. Acad. Sci.* **2013**.

(487) Pajkossy, T.; Kolb, D. M. *Electrochem. Commun.* **2011**, *13*, 284.

(488) Zheng, J.; Goonetilleke, P.; Pettit, C.; Roy, D. *Talanta* **2010**, *81*, 1045.

(489) Zheng, J. P.; Moganty, S. S.; Goonetilleke, P. C.; Baltus, R. E.; Roy, D. *J. Phys. Chem. C.* **2011**, *115*, 7527.

(490) Silva, F.; Gomes, C.; Figueiredo, M.; Costa, R.; Martins, A.; Pereira, C. M. *J. Electroanal. Chem.* **2008**, *622*, 153.

(491) Costa, R.; Pereira, C. M.; Silva, F. *Phys. Chem. Chem. Phys.* **2010**, *12*, 11125.

(492) Roling, B.; Drüschler, M. *Electrochim. Acta.* **2012**, *76*, 526.

(493) Roling, B.; Drüschler, M.; Huber, B. *Faraday Discuss.* **2011**, *154*, 303.

(494) Mezger, M.; Schröder, H.; Reichert, H.; Schramm, S.; Okasinski, J. S.; Schöder, S.; Honkimäki, V.; Deutsch, M.; Ocko, B. M.; Ralston, J.; Rohwerder, M.; Stratmann, M.; Dosch, H. *Science* **2008**, *322*, 424.

(495) Mezger, M.; Schramm, S.; Schröder, H.; Reichert, H.; Deutsch, M.; De Souza, E. J.; Okasinski, J. S.; Ocko, B. M.; Honkimäki, V.; Dosch, H. *J. Chem. Phys.* **2009**, *131*, 094701.

(496) Mezger, M.; Ocko, B. M.; Reichert, H.; Deutsch, M. *P. Natl. Acad. Sci.* **2013**, *110*, 3733.

(497) Nishi, N.; Yasui, Y.; Uruga, T.; Tanida, H.; Yamada, T.; Nakayama, S.-i.; Matsuoka, H.; Kakiuchi, T. *J. Chem. Phys.* **2010**, *132*, 164705.

(498) Nishi, N.; Uruga, T.; Tanida, H.; Kakiuchi, T. *Langmuir* **2011**, *27*, 7531.

(499) Yamamoto, R.; Morisaki, H.; Sakata, O.; Shimotani, H.; Yuan, H.; Iwasa, Y.; Kimura, T.; Wakabayashi, Y. *Appl. Phys. Lett.* **2012**, *101*, 053122.

(500) Atkin, R.; Warr, G. G. *J. Phys. Chem. C* **2007**, *111*, 5162.

(501) Wakeham, D.; Hayes, R.; Warr, G. G.; Atkin, R. *J. Phys. Chem. B* **2009**, *113*, 5961.

(502) Hayes, R.; El Abedin, S. Z.; Atkin, R. *J. Phys. Chem. B* **2009**, *113*, 7049.

(503) Hayes, R.; Borisenko, N.; Tam, M. K.; Howlett, P. C.; Endres, F.; Atkin, R. *J. Phys. Chem. C* **2011**, *115*, 6855.

(504) Perkin, S.; Cousen, N. Personal Communication. 2013.

(505) Smith, A. M.; Lovelock, K. R. J.; Gosvami, N. N.; Licence, P.; Dolan, A.; Welton, T.; Perkin, S. *J. Phys. Chem. Lett.* **2013**, 378.

(506) Zhang, X.; Zhong, Y.-X.; Yan, J.-W.; Su, Y.-Z.; Zhang, M.; Mao, B.-W. *Chem. Commun.* **2012**, *48*, 582.

(507) Carstens, T.; Hayes, R.; Abedin, S. Z. E.; Corr, B.; Webber, G. B.; Borisenko, N.; Atkin, R.; Endres, F. *Electrochim. Acta.* **2012**, *82*, 48.

(508) Baldelli, S. *J. Phys. Chem. Lett.* **2013**, *4*, 244.

(509) Santos, C. S.; Baldelli, S. *J. Phys. Chem. B* **2009**, *113*, 923.

(510) Martinez, I. S.; Baldelli, S. *J. Phys. Chem. C.* **2010**, *114*, 11564.

(511) Baldelli, S.; Bao, J.; Wu, W.; Pei, S.-s. *Chem. Phys. Lett.* **2011**, *516*, 171.

(512) Peñalber, C. Y.; Baldelli, S. *J. Phys. Chem. Lett.* **2012**, *3*, 844.

(513) Baldelli, S. *Accounts. Chem. Res.* **2008**, *41*, 421.

(514) Pan, G.-B.; Freyland, W. *Chem. Phys. Lett.* **2006**, *427*, 96.

(515) Castillo, M. R.; Fraile, J. M.; Mayoral, J. A. *Langmuir* **2012**, *28*, 11364.

(516) Liu, Y.; Zhang, Y.; Wu, G.; Hu, J. *J. Am. Chem. Soc.* **2006**, *128*, 7456.

(517) Yokota, Y.; Harada, T.; Fukui, K.-i. *Chem. Commun.* **2010**, *46*, 8627.

(518) Henderson, J. R.; Sabeur, Z. A. *J. Chem. Phys.* **1992**, *97*, 6750.

(519) Drüschler, M.; Borisenko, N.; Wallauer, J.; Winter, C.; Huber, B.; Endres, F.; Roling, B. *Phys. Chem. Chem. Phys.* **2012**, *14*, 5090.

(520) Ivaništšev, V.; Ruzanov, A.; Lust, K.; Lust, E. *J. Electrochem. Soc.* **2013**, *160*, H368.

(521) Myamlin, V. A.; Pleskov, Y. V. *Electrochemistry of semiconductors*; Plenum, 1967.

(522) Endres, F.; El Abedin, S. Z. *Phys. Chem. Chem. Phys.* **2006**, *8*, 2101.

(523) Abbott, A. P.; McKenzie, K. J. *Phys. Chem. Chem. Phys.* **2006**, *8*, 4265.

(524) Abbott, A. P.; Frisch, G.; Hartley, J.; Ryder, K. S. *Green. Chem.* **2011**, *13*, 471.

(525) Endres, F. *Chem. Ing. Tech.* **2011**, *83*, 1485.

(526) Hagiwara, R.; Ito, Y. *J. Fluorine Chem.* **2000**, *105*, 221.

(527) Levich, V. G. *Physicochemical hydrodynamics: (by) veniamin G. Levich. Transl. by scripta technica, inc*; Prentice-Hall, 1962.

(528) Bard, A.; Faulkner, L. R. *Electrochemical Methods. Fundamentals and Applications*; John Wiley & Sons: New York, 2001.

(529) Lloyd, D.; Vainikka, T.; Schmachtel, S.; Murtomäki, L.; Kontturi, K. *Electrochim. Acta.* **2012**, *69*, 139.

(530) Boxall, D. L.; O'Dea, J. J.; Osteryoung, R. A. *J. Electrochem. Soc.* **2002**, *149*, E468.

(531) Kuznetsov, A.; Ulstrup, Jens., *Electron transfer in chemistry and biology: an introduction to the theory.*; Wiley: Chichester, 1999.

(532) Kornyshev, A. A.; Kuznetsov, A. M.; Ulstrup, J. *J. Phys. Chem* **1993**, *98*, 3832.

(533) Marcus, R. A. *Annu. Rev. Phys. Chem.* **1964**, *15*, 155.

(534) Marcus, R. A. *J. Chem. Phys.* **1965**, *43*, 679.

(535) Marcus, R. A. *Rev. Mod. Phys.* **1993**, *65*, 599.

(536) Marcus, R. A. *J. Chem. Phys.* **1956**, *24*, 966.

(537) Pekar, S. *Untersuchungen uber die Elektronentheorie der Kristalle*; Akademie-Verlag: Berlin, 1954.

(538) Phelps, D. K.; Kornyshev, A. A.; Weaver, M. J. *J. Phys. Chem* **1990**, *94*, 1454.

(539) Dzhavakhidze, P.; Kornyshev, A.; Krishtalik, L. *J. Electroanal. Chem.* **1987**, *228*, 329.

(540) Kuznetsov, A. M.; Medvedev, I. G. *J. Phys. Chem.* **1996**, *100*, 5721.

(541) Medvedev, I. *J. Electroanal. Chem.* **2000**, *481*, 215.

(542) Kornyshev, A.; Ulstrup, J. *Chem. Phys. Lett.* **1986**, *126*, 74.

(543) Kornyshev, A. A.; Sutmann, G. *Electrochim. Acta.* **1997**, *42*, 2801.

(544) Dogonadze, R. R., Kalman, E., Kornyshev, A. A., Ulstrup, J., Eds. *The Chemical Physics of Solvation. Part A*; Elsevier: Amsterdam, 1985.

(545) Kornyshev, A. A. *Electrochim. Acta.* **1981**, *26*, 1.

(546) Lynden-Bell, R. M. *J. Phys. Chem. B.* **2007**, *111*, 10800.

(547) Lynden-Bell, R. *Electrochem. Commun.* **2007**, *9*, 1857.

(548) Shim, Y.; Kim, H. J. *J. Phys. Chem. B.* **2007**, *111*, 4510.

(549) Dogonadze, R. R.; Kuznetsov, A. M.; Vorotyntsev, M. A. *Phys. Status Solidi B* **1972**, *54*, 125.

(550) Vorotyntsev, M.; Dogonadze, R. R.; Kuznetsov, A. *Dokl. Akad. Nauk SSSR* **1970**, *195(5)*, 1135.

(551) Kornyshev, A. A.; Kuznetsov, A. M.; Phelps, D. K.; Weaver, M. J. *J. Chem. Phys.* **1989**, *91*, 7159.

(552) Medvedev, I. *J. Electroanal. Chem.* **2001**, *517*, 1.

(553) Frumkin, A. *Z. Phys. Chem.* **1933**, *A164*, 121.

(554) Krishtalik, L. In *Comprehensive treatise of electrochemistry*; Conway, B. E., Ed.; Plenum Press: New York, 1983.

(555) Krishtalik, L. I. *Charge transfer reactions in electrochemical and chemical processes*; Consultant's Bureau,New York, NY, 1986.

(556) Kornyshev, A. A.; Vorotyntsev, M. A. *Electrochim. Acta.* **1981**, *26*, 303.

(557) Marx, D.; Hutter, J. *Modern methods and algorithms of quantum chemistry*; Jülich, Germany, 2000; 301.

(558) Lagrost, C.; Carrié,; Vaultier, M.; Hapiot, P. *J. Phys. Chem. A.* **2003**, *107*, 745.

(559) Silvester, D. S.; Aldous, L.; Hardacre, C.; Compton, R. G. *J. Phys. Chem. B.* **2007**, *111*, 5000.

(560) Bautista-Martinez, J. A.; Tang, L.; Belieres, J.-P.; Zeller, R.; Angell, C. A.; Friesen, C. *J. Phys. Chem. C.* **2009**, *113*, 12586.

(561) Matsumiya, M.; Terazono, M.; Tokuraku, K. *Electrochim. Acta.* **2006**, *51*, 1178.

(562) Bard, A. J., Stratmann, M., Calvo, E. J., Eds. *Encyclopedia of Electrochemistry: Interfacial Kinetics and Mass Transport*; Wiley VCH: Weinheim, 2003; Vol. 2.

(563) Taylor, A. W.; Qiu, F.; Hu, J.; Licence, P.; Walsh, D. A. *J. Phys. Chem. B.* **2008**, *112*, 13292.

(564) Belding, S. R.; Rees, N. V.; Aldous, L.; Hardacre, C.; Compton, R. G. *J. Phys. Chem. C.* **2008**, *112*, 1650.

(565) Lovelock, K. R. J.; Cowling, F. N.; Taylor, A. W.; Licence, P.; Walsh, D. A. *J. Phys. Chem. B.* **2010**, *114*, 4442.

(566) Walsh, D. A.; Ejigu, A.; Smith, J.; Licence, P. *Phys. Chem. Chem. Phys.* **2013**, *15*, 7548.

(567) Meng, Y.; Aldous, L.; Belding, S. R.; Compton, R. G. *Phys. Chem. Chem. Phys.* **2012**, *14*, 5222.

(568) Meng, Y.; Aldous, L.; Belding, S. R.; Compton, R. G. *Chem. Commun.* **2012**, *48*, 5572.

(569) Martindale, B. C. M.; Menshykau, D.; Ernst, S.; Compton, R. G. *Phys. Chem. Chem. Phys.* **2013**, *15*, 1188.

(570) Wibowo, R.; Ward Jones, S. E.; Compton, R. G. *J. Phys. Chem. B.* **2009**, *113*, 12293.

(571) Wibowo, R.; Jones, S. E. W.; Compton, R. G. *J. Chem. Eng. Data* **2010**, *55*, 1374.

(572) Miller, J. R.; Simon, P. *Science* **2008**, *321*, 651.

(573) Walcarius, A. *Chem. Soc. Rev.* **2013**, *42*, 4098.

(574) Daikhin, L. I.; Kornyshev, A. A.; Urbakh, M. *Phys. Rev. E* **1996**, *53*, 6192.

(575) Daikhin, L. I.; Kornyshev, A. A.; Urbakh, M. *J. Chem. Phys.* **1998**, *108*, 1715.

(576) Hutchins, O. U.S. Patent 1271713, 9 July, **1918** .

(577) Mohun, W. A. Mineral Active Carbon and Process for Producing Same. U.S. Patent 3066099, 27 Nov, **1962**.

(578) Shipton, G. Improvements in and relating to mineral active carbons and to a process for their preparation. U.K. Patent GB971943 (A), 7 Oct, **1964** .

(579) Gordeev, S.; Vartanova, A. *Russ. J. Appl. Chem.* **1991**, *64*, 1040.

(580) Gogotsi, Y. G.; Yoshimura, M. *Nature* **1994**, *367*, 628.

(581) Gogotsi, Y.; Welz, S.; Ersoy, D. A.; McNallan, M. J. *Nature* **2001**, *411*, 283.

(582) Leis, J.; Perkson, A.; Arulepp, M.; Käärik, M.; Svensson, G. *Carbon* **2001**, *39*, 2043.

(583) Stoeckli and Centeno[585] debated these findings claiming that the internal surface area of accessible pore space – the quantity critical for the conclusions about the value of the specific capacitance – is not the one assessed in Simon-Gogotsi experiments. However, we note that the latter groups have used several independent methods of evaluation of the true surface area of the carbide-derived carbon electrodes, and in the absence of other counter-evidences we will refrain from dismissing the Simon-Gogotsi 'anomalous capacitance' as an artifact .

(584) Centeno, T. A.; Sereda, O.; Stoeckli, F. *Phys. Chem. Chem. Phys.* **2011**, *13*, 12403.

(585) Stoeckli, F.; Centeno, T. A. *Phys. Chem. Chem. Phys.* **2012**, *14*, 11589.

(586) Laudisio, G.; Dash, R. K.; Singer, J. P.; Yushin, G.; Gogotsi, Y.; Fischer, J. E. *Langmuir* **2006**, *22*, 8945.

(587) Chmiola, J.; Largeot, C.; Taberna, P.-L.; Simon, P.; Gogotsi, Y. *Science* **2010**, *328*, 480.

(588) Largeot, C.; Portet, C.; Chmiola, J.; Taberna, P.-L.; Gogotsi, Y.; Simon, P. *J. Am. Chem. Soc.* **2008**, *130*, 2730.

(589) Cavazzoni, C.; Chiarotti, G. L.; Scandolo, S.; Tosatti, E.; Bernasconi, M.; Parrinello, M. *Science* **1999**, *283*, 44.

(590) Panofsky, W. K. H.; Phillips, M. *Classical Electricity and Magnetism: Second Edition*; Dover Publications, Incorporated, 2012.

(591) Vekilov, P.G., Personal Communication. 2011.

(592) Vorotyntsev, M.; Kornyshev, A. *Zh. Eksp. Teor. Fiz+* **1980**, *78*, 1008.

(593) Kornyshev, A. A.; Rubinshtein, A. I.; Vorotyntsev, M. A. *Phys. Status Solidi B* **1977**, *84*, 125.

(594) Kiyohara, K.; Asaka, K. *J. Chem. Phys.* **2007**, *126*, 214704.

(595) Kondrat, S.; Georgi, N.; Fedorov, M. V.; Kornyshev, A. A. *Phys. Chem. Chem. Phys.* **2011**, *13*, 11359.

(596) Typical experimental values lie in between these two results. However, real experimental systems can not be literally compared with the idealized models, such as treated in Refs.[372,594] One should therefore focus only on qualitative correspondence between the theoretical/computational results and available experimental data .

(597) There is a discussion what capacitance has been reported by Gogotsi-Simon group: integral or differential. Assessing it from dq/dt dV/dt = dq/dV of cyclic voltammograms one gets differential capacitance, but in the voltage region where the capacitance seems to be practically constant, the difference would be unnoticeable .

(598) Kondrat, S.; Pérez, C. R.; Presser, V.; Gogotsi, Y.; Kornyshev, A. A. *Energ. Environ. Sci.* **2012**, *5*, 6474.

(599) Kornyshev, A. *Faraday Discuss.* **2013**, *164*.

(600) In the theory of magnetism, α is the so called coupling parameter that characterises the interactions of real spins (with positive $\alpha >$ causing propensity for antiferromagnetic order) and the last term describing interaction of spins with the external magnetic field .

(601) Baxter, R. J. *Exactly solved models in statistical mechanics*; Academic Press, 1982.

(602) Feng, G.; Cummings, P. T. *J. Phys. Chem. Lett.* **2011**, *2*, 2859.

(603) Katayama, Y. In *Electrochemical Aspects of Ionic Liquids*; Ohno, H., Ed.; A John Wiley & Sons, Inc.: Hoboken, New Jersey, 2005; p 111.

(604) Aal, A. A.; Al-Salman, R.; Al-Zoubi, M.; Borissenko, N.; Endres, F.; Höfft, O.; Prowald, A.; Zein El Abedin, S. *Electrochim. Acta.* **2011**, *56*, 10295.

(605) Linden, D.; Reddy, T. B. *Handbook of batteries*; McGraw-Hill, 2002.

(606) Madria, N.; Arunkumar, T.; Nair, N. G.; Vadapalli, A.; Huang, Y.-W.; Jones, S. C.; Reddy, V. P. *J. Power. Sources.* **2013**, *234*, 277.

(607) Scrosati, B.; Garche, J. *J. Power. Sources.* **2010**, *195*, 2419.

(608) Currently lithium-metal serves usually as a counter electrode and as a commonly accepted Li/Li+ reference electrode in test cells (see Ref.[107]) .

(609) Shin, J.-H.; Henderson, W. A.; Passerini, S. *Electrochem. Commun.* **2003**, *5*, 1016.

(610) Sakaebe, H.; Matsumoto, H. *Electrochem. Commun.* **2003**, *5*, 594.

(611) Garcia, B.; Lavallée, S.; Perron, G.; Michot, C.; Armand, M. *Electrochim. Acta.* **2004**, *49*, 4583.

(612) Howlett, P. C.; MacFarlane, D. R.; Hollenkamp, A. F. *Electrochem. Solid-State Lett.* **2004**, *7*, A97.

(613) Nakagawa, H.; Fujino, Y.; Kozono, S.; Katayama, Y.; Nukuda, T.; Sakaebe, H.; Matsumoto, H.; Tatsumi, K. *J. Power. Sources.* **2007**, *174*, 1021.

(614) Schweikert, N.; Hofmann, A.; Schulz, M.; Scheuermann, M.; Boles, S. T.; Hanemann, T.; Hahn, H.; Indris, S. *J. Power. Sources.* **2013**, *228*, 237.

(615) Bruce, P. G.; Freunberger, S. A.; Hardwick, L. J.; Tarascon, J.-M. *Nat. Mater.* **2012**, *11*, 19.

(616) Schaefer, J.; Lu, Y.; Moganty, S.; Agarwal, P.; Jayaprakash, N.; Archer, L. *Appl. Nanosci.* **2012**, *2*, 91.

(617) Li, F.; Zhang, T.; Zhou, H. *Energ. Environ. Sci.* **2013**, *6*, 1125.

(618) Eguizábal, A.; Lemus, J.; Pina, M. *J. Power. Sources.* **2013**, *222*, 483.

(619) Gorlov, M.; Kloo, L. *Dalton Trans.* **2008**, 2655.

(620) Jhong, H.-R.; Wong, D. S.-H.; Wan, C.-C.; Wang, Y.-Y.; Wei, T.-C. *Electrochem. Commun.* **2009**, *11*, 209.

(621) Guo, L.; Pan, X.; Wang, M.; Zhang, C.; Fang, X.; Chen, S.; Dai, S. *Sol. Energy* **2011**, *85*, 7.

(622) Wang, G.; Wang, L.; Zhuo, S.; Fang, S.; Lin, Y. *Chem. Commun.* **2011**, *47*, 2700.

(623) Pushparaj, V. L.; Shaijumon, M. M.; Kumar, A.; Murugesan, S.; Ci, L.; Vajtai, R.; Linhardt, R. J.; Nalamasu, O.; Ajayan, P. M. *P. Natl. Acad. Sci.* **2007**, *104*, 13574.

(624) Wei, D.; Wakeham, S. J.; Ng, T. W.; Thwaites, M. J.; Brown, H.; Beecher, P. *Electrochem. Commun.* **2009**, *11*, 2285.

(625) Shahinpoor, M.; Kim, K. J. *Smart Mater. Struct.* **2001**, *10*, 819.

(626) Kim, K. J.; Shahinpoor, M. *Smart Mater. Struct.* **2003**, *12*, 65.

(627) Shahinpoor, M.; Kim, K. J. *Smart Mater. Struct.* **2004**, *13*, 1362.

(628) Shahinpoor, M.; Kim, K. J. *Smart Mater. Struct.* **2005**, *14*, 197.

(629) Shahinpoor, M.; Bar-Cohen, Y.; Simpson, J. O.; Smith, J. *Smart Mater. Struct.* **1998**, *7*, R15.

(630) Löfdahl, L.; Gad-el Hak, M. *The MEMS Handbook*; CRC Press, 2005.

(631) Tan, X. *Mar. Technol. Soc. J.* **2011**, *45*, 31.

(632) Keshavarzi, A.; Shahinpoor, M.; Kim, K. J.; Lantz, J. W. *Proc. SPIE* **1999**, 369.

(633) Ferrara, L.; Shahinpoor, M.; Kim, K. J.; Schreyer, H. B.; Keshavarzi, A.; Benzel, E.; Lantz, J. W. *Smart Mater. Struct* **1999**, 394.

(634) Etebari, A.; Bennett, M. D.; Leo, D. J.; Vlachos, P. P. *A dynamic wall shear stress sensor based on ionic polymers*; ASME: New York, 2005 .

(635) Biddiss, E.; Chau, T. *Med. Eng. Phys.* **2006**, *28*, 568.

(636) Aureli, M.; Prince, C.; Porfiri, M.; Peterson, S. D. *Smart Mater. Struct* **2010**, *19*, 015003.

(637) Giacomello, A.; Porfiri, M. *J. Appl. Phys.* **2011**, *109*, 084903.

(638) Davidson, J. D.; Goulbourne, N. C. *J. Appl. Phys.* **2011**, *109*, 084901.

(639) Davidson, J. D.; Goulbourne, N. C. *IInt. J. Appl. Mech. Eng.* **2011**, *03*, 365.

(640) Lee, A. A.; Colby, R. H.; Kornyshev, A. A. *Soft. Matter.* **2013**, *9*, 3767.

(641) Lee, A. A.; Colby, R. H.; Kornyshev, A. A. *J. Phys.: Condens. Matter* **2013**, *25*, 082203.

(642) Kondrat, S.; Kornyshev, A. *J. Phys. Chem. C.* **2013**, *117*, 12399.

Dr. Maxim V. Fedorov an expert in computational physical chemistry, electrochemistry and molecular biophysics. His research interests focus on (i) ionic liquids at electrified interfaces; (ii) ion effects on macromolecules and nanobjects; (iii) modeling molecular effects of solvation. He published over 70 peer-reviewed publications and presented about 70 invited talks and lectures on these subjects.

He received his Ph.D. degree at the Institute of Theoretical and Experimental Biophysics of the Russian Academy of Sciences, Pushchino, Russia, in 2002, in Biophysics with Prof. S.E. Shnoll, an expert in physical biochemistry. After his PhD he worked as a researcher at the same institute until the beginning of 2004 when he moved to the University College Dublin, Republic of Ireland, as a postdoc at the Department of Chemistry. In 2005 he moved to the University of Cambridge, UK, where he spent three years working at the Department of Chemistry as a Research Associate in the Unilever Centre for Molecular Science Informatics. Since 2007 he was a Group Leader at the Max Planck Institute for Mathematics in the Sciences, in Leipzig, Germany. In 2010-2011 he was also an external Privat-Dozent at the Department of Chemistry, University of Duisburg-Essen, Germany. In 2007 he received his Doctor of Sciences (Doktor Nauk) degree in Physical Chemistry from the Institute of Solution Chemistry of the Russian Academy of Sciences, Ivanovo, Russia. As a visiting scientist he worked at the University of Kassel in 2003 (with Prof. D. Kolb, as a DAAD scholar); Imperial College London in 2007 (with Prof. A.A. Kornyshev); and at the University of Osaka in 2009 (with Prof. Y. Goto). In 2011 he spent a month in the University of Lille as a Visiting Professor. 2012 he received the Helmholtz Award from the International Association of the Properties of Water and Steam (IAWPS).

In 2011 he moved to the University of Strathclyde in Glasgow (UK) as a Professor in Physics and Life Sciences. Since 2012 he is also Director of the West of Scotland Academia-Industry Supercomputer Centre (aka ARCHIE-WeST) at the University of Strathlcyde.

Professor Alexei Kornyshev is an expert in condensed matter theoretical chemical physics and its applications to biophysics, electrochemistry, nanoscience, and energy generation and storage. His areas of research were -- hydration, the structure and dynamics of metal/electrolyte and liquid-liquid interfaces, electron and proton transfer processes (in the bulk of solutions, at electrochemical interfaces, through nano-junctions and single molecules, in complex environment), transport phenomena in solid electrolytes and polymer electrolyte membranes, aggregation and recognition of helical biopolymers and the structure of chiral liquid crystals, theory of modern fuel cells and super-capacitors, electrowetting. He has over 200 publications and 30 review articles in leading journals, several patents, edited 5 multi-author books and a number of special issues.

Current projects of his research group focus on: (i) DNA biophysics and molecular genetics, (ii) electrovariable optofluidics and nanophotonics; (iii) molecular electronics and machines; (iv) ionic liquids and their applications, (v) sensors and electroactuators.

He received his Master's degree from Moscow Physical Engineering Institute in theoretical nuclear physics in 1970. After getting in 1974 his PhD in Physical and Mathematical Sciences (under the guidance of R.R. Dogonadze), he worked as researcher at the Frumkin Institute of Electrochemistry (Acad.Sci.), Moscow (1973 - 1991), with his DSc degree defended in 1986. In 1991 he was awarded *Humboldt Prize in Electrochemistry and Physical Chemistry*, and spent consequently a year at TU Munich, as Humboldt Guest Professor. He was then invited to the Research Centre Juelich, Germany, to lead a Theory Group in a new Institute of Energy Processing with a focus on fundamentals of fuel cells. In 1997 he was promoted there to Head of Division of Theoretical Physical Chemistry, and later got a joint appointment between the Research Centre Juelich and the Heinrich-Heine University of Dusseldorf as Professor of Theoretical Physics. In 2002 he moved to Imperial College, appointed to Chair of Chemical Physics, supported by 2001*Royal Society Wolfson Research Merit Award*.

He is an elected Fellow of IUPAC, Institute of Physics, International Society of Electrochemistry, and a Member of Royal Danish Academy of Science. His achievements were also celebrated by 2003 Christian-Friedrich Schönbein Contribution-to-Science Medal and 2006 RSC Geoffrey Barker Electrochemistry Medal. This year he was awarded an RSC 2010 Interdisciplinary Prize, Medal and Endowed Lectureship; this article will cover the material of one of these lectures. See more in http://www3.imperial.ac.uk/people/a.kornyshev